CHEMICAL IMPACTS FROM ACID MINE DRAINAGE IN A DAM ECOSYSTEM – AN EPILIMNION AND SEDIMENT ANALYSIS

Kirstin Olsen

A Dissertation submitted to the Faculty of Science, University of the Witwatersrand, Johannesburg, in fulfilment of the requirements for the degree of Master of Science

Supervision undertaken by Dr. Gavin Snow and Dr. Marc Humphries

Johannesburg, 2015

The financial assistance of the National Research Foundation (NRF) towards this research is hereby gratefully acknowledged. Opinions expressed and conclusions arrived at, are those of the author and not necessarily to be attributed to the NRF.

AP&ES
School of Animal, Plant & Environmental Sciences
The Biology of a Changing World: Conserving African Biodiversity

DECLARATION

I declare that this Dissertation is my own, unaided work. It is being submitted for the Degree of Master of Science at the University of the Witwatersrand, Johannesburg. It has not been submitted before for any degree or examination at any other University.

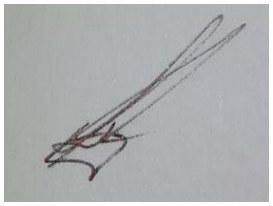

Kirstin Addison Aleksander Olsen

On the 10th day of May 2016 at the University of the Witwatersrand, Johannesburg.

ABSTRACT

Acid Mine Drainage (AMD) can result in significant and permanent ecological, chemical and physical alterations to the receiving environment. In 2002 a major surface decant of AMD effluent first entered the Tweelopies River upstream of the Krugersdorp Game Reserve, near Johannesburg. Within the game reserve the Tweelopies River intersects the Charles-Fourie Dam. The function of this dam, as a a sink of dissolved AMD contaminants (sulfate and iron), in the contaminated river was investigated in this study between September 2013 and August 2014. A water mass balance approach was used to estimate fluxes of dissolved contaminants. Additionally, compositional changes in sediment chemistry (total Fe, S, Al, Mg, Ca, Cu, Ni, Pb, V, and Zn) were investigated in order to quantify the storage or accumulation of contaminants in the sediment, which would indicate the long-term mitigatory function of the dam.

The accumulation of high concentrations of metals and non-metals in the sediment of the dam (including 121.0 g $S.kg^{-1}$ and 34.7 g $Fe.kg^{-1}$) indicate that the dam stored both total iron and sulfur (AMD constituents) in the long term. Assuming that there was an average sediment depth of 19.3 cm in the dam, it was estimated that 18 tons of total iron, and 5 tons of total sulfur were present in the sediments of the dam. Additionally, the mass balance indicated that in total the dam acted as a sink for both sulfate and iron (14 853 kg SO_4^{2-} and 5.5 kg Fe respectively) between September 2013 and February 2014, when the pH of the Tweelopies River was circumneutral (pH 6.1 – 7.6). However, the storage of contaminants in the dam also allowed iron and sulfate to be remobilised from the species and compounds it was stored in in the dam over the 2013-2014 study period. This is the result of changes in the water quality between March and July, when the pH of the river was lower (pH 2.9 – 3.6) and both dissolved iron and sulfate were remobilised (18 219 kg SO_4^{2-} and 210 kg Fe respectively). In total the dam remobilised sulfate and iron in the 2013-2014 study period (increasing the flux by 0.4% or 3 366 kg and 8.7% or 202 kg Fe respectively).

The data collected indicate that pH is the primary driver governing the dam to act as a sink and also remobilise dissolved iron and sulfate from the species and compounds they are stored in in the dam. When the pH is low the dam remobilises AMD constituents and acts as a sink when the pH is circumneutral. Therefore, it is

evident that continual neutralisation of the water limits the degree to which the dam remobilises dissolved contaminants from the species and compounds they were stored in and that maintaining a neutral pH in the river should be prioritised by management. Additionally, the concentrations of total Fe, S, Ni, Pb, and Zn in the sediments exceeded the maxima probable effect level for the protection of aquatic life (by 3, 69, 20, 1.6, and 4.9 times respectively). The accumulation of contaminants in the sediment have very likely had a long-term adverse impact upon biodiversity and may present challenges to future rehabilitation efforts. Future management plans should avoid high investment loss to short-term remediation efforts and rather take a long term approach that incorporates these findings.

ACKNOWLEDGEMENTS

I would like to thank and acknowledge the staff of the Krugersdorp Game reserve for their tireless support of this research, Martin and Dean in particular, for not only granting me access but also for keeping an eye out for the hippos at all times on my behalf. I would also like to thank the Department of Environmental Affairs and the National Groundwater Archive, Ernest Bertram, Nico Du Toit and Theo Moolman in particular – without whom groundwater sampling would not have been possible. I would like to thank Professor Christopher Curtis from the Wits School of Geography, Archaeology and Environmental Studies for the extended use of his inflatable boat during the sediment coring attempts, as well as Brad Robinson for his assistance in extruding the sediment core. I would also like to thank the South African Weather Service and iWeathar for granting me access to their meteorological databases and the National Research Foundation for their financial support of this research.

Finally I would like to thank my supervisors for their advice and support.

TABLE OF CONTENTS

LIST OF FIGURES

LIST OF TABLES

1 LITERATURE REVIEW

1.1 INTRODUCTION AND RATIONALE

Gold mining in South Africa first began in 1886, with the industry rapidly growing in the far West Rand which contains the largest gold deposit in the world (Adler *et al.*, 2007). The first complaints of water pollution from mining activity were filed by farmers in 1905. However, during this time government seconded 57% of mining profit in the form of tax and the mining industry was given special privileges regarding water use that enabled profit maximization (Adler *et al.*, 2007). Thus it was only 50 years after the first complaints of mine effluent in 1905, that an Interdepartmental Government Committee was established to investigate the effects of mines (Adler *et al.*, 2007). There are still many management obstacles present within the South African government including a lack of interdepartmental collaboration, a lack of proactive governance (Adler *et al.*, 2007), as well as a misunderstanding of the pollutants (Turton *et al.*, 2014). Therefore, it is apparent that socio-economic and political motives played a highly influential role in creating this historical problem.

The South African mining sector is the fifth largest globally, employing 1 million individuals, contributing 18% to the GDP and generating 94% of the country's electricity via coal mining (Oxford Business Group, 2012; Smit, 2013). Acid mine drainage (AMD) has only recently become a widely-publicised critical issue in Gauteng beginning with the 2002 decant in the Western Basin of the Witwatersrand Goldfields (Department of Water Affairs, 2010). If acid mine drainage is not effectively managed in South Africa it is very likely that it will become a problem proportional to damage seen in other countries. The impacts from mining effluent have been well documented in other countries and caused severe environmental damage and highly expensive costs across the world. The United States Environmental Protection Agency (USEPA) has weighted the significance of the ecological impacts from mining below only global warming and stratospheric ozone depletion (Hontelez, 2000; Oelofse *et al.*, 2007). Acid mine drainage is a serious international issue – ~R32 billion per annum is spent to remediate contaminated rivers in Canada, and ~R163 billion per annum in the USA (Harries, 1997; Costello, 2003; Department of Water Affairs, 2010).

Acid mine drainage contamination can persist for millennia – for instance, without treatment mining lakes under Iron Mountain in California are predicted to decant for up to 3000 years (Nordstrom & Alpers, 1999). While the Iberian pyrite belt contains the world's oldest operating mine (~4500 years old, dating from the bronze age) which still discharges AMD today (Hudson-Edwards *et al.*, 1999). Acid mine drainage is very expensive to address and can transform aquatic ecosystems into permanently, critically modified ecosystems from significant ecological and environmental alterations (Department of Water Affairs, 2010; Nordstrom, 2011). These alterations are the result of the oxygenation and hydrolysis of a sulfide-based ore. This natural process is accelerated by mining activities which expose a greater amount of ore over a shorter time period (in South Africa ~495 metric tons of pyrite (FeS_2) were extracted from gold mines alone between 2002-2011 (McCarthy, 2011; Chamber of Mines South Africa, 2012)). Alterations to aquatic ecosystems frequently include a pH below 3, which mobilises heavy metal contaminants. This – paired with the high concentrations of dissolved sulfate – disrupts metabolic activities and generates iron precipitates on both the exposed surfaces of organisms and the aquatic ecosystem (Figure 1).

Figure 1: Dipteran, Chironomidae larvae of the AMD contaminated Tweelopies River coated in iron precipitate (2012).

This study quantified the accumulation of total sulfur and iron that resulted from ~11 years of AMD contamination in the Charles-Fourie Dam, Krugersdorp (Hobbs & Cobbing, 2007), and provided some insight into the depth of the

contamination and the annual rate of deposition. The study also investigated whether dissolved contaminants (sulfate and iron) were retained or remobilised from the dam.

Acidification and the impact of AMD is well documented in many natural lakes, particularly in the USA and along the European-Iberian pyrite belt (Charles *et al.*, 1990; Grande *et al.*, 2004), but there appear to be few or no studies conducted on the retention of AMD in dams that existed prior to contamination. A number of studies, however, address the building of remediation/retention dams, and slime and tailings dams (Akcil & Koldas, 2006; Oelofse *et al.*, 2007). This study provided insight into this apparent gap in the scientific literature and on this demonstrated economically and environmentally important area of research.

Additionally, surface water is the sole focus of many AMD impact assessments (Luoma & Rainbow, 2011). Acid mine drainage contamination of sediments appears to have been largely overlooked in the geological context of South Africa. Sediments can support a large amount of primary production, nutrient cycling and transport, and invertebrate communities. Additionally, a reservoir of AMD contaminants in dam sediments may confound improvements in water quality if flood events or changes in pH cause chemical transformations and re-suspensions. This study examines both the epilimnic and sedimentary changes in a dam associated with acid mine drainage in South Africa, thereby providing insight into this apparently under-investigated topic.

Sediments contaminated with AMD may also constitute an economic opportunity depending upon the amounts of contaminants in them. Marketable iron oxide and sulfur compounds have been extracted from sludge/slurry in AMD contaminated sediments (Hedin, 2003; Maree *et al.*, 2005; McCullough & Lund, 2006; Michalková *et al.*, 2013; Weaver, 2014). Sulfur in particular is often imported into Africa to meet demand (Maree *et al.*, 2005). The above highlights the economic importance of the potential implications of this study, which quantifies the accumulation of AMD constituents in the sediment of a dam. Additionally, assessment of the storage of metals and salts in dam sediment will help predict future contamination scenarios. Data on the specific, successive impacts associated with the progression of AMD pollution in this study can potentially be used to minimise or address ecological impacts prior and post decant into other areas.

The location of the study site also adds important context to the motivation for the study (Figure 3). The dam lies in a conservation area (the Krugersdorp Game Reserve) that was highly contaminated and is upstream of the Cradle of Humankind World Heritage Site (Hobbs & Cobbing, 2007). The data produced in this study will potentially provide valuable and novel scientific insight, which could be used by the Krugersdorp Game Reserve management; for example quantification of contaminant sediment storage and residence time of water in the dam. By facilitating more informed management of the pollution, the results of this study may assist in the protection of the World Heritage Site, which is located just 10 kilometres downstream. Additionally, the quality of the water discharged by the dam was examined and will have varied annually depending upon discharges (precipitation, groundwater, etc.). From a managerial perspective it will be useful to understand these seasonal changes. For instance, a flood event may drastically decrease a river's water quality (which needs to be planned for) or cause the dam to remobilised contaminants from the species and compound they are stored in in the sediments.

There are at least 48 000 dams over 15 m high worldwide, 500 are in South Africa and store approximately half of the country's mean annual runoff (MAR) (The World Commission on Dams, 2000; Department of Water Affairs, 2010). The impacts of dam releases, retention during floods, as well as the physical barrier to wildlife have widespread affects across many of South Africa's aquatic ecosystems. Thus the impacts and the storage or remobilisation of AMD contaminants from dams have quite widespread implications that needed to be quantified.

Finally, major AMD surface decants are predicted to appear soon in other Witwatersrand basins which arise from the same reef as the study site (the Central and Eastern Witwatersrand Basins) (Department of Agriculture and Rural Development, 2014; Turton *et al.*, 2014). Knowledge of the potential amount and rate of AMD constituent removal, and the quality of water being discharged from the Charles-Fourie Dam will provide some insight when evaluating new decants, increase the accuracy of risk prediction and increase the efficiency of amelioration targeting in these highly populated areas.

1.2 AIM, OBJECTIVES AND KEY QUESTIONS:

The aim of this study was to determine the mitigatory function of a dam on dissolved sulfate and iron (acid mine drainage contaminants) in a river and to quantify the reservoir of total iron and sulfur in the dam sediment.

The key questions are presented below:

1) Does the dam act as a sink for dissolved sulfate[1] and iron (AMD contaminants)?
2) What is the estimated reservoir of total sulfur[1] and iron (AMD contaminants) in the dam sediment?
3) Do the sediments of the dam show reliable temporal trends?

[1] It should be noted that key question 1 pertains to dissolved sulfate, while key question 2 pertains to total sulfur (including the species of sulfur such as sulfate). It was assumed that the majority of dissolved sulfur would be present in the form of sulfate, whereas sulfur occurs in multiple species in the sediment.

1.3 SCIENTIFIC BACKGROUND

The scientific background below discusses 1) the study site, 2) AMD generation and pH dependencies, 3) the mechanisms governing chemical transformations of AMD pollutants from the dam (decomposition, aeration and iron precipitation), and 4) the conditions (groundwater influx, and heavy rainfall) that may cause natural variation of these mechanisms over a year. These aspects were considered important as AMD generation was the basis for the contaminants chosen to be the focus of this study. The speciation of iron is highly dependent upon pH. The mechanisms facilitating retention or release of contaminants and the conditions affecting them, justify and explain trends in the time series taken.

The final section of the scientific background section of the literature review presents a discussion and examples of mass balance models and calculations as background to the methodology.

1.3.1 Study site

1.3.1.1 Location and notable geographic sites

The study site is the Charles-Fourie Dam on the Tweelopies River, located within the Krugersdorp Game Reserve (26°5'19.12"S; 27°42'55.39"E) (Figures 2 and 3). The Charles-Fourie Dam and Tweelopies River are located in West Krugersdorp within the Crocodile (West) and Marico Catchment of the Limpopo River basin (A21D) (Figure 2). The catchment is 5.8 km^2 in extent, and it was reported that the Present Ecological State is in a seriously modified (Class E) condition (Department of Water Affairs, 2012). Krugersdorp was founded in 1887 and mining in the area dates back to this time. However, impacts from contamination in the game reserve have only been reported since a major surface decant of effluent began in August 2002 (Department of Water Affairs, 2010).

The source of the acid mine drainage contamination is discharge from a flooded mine shaft, which confluences with the Tweelopies River (Figure 3). The mining site was developed by Rand Uranium for gold, uranium and sulfur extraction. The company's primary activity sites are designated: Randfontein Surface Operations and Cooke Underground Operations. Three shafts were still operating in

2012 and vast tailings storage facilities, the West Wits Pit, overlook the reserve (Figure 3).

At the time of this study the closest borehole to the dam was located approximately 500 m to the south-east of the dam (Figure 3).

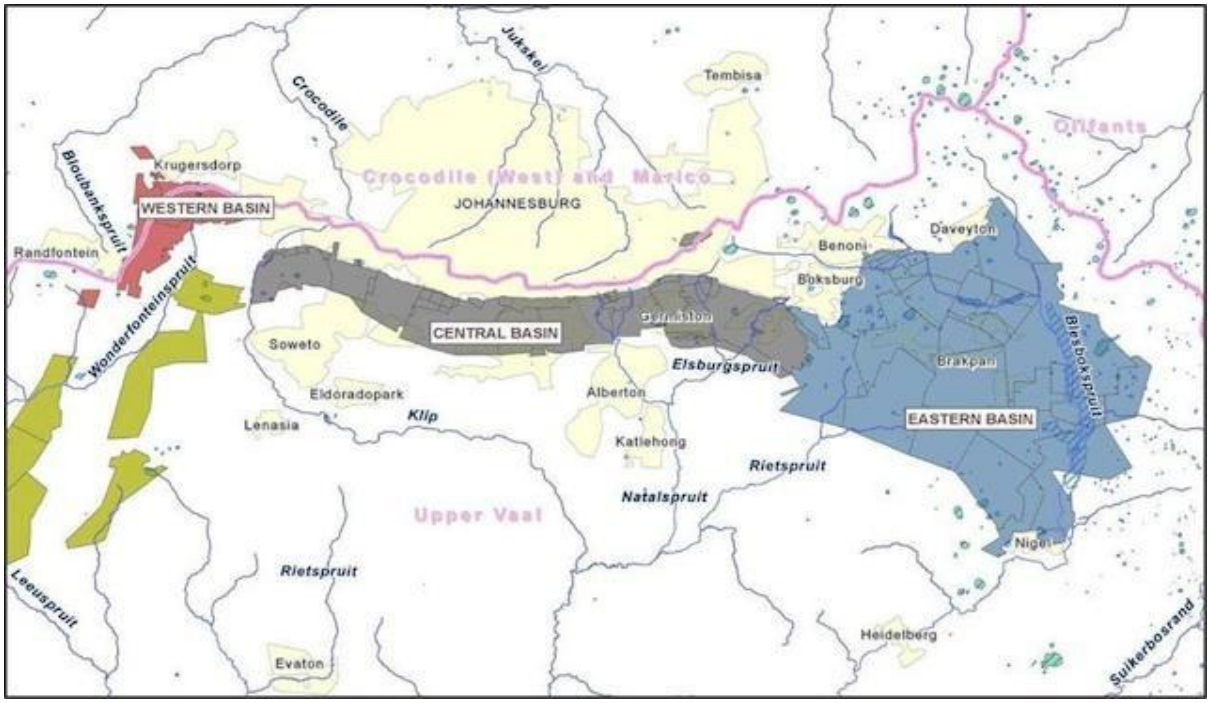

Figure 2: Map showing the Far Western, Western, Central and Eastern Basins of the Witwatersrand and their positions relative to major catchments (Upper Vaal, Crocodile (West) and Marico, and Olifants). The town of Krugersdorp is shown in the top left hand corner (Department of Water Affairs, 2010).

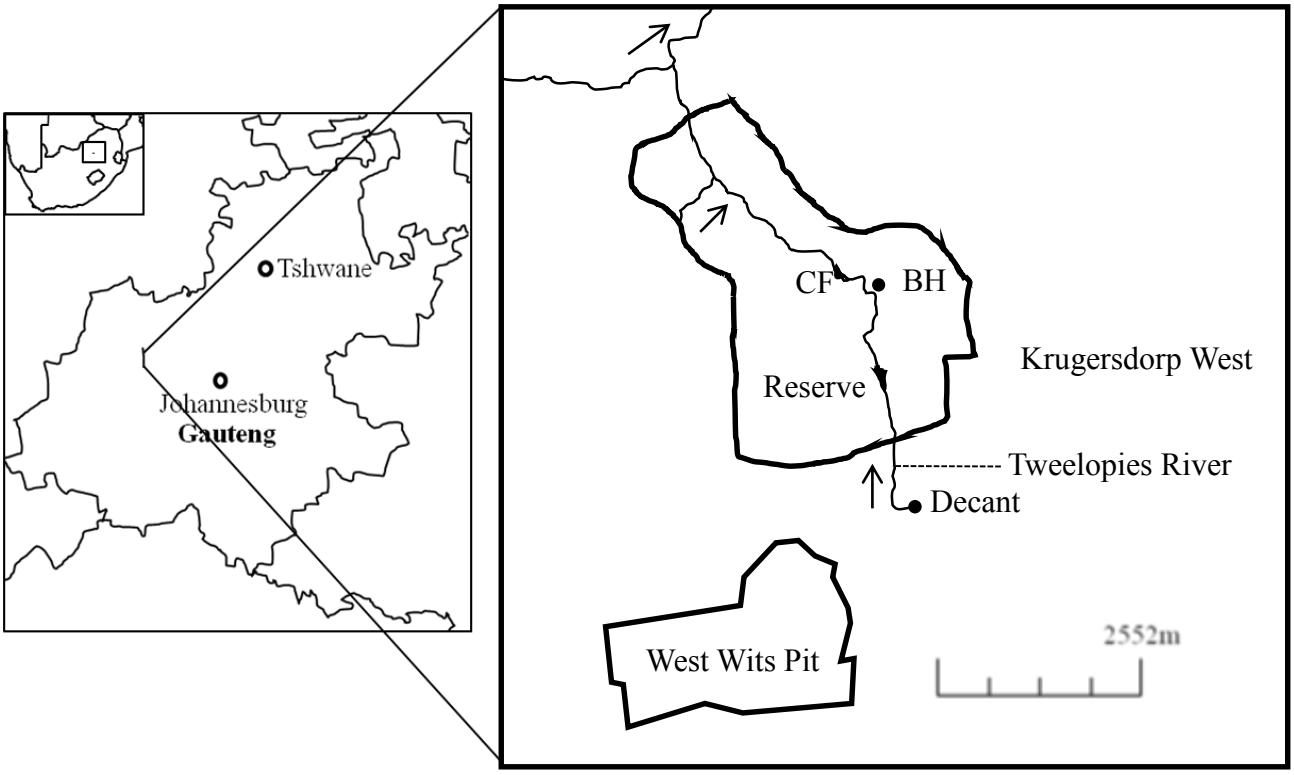

Figure 3: Scaled map of the Charles-Fourie Dam (CF) located within Gauteng, South Africa. The borehole (BH) closest to the Charles-Fourie Dam and the Tweelopies River are shown. The AMD decant and the Tweelopies is shown with the West Wits Pit around which several mines congregate. Direction of river flows are indicated by arrows.

1.3.1.2 Dam description

The Charles-Fourie Dam is an overflow dam that was constructed of concrete with an arch design (curved upstream) and an artificially constructed abutment on the far left side (Figure 4). It was constructed by Charles Fourie – a manager of the Krugersdorp Game Reserve - for recreational tourism (mainly fishing activities) in 1978 (*pers comm.*, M. Yamaha).

Figure 4: The Charles-Fourie Dam water surface from the wall towards the inlet (top left), atop and below the dam wall (top right, left bottom) and the abutment from below the dam wall (right bottom) (2013).

1.3.1.3 Geology

Designated as the West Rand Gold Field of the Witwatersrand Gold Reef, the area's geology lies within the Zwartkrans Compartment and is part of the Witwatersrand and Transvaal Supergroups (Figure 5). It falls in the Black Reef quartzite formation, but also contains shale and other deposits including the carbonate mineral dolomite, $CaMg(CO_3)_2$ (Keyser *et al.*, 1986; Els *et al.*, 1995).

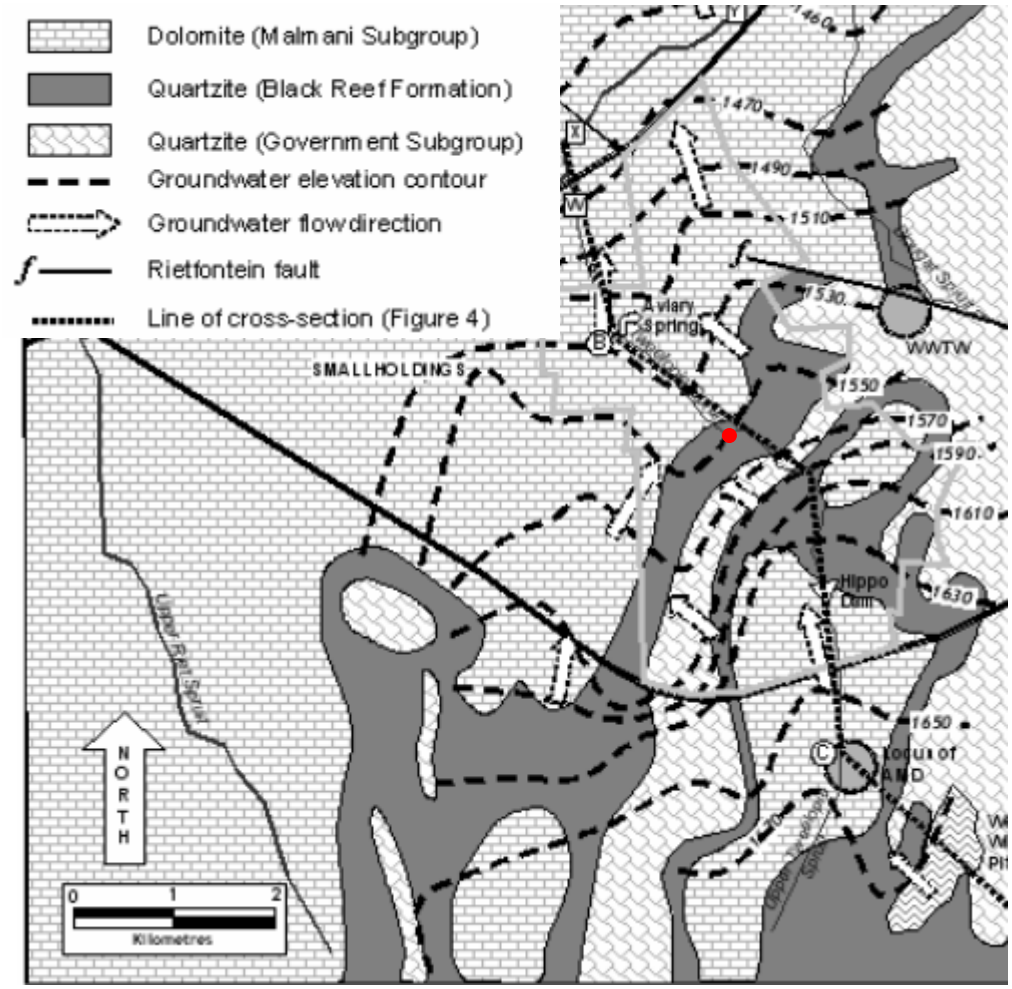

Figure 5: Geological map showing Black Reef Quartzite formations, groundwater elevation contour and groundwater flow direction. A red waypoint identifies the Charles-Fourie Dam near the centre of the figure (Hobbs & Cobbing, 2007).

1.3.1.4 Climate

Krugersdorp receives summer rainfall (December-February) and winter frost (June-August). Annual precipitation is ~720 mm (based on a 10 year average). Highest rainfall usually occurs in January (~125 mm) and the lowest in July (~5 mm) (World Weather Online, 2013) (Appendix 1). The surrounding topography creates a natural barrier and watershed to the west and east of the reserve, limiting agricultural

and urban pollution occurring in runoff from the surrounding landscape (Olsen *et al.*, 2012).

1.3.1.5 Current management practices

This study took place from September 2013 to August 2014. As of August 2012 a short-term action plan was implemented at the site – a new emergency neutralization plant began abstraction and treatment of the water at the point source of the decant (a flooded mine shaft) increasing the amount of water neutralized from 15 million litres per day to 25 - 35 million litres per day (Department of Water Affairs *et al.*, 2010; Bege, 2014; Department of Agriculture and Rural Development, 2014; Turton *et al.*, 2014). Neutralization increases the pH and decreases the concentration of dissolved heavy metals (by facilitating precipitation) – however neutralization does not remove all salts. This is discussed further in section 3.2 below.

Following seasonal heavy rainfall at the end of February 2014 between 26 and 30 million litres of acid mine drainage overwhelmed the treatment plant, and were released untreated into the Tweelopies River (Bege, 2014; Turton *et al.*, 2014).

1.3.2 AMD generation and pH dependencies

Acid mine drainage originates from the weathering of sulfide mineral deposits such as pyrite (FeS_2), chalcopyrite (CuS_2), galena (PbS) and numerous other sulfide ores (Gray, 1997). Although this weathering can be natural, the process is accelerated by mining activities which expose the ore to oxygen and water. Mining-based sources of AMD include opencast pits, underground workings and shafts, tailing slime dams, tailing dumps/storage facilities, diffuse seepage from rehabilitated areas, and rock exposed from construction (Akcil & Koldas, 2006). Opencast pits and tailing storage facilities can also serve as diffuse sources through dust blown into aquatic ecosystems (Luoma & Rainbow, 2011).

A flooded mine shaft in the Western Basin of the Witwatersrand Reef is the point source of AMD to the Tweelopies River (Figure 6) but diffuse decants have been quantified too (Olsen *et al.*, 2012). Approximately 2.6 km downstream of the

decant the river becomes an inlet to the Charles-Fourie Dam – the focus of this study. Mining of the Witwatersrand reef in this vicinity was conducted by Rand Uranium Ltd. (Hobbs & Cobbing, 2007). Rand Uranium Ltd. was a subsidiary of Harmony Gold at the time, and was ultimately bought by Gold One in 2012 (Gold One International Limited, 2012) for gold, uranium and sulfur extraction. The mining exposed underground pyrite-bearing ores which are a major source of AMD in addition to the potential diffuse seepage from the tailings storage facilities and slimes dams.

When these pyrite deposits are exposed they undergo oxidation and hydrolysis to produce sulfate, ferrous iron and hydrogen ions (Equation 1). Natural bacteria can substantially increase the rate at which acid is generated (Akcil & Koldas, 2006).

$4FeS_2 + 14O_2 + 4H_2O \rightarrow 4Fe^{2+} + 8\ SO_4^{2-} + 8H^+$ *Equation 1*

Mass inputs of these by-products into aquatic ecosystems over as little as a month cause significant hydro- and geo-chemical changes including acidification, metal precipitation, efflorescent salt formation and salinisation.

Acidification from AMD has occurred multiple times in different ecosystems; a record pH of -3.6 was measured in mining lakes beneath Iron Mountain, California (Nordstrom *et al.*, 2000). Acidification dominates several chemical responses in water and sediment. For instance, the behaviour of metals is pH dependent, with most metals (Fe, Co, Zn, etc.) becoming increasingly mobile in an acidic medium. Ferrous iron will oxidise to ferric iron provided there is sufficient oxygen, catalysing iron-oxidising bacteria and archea bacteria (Moses *et al.*, 1987; Akcil & Koldas, 2006) (Equation 2)

$Fe^{2+} + O_2 + H^+ \rightarrow Fe^{3+} + H_2O$ *Equation 2*

Once this has taken place, if the pH is above 3.5 the ferric iron will precipitate onto suspended particles and sediment as mostly insoluble $Fe(OH)_3$, also known as ‘yellow boy’ (Equation 3) (Akcil & Koldas, 2006) (Figure 6).

$Fe^{3+} + O_2 + H_2O \rightarrow Fe(OH)_3 + 2SO_4^{2-} + 4H^+$ *Equation 3*

Figure 6: 'Yellow boy' coating the riverbed of the Tweelopies River, Krugersdorp Game Reserve, Gauteng Province (2012).

The formation of insoluble ferric hydroxides from dissolved ferric iron is strongly dependent upon pH (Hem & Cropper 1959; Stumm & Lee, 1961; Brock & Gustafson 1976; Akcil & Koldas 2005). This dependency is explained by the relationship between pH and hydroxyl ions, where the concentration of hydroxyl ions strongly influences the reaction rate. It was determined by Stumm and Lee (1961) that for an increase in pH by a single unit the oxidation rate increases 100 fold (Figure 7). In a low pH environment (pH of less than 3.5) ferric iron will remain mostly dissolved and only precipitate into insoluble ferric hydroxides at a significantly low rate (Hem & Cropper 1959; Stumm & Lee, 1961; Brock & Gustafson 1976; Akcil & Koldas 2005). This explains the relationship between the concentration of dissolved iron in water and pH, and also the addition of alkaline substances, such as calcium carbonate, as an effective method used to remove dissolved iron (Akcil & Koldas 2005).

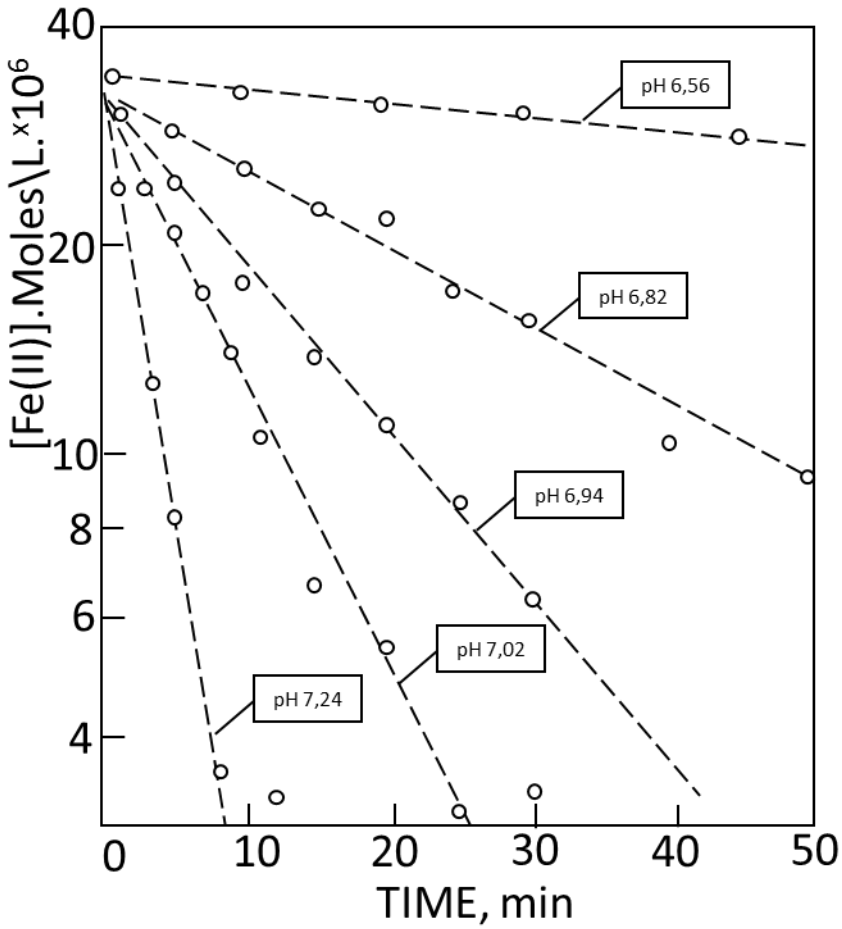

Figure 7: Oxygenation rate of ferrous iron under varying pH conditions (Stumm and Lee, 1961).

The pH of water also controls the formation of efflorescent iron sulfate salts such as melanterite ($FeSO_4 \cdot 7H_2O$) and copiapite ($Fe^{2+}Fe^{3+}4(SO_4)6(OH)_2 \cdot 20H_2O$). These generally form between pH of 1.0 and -3.5 on pyritic waste or dried surfaces that were in contact with AMD (Nordstrom & Alpers, 1999; Nordstrom, 2011). Gypsum ($CaSO_4 \cdot 2H_2O$) is a salt that may also cover contaminated environments (Nordstrom & Alpers, 1999) where interaction of the water with limestone or dolomite takes place, however it is readily dissolved in water (Figure 8). Of note; salt formation in the study area had been observed in a previous study (Olsen *et al.*, 2012).

Sulfate concentrations are high in these salts and before precipitation the dominant source of high salinity in AMD-contaminated ecosystems. The record high sulfate concentration was measured at 760 g $SO_4.L^{-1}$ under Iron Mountain, California (Nordstrom & Alpers, 1999; Nordstrom *et al.*, 2000). This concentration exceeds that

of pristine South African rivers by ~3800 times (DWAF 1996). In 2012 the dissolved sulfate concentration in the Tweelopies River was 1.97 $g.L^{-1}$, 117 times greater than an unaffected spring in the area (Olsen *et al.*, 2012).

Total dissolved iron and sulfate loads in the river are generated directly from pyritic oxidation (Equation 1) and, as there are no other large sources of iron and sulfate present, are representative measurements of AMD contamination which is why these two components were chosen as the focal elements examined. However, dissolved sulfate can transform into solid phase sulfide mineral compounds, as well as sulfate mineral compounds, therefore total sulfur was focused upon in the sediment component of the study.

1.3.3 Mechanisms driving the chemical transformations of species of iron (ferrous and ferric iron) and sulfur (sulfate and sulfide).

The mechanisms facilitating storage/remobilisation of contaminants explain trends in the time series taken and are therefore important to address. Decomposition of AMD-coated organic matter collected by the dam is a potential conduit by which dissolved iron and sulfate in the dam can be remobilised. Removal of dissolved iron occurs via the formation and precipitation of ferric iron – which is dependent upon pH and oxygen availability. The removal of dissolved sulfate is linked to co-precipitation with iron. These processes are discussed in-depth below.

1.3.3.1 Biologically induced changes to water quality in a dam ecosystem

Photosynthesis and decomposition will take place in a dam (Boehrer & Schultze, 2008). Aerobic and anaerobic decomposition by sulfate- and iron-reducing bacteria (SRBs and FRBs) and sulfide-oxidising bacteria (SOBs) are of primary interest to this study due to their chemical transformations of AMD-contaminants.

In an AMD-contaminated river organic debris is coated in iron hydroxide, iron oxides and metal sulfides (this ‘yellow boy’ and often coats the riverbed in an orange colour) (Figures 6 and 8).

The decomposition and oxidation of this material by bacteria wanting to gain energy and nutrients for protein formation inadvertently releases these contaminants from the debris, either for the bacteria's use or into the water as a by-product (Boehrer & Schultze, 2008).

Figure 8: Salt formation on vegetation in the Tweelopiespruit, Krugersdorp Nature Reserve, Gauteng Province (photo: D. Furniss, 2012).

1.3.3.1.1 Sulfate reducing and sulfide oxidising bacteria

Sulfur is a non-metal chemical element that is abundant in the natural environment, and occurs in multiple species, and minerals. The species of sulfur that are relevant in the context of this study include elemental sulfur (S^0), sulfide (S^{-2}) and sulfate (SO_4^{2-}). These species are key focus points in the context of this study, and the quantification of total sulfur in the sediments and dissolved sulfate in the dam form the basis upon which the key questions and aim of the study are answered and met.

Sulfide minerals include pyrite (FeS_2) which is a metal ore and a source from which acid mine drainage is generated, as described in section 1.3.2 above. Most metal sulfides have a very low solubility in water, whereas metal sulfates, such as gypsum are soluble in water (Brown, 2009). Therefore, the formation of sulfide

minerals in an aquatic ecosystem is a mechanism by which the concentration of dissolved sulfate can be removed. Furthermore, sulfide also occurs as hydrogen sulfide, which is a naturally occurring gas. There is a significant amount of scientific literature that indicates that sulfate-reducing bacteria use sulfate as an energy source in order to decompose organic material, and hydrogen sulfide forms as a by-product. Therefore, sulfate-reducing bacteria have the potential to remove dissolved sulfate (Herlihy & Mills, 1985; Machel, 1989; Baker & Banfield, 2003). This is discussed in more detail below.

Organic decomposition is primarily be facilitated by sulfate reduction in anoxic freshwater environments, but only where high concentrations of sulfate are present (Herlihy & Mills, 1985). Sulfate reduction refers to the process whereby SO_4^{2-} is reduced (i.e. loses an electron) to sulfide (i.e. H_2S, and HS^-) (Machel, 1989) (Equation 4). Anaerobic sulfate-reducing bacteria oxidize organic compounds that often accumulate in dams to gain energy and for the production of amino acids, in doing so they reduce sulfate to hydrogen sulfide. Most sulfate reducing bacteria are obligate anaerobes (Nicholas, 1967) and, because using oxygen yields a greater energy gain, most sulfate reduction happens only in an environment where oxygen has already been depleted such as bottom sediment in a dam. In oxygen-rich environments aerobic respiration will outcompete anaerobic respiration.

$$2CH_2O + SO_4^{2-} + 2H^+ \rightarrow 2CO_2 + H_2S + 2H_2O \qquad \textit{Equation 4}$$

Several sulfate-reducing bacteria (SRB) are closely associated with acid mine drainage. *Acidithiobacillus* spp. and *Thiobacillus* spp. are the most common, producing hydrogen sulfide in anoxic environments (Baker & Banfield, 2003). When hydrogen sulfide comes into contact with metals (such as iron, manganese and zinc) it forms insoluble metal sulfides (Herlihy & Mills, 1985; Webb *et al.*, 1998) (Equation *5*). Metals oxidized by oxygen can oxidize sulfides too (Luther *et al.*, 2011).

$$M^{2+} + S^{2-} \rightarrow MS\downarrow \qquad \textit{Equation 5}$$

(M^{2+} is a positively charged metal ion)

Hydrogen sulfide can react with oxygenated water (either near the surface or deeper from groundwater influx) to form sulfate (Herlihy & Mills, 1985), exit the water as a gas or form metal sulfides. In the case of the former, one can state that sulfate is ‘remobilized’ to sulfate from the sediment into the surface water. As organic

material will often contain many species of the element sulfur – an essential element – this natural source of sulfur adds to sulfur loads in dams and can be enhanced under certain conditions. Increased deposition of organic debris into a dam from a high rainfall event for instance, has been shown to enhance sulfate reduction and the production of hydrogen sulfide in anoxic lake environments (Gray, 1998; Dabrowski *et al.*, 2013). Organic material is likely to contain higher amounts of sulfate in an AMD-contaminated system than in a pristine river and therefore has the potential to be a greater conduit of sulfate, or metal sulfides or hydrogen sulfide, than in a pristine system. Organic material in a river impacted by acid mine drainage is a well-known material to which iron- and metal-sulfides and sulfates adsorb (Gray, 1998). Therefore, sulfate reduction in dams (which accumulate organic matter and often have anoxic bottom sediments) can serve as a mechanism by which dissolved sulfate and iron are removed from the water.

Conversely, bacteria can also oxidise sulfide minerals and hydrogen sulfide into elemental sulfur, and sulfate (Dunn, 1997; Friedrich *et al.*, 2001). The oxidation of hydrogen sulfide and metal sulfides such as pyrite, into sulfate can also occur naturally without bacterial activity (Luoma & Rainbow, 2011). Multiple studies show that metal sulfides form and precipitate onto the bed, banks, and suspended organic matter in aquatic ecosystems (Boerher & Shultze, 2008; Luoma & Rainbow, 2011) and this is also evident in a visual analysis of an AMD contaminated aquatic resource (Figure 6). Therefore, the organic matter collected in the dam may have a significant potential to remobilise dissolved sulfate.

In the context of this study the formation of metal sulfides, and the reduction of sulfate into hydrogen sulfide by sulfate-reducing bacteria are mechanisms by which the concentration of dissolved sulfate in an aquatic ecosystem can be lessened. Conversely, bacterial oxidation of sulfide minerals, and the oxidation of hydrogen sulfide, represents mechanisms by which dissolved sulfate can enter an aquatic ecosystem.

1.3.3.1.2 Iron precipitation and iron-reducing bacteria

Iron-reducing bacteria will outcompete sulfate-reducing bacteria for organic substances and hydrogen ions in acidic sediments and where there are high

concentrations of ferric iron (Fe^{3+}) (Küsel *et al.*, 2001). Reduction of iron occurs where organic material is used as a reducing agent by iron-reducing bacteria (FRBs) (Equation 6 (Boehrer & Schultze, 2008)).

$$CH_2O + 4Fe(OH)_3 + 8H^+ \rightarrow CO_2 + 4Fe^{2+} + 11H_2O \qquad \textit{Equation 6}$$

The speciation of iron in freshwater is highly dependent upon pH, temperature and oxygen availability (Figure 9). In the presence of oxygen and high pH conditions, iron generally precipitates as insoluble ferric hydroxide. Under low pH and anoxic conditions, iron exists predominantly in the soluble ferrous iron (Fe^{2+}) form. In fact adding an alkaline inducing agent (such as lime, calcium carbonate, sodium hydroxide etc.) is commonly used in AMD remediation as it increases the pH and results in the removal of iron (and other metals) from the water through precipitate formation (Johnson & Hallberg, 2005).

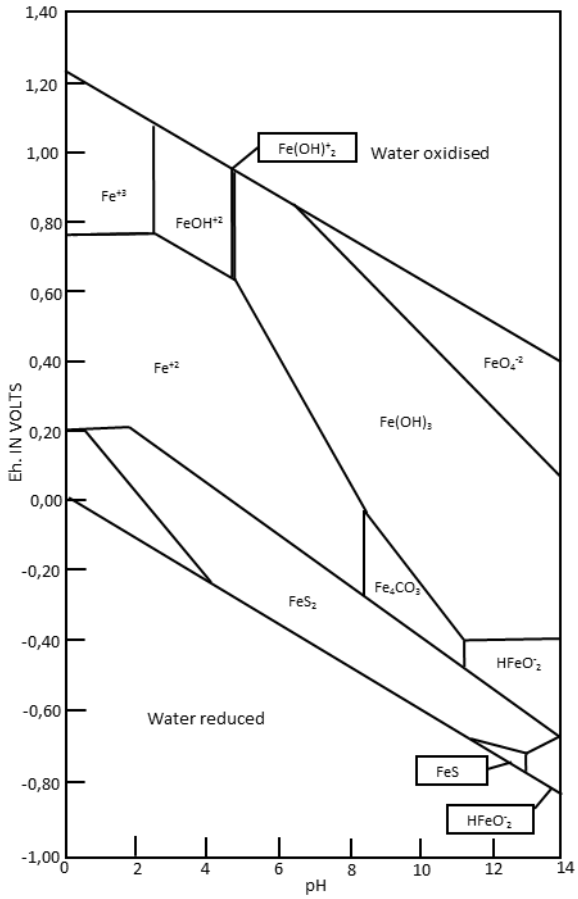

Figure 9: Solubilisation of iron as a function of pH and oxidation-reduction potential (Hem, 1975).

Of note, during low pH conditions (2.8 – 4.5) the ferric hydroxide precipitate is predominantly swertmannite ($Fe_8O_8(OH)6SO_4$) and at 2.6 it is jarosite ($KFe^{3+}3(OH)_6(SO4)_2$), whereas at 6.5 or higher pH conditions, the ferric hydroxide tends to be ferrihydrite ($FeHO^8$) and goethite (FeO(OH)) (Luoma & Rainbow, 2011) So during low pH conditions iron precipitation removes more sulfate from the water than under high pH conditions. However, as stated previously, the formation of iron hydroxides in a low pH environment is significantly slowed, and at a pH less than 3.5 ferrous and ferric iron will precipitate at an extremely low rate (Hem & Cropper 1959; Stumm & Lee, 1961; Brock & Gustafson 1976; Akcil & Koldas 2005) (Figure 9).

Kindly note that iron-oxidising bacteria are discussed as part of the oxidation of pyrite and the formation of AMD in section 1.3.2 above.

1.3.3.2 Aeration

As discussed in the above section – iron will oxidise and precipitate above pH 3.5 conditions where oxygen is present (Equation 3). Aeration is a commonly used remediation option to remove iron from AMD effluent (Kirby *et al.*, 2009). Waterfalls are natural vehicles for aeration and saturate the water flowing over them with oxygen. The water exits the study dam solely at the top with a drop of ~8 meters (Figure 10). Therefore, the dam wall might be affecting iron speciation and precipitation of the water flowing over it. A 2012 study on the influence of waterfall aeration on iron attenuation in a low pH (2.7-3.0) river contaminated with AMD (Chen & Jiang, 2012) found that a waterfall increased the rates of iron oxidation and precipitation by two orders of magnitude throughout the year (except during high flows in winter where the precipitation rate of iron was even more enhanced), and that the concentrations of ferrous and ferric iron were three to eight times lower after the waterfall section (Chen & Jiang, 2012).

Figure 10: Dam wall of the Charles-Fourie Dam, Krugersdorp Game Reserve, Gauteng Province (2013).

1.3.4 Natural conditions affecting seasonal and annual contaminant retention or release mechanisms

1.3.4.1 Heavy rainfall

Dams and lakes are traditionally depositional systems (as opposed to sediment carrying rivers). During flood/high flow events in a river large amounts of suspended material are commonly recorded (Meade, 1982; McCully, 1996; Boehrer & Schultze, 2008). Thus during flood events high amounts of organic material may collect in the dam and increase releases of dissolved sulfate and iron via decomposition for the short or medium future.

Heavy rainfall can also create turbidity currents – where fine particles are carried along a river bottom at an increased velocity. Upon reaching the dam, these

currents increase mixing between the sediment-water interface and can potentially release stored contaminants (Cesare *et al.*, 2001).

Rain/fresh water is less dense than AMD contaminated surface water and therefore direct rain and runoff may create a thin layer of less dense surface water in the dam (Alavian *et al.*, 1992).

1.3.4.2 Groundwater flux

Net groundwater gain will affect the water quality coming out from an AMD contaminated dam, through either dilution or increased contamination (should it be more polluted). The differences in salinity, and turbidity, from groundwater entering the dam and the water residing in it can create or increase mixing. The extent of mixing depends upon the net volume gained, as well as how the groundwater enters the dam – at one or many points. Mixing from below is likely to increase the release of contaminants from the sediments into the surface water via mixing. Aside from this – should the groundwater be oxygenated and/or carrying SO_4^{2-} when it enters the dam then this will induce a peak in sulfate levels (Herlihy & Mills, 1985). Oxygenated groundwater entering an anoxic, high pH environment will cause ferrous iron to precipitate onto suspended particulates or bedrock removing it from the water.

1.3.5 A review of mass balance models and applications in the field of acid mine drainage research.

A mass balance of all inputs and outputs of dissolved sulfate and iron into and from the dam was used to assess the accumulation of dissolved sulfate and iron in the dam. The calculation also included an integrated water balance, and is detailed in section 2.1.3.3 of the methods below. The following information presents background, context and motivation for use of the mass balance model that was developed for this study. (For further information on the need, desirability and importance of the study, kindly refer to the previously mentioned rationale in section 1.1 of the literature review).

A mass balance, also known as a material balance and budget calculation, is a model based on the conservation of mass, whereby accounting for material

entering and exiting a system allows for the indirect determination of unquantified mass flows or fluxes. The premise for a mass balance is the law of conservation of matter which states that all matter is neither created nor destroyed. The underlying application of this is that if the mass fluxes from different reservoirs or pools are known except one, then the remainder of the sum of the mass fluxes quantifies the unknown mass flux.

Mass balance calculations are well established methods used to determine chemical transport between and storage within different pools and reservoirs (Diamond, 1995; Runkel & Kimball, 2002; National Research Council *et al.*, 2005; Luoma & Rainbow, 2011). An example of a mass balance application is the determination of a pipe leak, where the difference in the mass of the water at the start of the pipe and at the end of the pipe represents the mass of water leaked. This would otherwise be practically difficult and costly to measure. The use of mass balances in research into acid mine drainage was investigated as part of the literature review. Although a significant amount of literature could be found on the use of mass balances in streams, the use of a mass balance in a dammed river contaminated by AMD could not be found, which highlights the importance of the study in the context of the available scientific literature.

Yu (1998) used a mass balance model to estimate the dilution and removal of pollutants in a stream polluted by AMD. Yu estimated the precipitation fractions of the most probable compounds formed by total iron, sulfate, and aluminium at different points in the stream, as well as the dilution factor of a perfectly conservative pollutant, and determined the removal rates of the pollutants. Yu highlighted that a mass balance approach can also be used to find unexpected inputs of pollutants into a stream. Although Yu takes a different approach to the one presented in this study, the same constituents, namely dissolved sulfate and total iron, were used. This study also incorporated the dilution potential that multiple influxes of water can have into the mass balance equation. Furthermore, the storage and remobilisation of dissolved sulfate and iron was determined with the assumption that precipitation is a mechanism by which the dam may store or acquire dissolved sulfate and iron from the Tweelopies River in various species and compounds.

Whitehead and Jeffrey (1995) developed a mass balance model in order to monitor and determine influxes of iron into the Pelenna River Catchment in the

United Kingdom. The model quantified the mass flux of iron at multiple points in the river, and after points of confluence in particular. This allowed Whitehead and Jeffrey to determine the iron load contribution from each tributary into the Pelenna River while taking into account the effect of the river's dilution. Bowman (2009) also conducted a similar iron mass balance study of the tributaries within the Upper Rush Creek Watershed in Ohio. The outcome of both of the studies enabled effective management prioritisation of the polluted tributaries, and led to an improvement in the ecological condition of the river. The study has multiple parallels with the proposed mass balance model (quantification of dissolved sulfate and total iron from an unquantified conduit), and further demonstrates how a mass balance can be used to quantify the conduit from which a pollutant is remobilised.

Bencala and Ortiz (1999) conducted a sulfate mass balance of a river in Colorado in order to determine diffuse points of contamination from groundwater in the river through an upstream-downstream site comparison. To quantify the mass flux the product of the concentration and discharge at each point in the river was used. The mass flux of the upstream site was summed with the inflow between the two sites and compared to the mass flux at the downstream site in order to determine any diffuse seeps. The mass sulfate balance was conducted using identical components and similar calculations as that proposed in this study. The quantification of net groundwater flux is in close parallel in particular.

2 METHODS

2.1 Mass balance

A mass balance model was used in order to answer key question 1 – whether the dam acts as a sink or remobilises dissolved sulfate and iron. In order to calculate the accumulation of sulfate and iron in the dam all unknown mass fluxes had to be quantified. This included the surface water entering and exiting the dam, the mass of dissolved sulfate or iron in the groundwater entering and exiting the dam, as well as the rain and dust. Due to the nature of the constituents, which exist as dissolved ions, in order to quantify the mass fluxes of each component (rain, groundwater etc. as listed above) it was necessary to quantify the concentration of the constituents in each component as well as the volume entering and exiting the dam. The following sections detail the field collections, laboratory analyses and the analytical calculations used in, or used to inform, the mass balance model. Section 2.1.3.3 details the mass balance calculation.

2.1.1 Field collections

2.1.1.1 Inlet and outlet sampling

Water samples were collected at the inlet and outlet at least once a month from September 2013 to August 2014. To assess monthly flow variability, water samples were collected daily for one week in February, April, and July 2014. Variation in flow from the start of the week until the end indicated how representative one sampling day in a month was of water quantity for the whole month. All collected water samples were stored frozen.

In situ discharge, pH and electrical conductivity (EC) measurements were taken concurrent with all water samples collected. The pH and EC were measured using a hand-held Thermo Scientific Orion 3 Star pH Portable Meter and a HANNA HI99300 meter, respectively. Buffer solutions of pH 4 and 7, and a 1413 µS/cm solution were used to calibrate the electrodes for pH and EC respectively on each sampling day. Each probe was held in flowing water at approximately 60% depth until a stable reading was obtained.

A SONTEK Flowtracker was used to measure the discharge of the Tweelopies River at the inlet and outlet of the Charles-Fourie Dam at 20 points in each river channel during each sampling period. The Flowtracker measured an averaged velocity over 30 seconds at each of the 20 points. These values were used by the software to develop and report standard error and are reported in the results. Measurement of discharge followed the USGS '6-tens' method (Hauer & Lamberti, 2011).

2.1.1.2 Groundwater sampling

Groundwater samples, groundwater pH, EC and water level measurements were collected from the nearby borehole (Figure 3) from February 2014 onwards due to delays in obtaining permission for access from the Department of Water Affairs. Fortunately pH and EC measurements in October, and water levels in September, October and November were available for the boreholes through the National Groundwater Archive (NGA) (The National Groundwater Information System, 2012).

Collection was done via a bailer consisting of a PVC pipe capped on one end attached to a weight. After depth measurement from the surface, the bailer was dropped down the borehole and consecutively moved up and down in the borehole to induce mixing for at least a minute before sample collection. This method was recommended by a Department of Water Affairs and NGA field technician (*pers. comm,* T. Moolman) due to the lack of an available purging vehicle that had already resulted in two months delay in sampling. Moolman had previously compared borehole water extracted with a purging vehicle against borehole water extracted with a bailer at this borehole and others in the area. Upon consultation Moolman indicated that in his opinion the quantified data did not differ when the two different methods were used – most likely because the aquifer lies close to the surface. The limitations of using a bailer, as opposed to purging the borehole, are discussed in the context of the results in section 4.4 below.

2.1.1.3 Sampling soluble contaminants in the dust and rain

The soluble mass of sulfate and iron in the dust and rain falling into the dam were quantified to eliminate the contaminant contributions from these sources when determining the pollutant loading of the dam.

A 15 L plastic bucket filled with de-ionized water was left on-site in a fenced area adjacent to the dam. Each month from September 2013, the water level of the bucket was recorded and a sample of water was collected (after a minute of stirring with a sterilized plastic spoon). After sampling the bucket was emptied, rinsed three times and filled with de-ionized water up to an identified level (about a third from the top to prevent overflow in case of rain). Other studies have similarly used a bucket filled with de-ionised water to collect dust (Dasch, 1985).

The water level measurement allowed for determination of the volume that was present in the bucket at the time of sampling. The water sample was analysed for iron and sulfate concentrations (see laboratory methods described in 2.2.1 and 2.2.2). Multiplying water volume by the concentration of iron or sulfate yielded the soluble mass of each present in the bucket (this included the masses from rainfall).

A rain gauge (whose funnel was of the same surface area as the bucket) was placed adjacent to the dust bucket. The gauge was designed with a curved ‘neck’ and the collection bottle was buried to minimize the influence of evaporation. Rain was collected and the volume recorded concurrently with the dust bucket measurements. Although the contaminant mass from rainfall had already been measured in the dust bucket, the rain gauge was installed as a way of measuring water quality of rainfall (to determine if rainfall or dust was the greater conduit of contaminants). The dissolved mass of sulfate and iron in the rain was subtracted from the mass in the dust bucket (which included the masses in rainfall) to determine the soluble mass of contaminants in the dust alone.

To determine the dissolved masses of iron and sulfate entering the dam the masses present in the bucket or rain gauge were divided by the surface area of those vessels and multiplied by the surface area of the dam.

2.1.1.4 Bathymetric mapping

A bathymetric survey was carried out to estimate the volume of the dam and calculate residence time/turnover rate. The GPS points recorded in the bathymetric mapping were also used to calculate the surface area of the dam – which was used to calculate daily evaporation rates (see section 2.3.1. for the calculation). The evaporation rates were quantified so that net groundwater volume could be estimated more accurately in the mass water balance. A bathymetric map was developed for reference purposes during coring and to add to the understanding of this specific dam environment (Appendix 3).

Five longitudinal, and eleven cross-sectional transects were used for bathymetry with paired GPS and depth recordings taken approximately every 5 m (Figure 11), thereafter recordings were taken approximately every 2 m around the perimeter of the dam and then for 30 minutes in a randomized manner. A Garmin Echo 100 Fish Finder was used to measure depth. Other studies have similarly used an echo-sounder to develop a bathymetric map (Moreno-Amich & Garcia-Berthou, 1989).

Figure 11: Satellite image of the Charles-Fourie Dam with overlain transects for bathymetric mapping. The orange points mark the positions where the sediment cores were extracted. The core lengths were, from left to right, a 27 cm core, 19 cm core and 8 cm core (Google Earth, 2014).

2.1.1.5 Sediment coring

Three sediment cores were extracted from the Charles-Fourie Dam, using a push corer (Aquatic Research Instruments), the core closest to the wall was the longest at 27 cm.

During coring, the boat was triple anchored and the depth to the sediment measured. The core barrel was held just above the sediment in the dam by extension rods and then pushed hard into the sediment in one fluid movement until the point of refusal. The barrel was then carefully pulled up, double capped and kept upright until extrusion could take place (Figure 12). The cores were extruded in 1 cm intervals and samples were stored frozen prior to analysis.

Figure 12: The 27 cm sediment core extracted from the Charles-Fourie Dam, Krugersdorp Nature Reserve, Gauteng Province (2014).

2.1.1.6 Monitoring dam temperature

In order to calculate evaporation from the dam, surface water temperature was recorded. The evaporation rate from the dam was calculated to improve the estimate of the net groundwater flux (described below). Two temperature loggers (Maxim iButton DS1921G loggers) were attached to the dam wall ~1 m below the water surface. Hourly measurements were recorded from September 2013 to August 2014.

2.1.2 Laboratory procedures

2.1.2.1 Iron analyses

Total dissolved iron concentrations were measured using a colorimeter (HACH DR/890 Colorimeter). The USEPA approved FerroVer Method (United States Environmental Protection Agency, 1980; Hach Company, 2013) with Ferrover Iron Reagent Powder Pillows (HACH 21057-69) was followed. The samples were filtered to eliminate interferences and the pH was adjusted to a range of 3 - 5 using sodium hydroxide (5.0 N) prior to analysis (Hach Company, 2013). Samples were diluted with de-ionized water to allow for measurement within the 0 – 3.00 $mg.L^{-1}$ iron range of the test. After dilution a Ferrover Iron Reagent Powder Pillow (HACH 21057-69) was added to the vial which was shaken. After a reaction time of three minutes the sample was measured in a DR/890 Hach colorimeter (Hach Company, 2013). The manufacturer stipulates precision of ±0.0017 $mg.L^{-1}$ and an estimated detection limit of 0.03 $mg.L^{-1}$.

2.1.2.2 Sulfate analyses

Water samples were analysed for sulfate concentrations using an unpublished (Bruyns, 2013) method and a standard spectrophotometer (MAPADA Instruments UV – 110 Spectrophotometer). This method was preferred over a less costly USEPA approved Hach colorimeter method based on the opinion that manually mixing reagents yields more accurate results than using a pre-mixed reagent (D. Drake *pers comm*). Samples were filtered with laboratory grade filter paper (47 mm 4160047, Macherey-Nagel) and those predicted to have high sulfate concentrations (namely the inlet, outlet and borehole water samples) were diluted by a factor of 50 using de-ionised water. The conditioning agent was created, consisting of 30 ml concentrated HCl added to 300 ml de-ionised water, 100 ml 95% ethanol and 75 g NaCl mixed with 50 ml glycerol until dissolved. Five millilitres of conditioning agent was added to 100 ml of diluted sample and, after the addition of approximately 5 ml of $BaCl_2$ crystals (measured in a spoon), stirred at a constant speed for one minute before immediate measurement at 420 nm.

Absorbance was plotted against a standard concentration curve (developed with Na_2SO_4 at concentrations of 2, 5, 10, 20 and 40 mg $SO_4^{2-}.L^{-1}$) to determine sulfate concentration and thereafter multiplied by the dilution factor.

A quality control test was conducted whereby one diluted AMD sample was processed six times to determine the precision of the test. The difference between the results of each replicate remained less than 1%, even after the dilution factor was taken into account.

2.1.2.3 Evaporation experiments

The evaporation calculation used (detailed in 2.1.3.1) incorporates a specific water evaporation co-efficient that was determined with pure water at room temperature. As water salinity can decrease the rate of evaporation (Brown, 2009) a self-designed comparison test was carried out for modification of the water evaporation coefficient. The evaporation rates of three water samples were each measured simultaneously 17 times over a three month period. Cylinders containing 50 ml of de-ionized water, low pH (3.1) AMD, and high pH (6.1) AMD respectively were used and exposed to constant identical conditions (30 ^{0}C, 70% humidity). Both the low and high pH samples had high salinities relative to an unpolluted river (~2400 $\mu S.cm^{-1}$ and ~1600 $\mu S.cm^{-1}$ respectively) and were sourced directly from the outlet of the dam during the sampling period.

The evaporation rate of high and low pH AMD samples and de-ionized water were compared over time. The Shapiro-Wilkinson test was used to determine the normality of the datasets compared. Parametric data were analysed with a one-way ANOVA. Non-parametric data were analysed using a Kruskal-Wallis test.

No significant difference existed between the evaporation rate in either measurements of volume or in weight, (ANOVA $F_{1,18} = 0.119$, $P > 0.05$ and ANOVA $F_{1,18} = 0.114$, $P > 0.05$ respectively) between de-ionized water, AMD with a 3.1 pH and 6.1 pH. Thus the evaporation co-efficient was used unchanged.

2.1.3 Analytical calculations

2.1.3.1 Evaporation rate

Daily evaporation rates of the dam's total surface were calculated as cubic metres per hour summed for 24 hours (Equation 7) (Daneshmand *et al.*, 2012). The daily evaporation rate used was then the average daily evaporation rate for the month in which the field sampling took place.

$$gh = e\,A\,(Xs - X) \qquad \text{Equation 7}$$

Where *gh* is the amount of water evaporated per hour ($kg.h^{-1}$), *e* represents the water evaporation coefficient (25 + 19v), *v* is the velocity of air above the water surface ($m.s^{-1}$), *A* is the surface area of the dam (m^2), *Xs* is the humidity ratio in saturated air at the same temperature as the water surface and *X* is the humidity ratio in the air.

A function detailing the maximum specific humidity of water vapour in dry air at different temperatures was calculated from the known saturation pressure of water vapour at different temperatures. The hourly temperatures of the water in the dam were then applied to this function to generate *Xs* (which did not need to be multiplied by relative humidity as it is the measure of saturated air and water is 100% saturated). Similarly, *X* was generated by inserting the ambient temperature of the air into the function to yield the maximum specific humidity of water above the dam's surface for each hour during the day – this number was then multiplied by the relative humidity of that hour.

Evaporation data were calculated hourly initially, as the meteorological readings were recorded every 10 minutes. Hourly data were summed into daily data and averaged across the month each time sampling took place for the water balance calculation. Approximately 8000 data points for wind velocity, relative humidity, maximum humidity, dam surface temperature and ambient temperature each were used, sourced from an iWeathar station approximately 1 km east of the dam. These weather measurements were a highly reliable data set as they were recorded every ten minutes throughout the study period.

2.1.3.2 Net groundwater discharge exchange

A water balance of daily volume (m^3) was used to quantify net groundwater gain or loss in the dam at each of the twelve observation points taken in the year (Equation 8).

$$Net\ groundwater\ gain = (Outlet + evaporation\ loss) - (inlet + rain) \quad \textit{Equation 8}$$

The daily volume (m^3) of rain and evaporative loss were determined from monthly data.

2.1.3.3 Chemical mass balance with an integrated water balance

A mass balance of dissolved constituents (iron and sulfate), was integrated with a water balance, and quantified the daily accumulation of the dam for each of the 12 observation points in the time series. All units were in $kg.day^{-1}$ as each input was a mass calculated as the product of the daily volume of water ($m^3.day^{-1}$) and the corresponding contaminant concentration (in $kg.m^{-3}$, where 1 $mg.L^{-1}$ was the equivalent of 0.001 $kg.m^{-3}$).

Daily dam accumulation of each of the observations was calculated as the sum of the outflow masses subtracted from the sum of the inflow masses. A conceptual diagram illustrates this where the accumulation left in the dam is the remainder after the mass of all the chemical inflows and outflows have been taken into account (Figure 13).

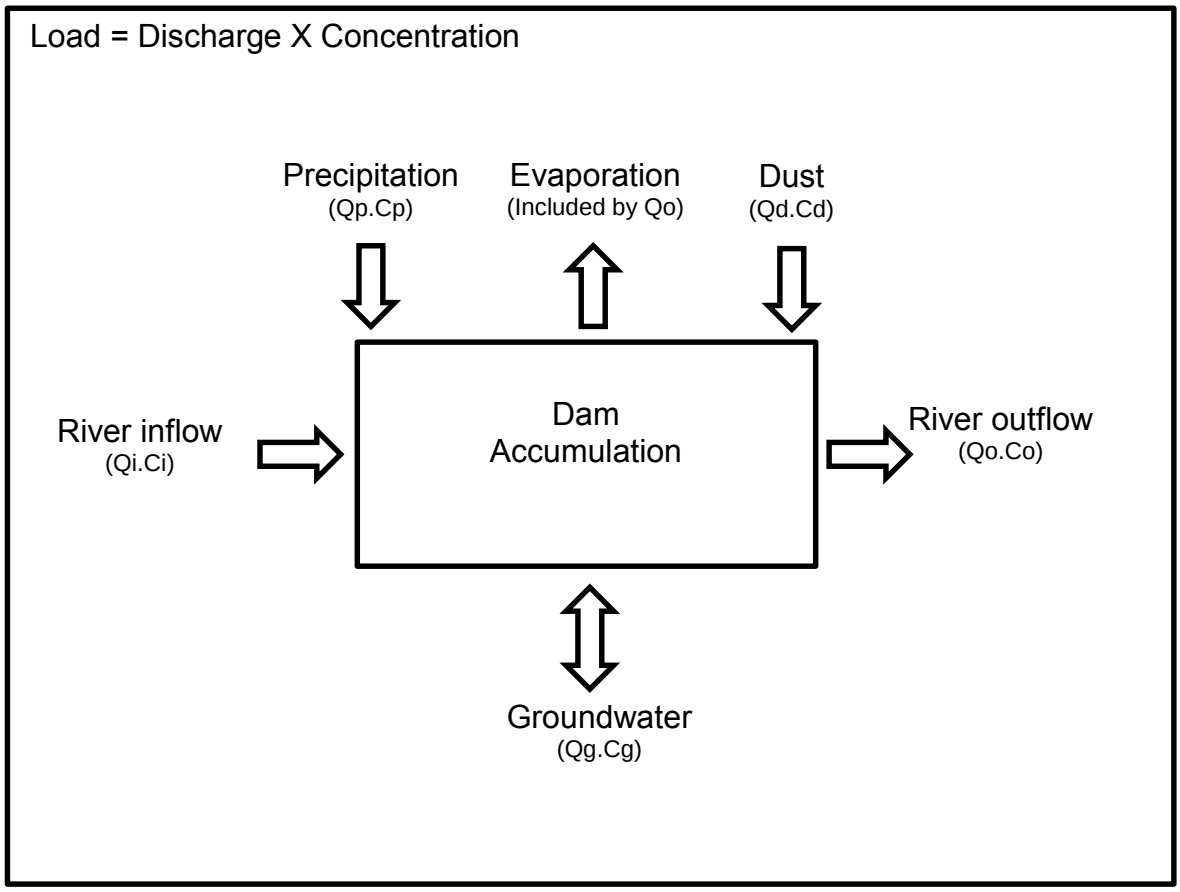

Figure 13: Conceptual influx and efflux diagram illustrating the input/inflows of chemicals via the river inlet, rain, dust and groundwater, and outflows in the form of the surface outlet of the dam and groundwater.

Input components were net groundwater gain (for the observation points where the mass water balance estimated a gain), rain, dust and the river inlet. Output components were net groundwater loss (where applicable) and surface outflow. It should be noted that the evaporative loss of discharge is inherently part of the discharge quantified for the surface outflow.

The equations below were developed based on background literature discussed in section 1.3.5 and the conceptual model (Figure 13). Equation 9 was used to calculate accumulation in the dam when there was a net loss of groundwater from the dam, and Equation 10 was used to calculate accumulation in the dam when there was a net gain of groundwater into the dam. Accumulation was negative where the outflow of mass exceeded the inflow, and the dam remobilised contaminants. Accumulation in the dam was positive where the inflow of mass exceeded the outflow mass, and the dam acted as a sink for contaminants.

$$\frac{dM}{dt} = Qi.Ci + Qp.Cp + Qd.Cd - Qg.Cg - Qo.Co$$ Equation 9

$$\frac{dM}{dt} = Qi.Ci + Qp.Cp + Qd.Cd + Qg.Cg - Qo.Co$$ Equation 10

Symbols and notations:

$\frac{dM}{dt}$: Accumulation term (kg.day^{-1}). May be a negative or positive term.

Q: Discharge of the applicable site (m^3.day^{-1}).

C: Concentration of the relevant constituent (dissolved sulfate or iron) at the applicable site (kg.m-3).

i: Denotes the surface water inflow entering the dam at the inlet.

p: Denotes precipitation/rainfall entering the dam.

d: Denotes the soluble contaminants of dust entering the dam.

g: Denotes the net groundwater flux exiting (Equation 9) or entering (Equation 10) the dam.

o: Denotes the surface water outflow exiting the dam at the outlet.

The accumulation values for each of the twelve observation points were summed in order to determine the net accumulation in the dam over the 2013-2014 study period.

2.1.3.4 Water residence time

The water residence time for the year studied was the number of days (*Tr*) taken for water to empty out of the dam if there were no inflows (Equation 11) (Bartram & Balance, 1996). Water residence time, as well as depth, indicates the likelihood of thermal stratification and an anoxic hypolimnion (Bushaw-Newton *et al.*, 2001).

$$Tr = \frac{V}{(Qo+Do)}$$ *Equation 11*

Symbols and notations:

Tr: The water residence time (days)

V: The volume of the dam (m^3) (the product of surface area and average depth).

Qo: The average daily outlet discharge (m^3.day^{-1}).

Do: The sum of diversions out of the dam. Here *Do* is taken as the average of the daily net groundwater flux over the study period (if this was negative) and evaporation.

2.1.3.5 Dam surface area relative to accumulation

In order to provide context to the accumulation of dissolved sulfate and iron from and to the dam it is necessary to place the data in the context of the dimensions of the Charles-Fourie Dam. As calculated in Section 2.1.3.4 above through the use of bathymetric mapping, the surface area of the dam is approximately 2 631 m^2. The accumulation per square meter of the dam was calculated as the accumulation divided by the surface area (Equation 12).

$$A = \frac{dM}{dt} \; X \; \frac{1}{S} \qquad \textit{Equation 12}$$

A: A measurement of the accumulation relative to the surface area of the dam (kg. day^{-1}. m^{-2}).

$\frac{dM}{dt}$: Accumulation term (kg.day^{-1}). May be a negative or positive term.

S: Surface area of the dam (m^2).

2.2 Sediment storage laboratory procedures

One sediment core was selected for detailed analysis.

2.2.1 Radiometric dating

An attempt to calculate sediment accumulation rates was done using Caesium-137 and Lead-210 radiometric dating. The use of gamma ray spectroscopy for the radiometric dating of lead and caesium is supported by the International Atomic Energy Agency (International Atomic Energy Agency, 2009). Thirteen samples were dried overnight at 110 ºC and ground to a fine powder using a pestle and mortar. Measurements of Cs-137 and Pb-210 were made by gamma ray spectrometry using a low-energy Germanium well type detector system. Total Pb-210 was determined by its emission at 46.5 keV and supported Pb-210 determination by measuring the Ra-226 activity of the sample via its daughter Pb-214 at 352 keV. Excess Pb-210 was calculated from the difference between total Pb-210 and the supported Pb-210 activity. Caesium-137 was determined using its gamma emission at 662 keV. Analysis was performed at the University of South Carolina by Dr. Claudia Benitez-Nelson.

2.2.2 Organic matter and bulk density

Bulk density was calculated by sequential weighing before and after drying 1 cm^3 sub-samples at 110 ^{0}C for 16 hours. This allowed for calculation of the water content (Abbot, 2005). Loss on ignition was then used to estimate the percentage of organic matter in sediment samples. 1 cm^3 samples were combusted at 550 ^{0}C for 16 hours (Abbot, 2005). Organic matter was then calculated using standard calculation (Equation 13).

$$\%\, Organic\ matter = \frac{Dry\ mass\ after\ 110^0\ C - mass\ after\ 550^0 C}{Dry\ mass\ after\ 110^0 C}\ X\ 100 \qquad \textit{Equation 13}$$

2.2.3 X-ray fluorescence

Ashed samples in alternating 1 cm sections of the sediment core (giving a total of 14 samples) were analysed for total sulfur and other major and minor elements using X-ray fluorescence (XRF). Pressed pellets were analysed using a Bruker S2 Ranger XRF spectrometer, following calibration against a range of local and USGS rock standards (Bruker AXS GmbH, 2013).

Concentrations were multiplied by bulk density (g/cm^3) and volume (cm^3) to calculate mass per section. Values for all core sections were summed to yield the total mass in a 13 cm core. This was divided by the surface area of the inner core barrel, and multiplied by the surface area of the dam to provide a rough estimate of the total mass of each element present in the dam sediments. This mass was then adjusted to an average sediment depth of 19.3 cm, based on the average depth of the three cores that were collected from the dam.

3 RESULTS

3.1 Water balance of the Charles-Fourie Dam

The average daily surface discharge (± SE) of water at the dam inlet was 34 081 ± 17 423 $m^3.day^{-1}$ over the 12 observation points measured, the surface outlet discharge was only fractionally higher at 34 646 ± 14 896 $m^3.day^{-1}$, while the average water input from rain and evaporative water loss were relatively lower (0.006 $m^3.day^{-1}$ and 11 $m^3.day^{-1}$, respectively) (Figure 14). Precipitation and evaporation contributed relatively little to average inflow and outflow (precipitation contributed 0.00% and evaporation 0.03%), however they were still included in the mass balance (Figures 14 and 15).

3.1.1 Surface inflow and outflow

Average monthly surface discharges were 25 985 $m^3.day^{-1}$ in September and October, and then decreased in November and December (16 639 $m^3.day^{-1}$) before increasing to 26 868 $m^3.day^{-1}$ in January and February (Figure 14). River discharge entering the dam was highest near the end of the rainfall season (from November to March) increasing by 237% from February to March (from 24 106 $m^3.day^{-1}$ to 81 328 $m^3.day^{-1}$). Average monthly discharges during the remaining dry season, from April to August, were greater (38 558 $m^3.day^{-1}$) than all other months measured except March.

3.1.2 Rainfall

The direct input of water into the dam from rainfall was calculated by multiplying the daily rainfall at the dam (where daily values were calculated from averaging monthly totals) into meters and multiplying it with the surface area of the dam. The average rain flux into the dam during the study period was 0.006 $m^3.day^{-1}$. Average rain flux was highest in March (0.02 $m^3.day^{-1}$) (Figure 14) and the wettest period of the study was clearly defined as December to March. No rainfall occurred in June or July, and the driest period of the study was from April to September (where a dry season is defined by months with less than 60 $mm.m^{-2}$ rainfall and a wet season vice versa (Chen & Chen, 2013)).

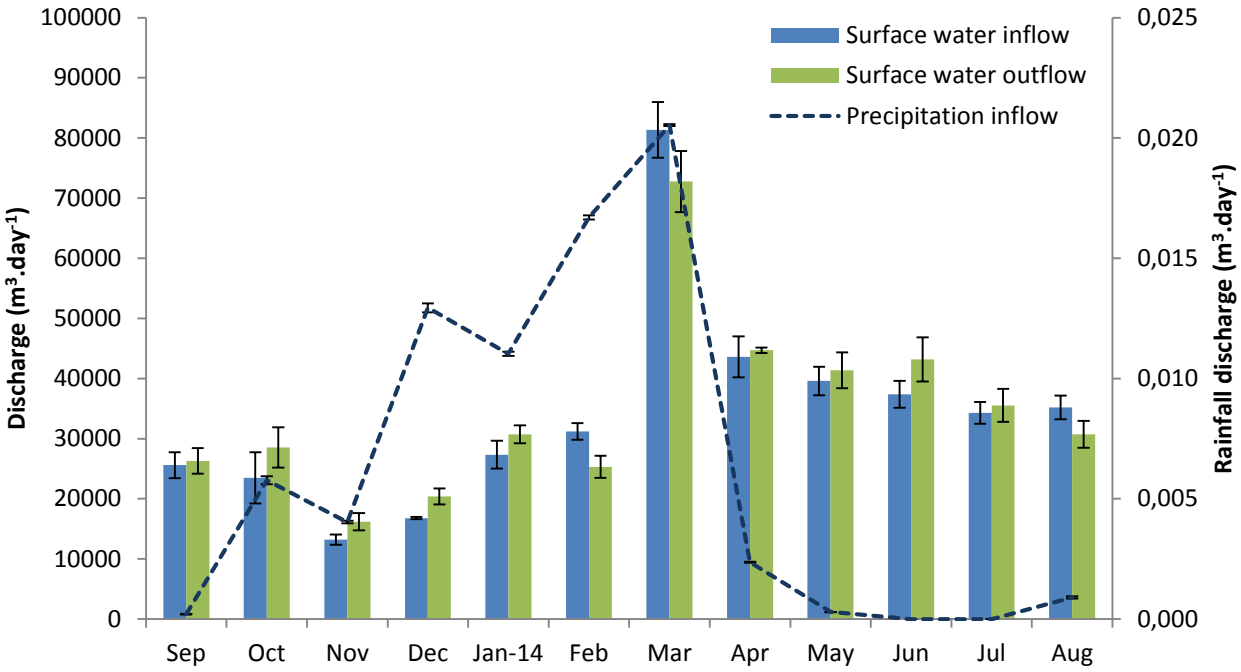

Figure 14: Fluxes ($m^3.day^{-1}$) for surface inflows and outflows with standard error of discharge, and rainfall with standard error in the Charles-Fourie Dam for 12 observation points measured over a year.

3.1.3 Daily evaporation from the Charles-Fourie Dam

The average evaporation rate from the Charles-Fourie Dam was 11.4 ± 2.5 $m^3.day^{-1}$. The highest evaporation rate was 30 $m^3.day^{-1}$ in August 2014, followed by 27 $m^3.day^{-1}$ in September 2013 (Figure 15). The lowest evaporation rate was recorded in October at 0 $m^3.day^{-1}$ due to a combination of high relative humidity (76%), wind velocity (4 $m.s^{-1}$) and low water temperature (14.5ºC) at the site (Appendix 1). The wind velocity in October was slightly below the average measured during the study period (2.9 $m.s^{-1}$), while the water temperature was slightly above the average water temperature (16.3ºC) (Appendix 1).

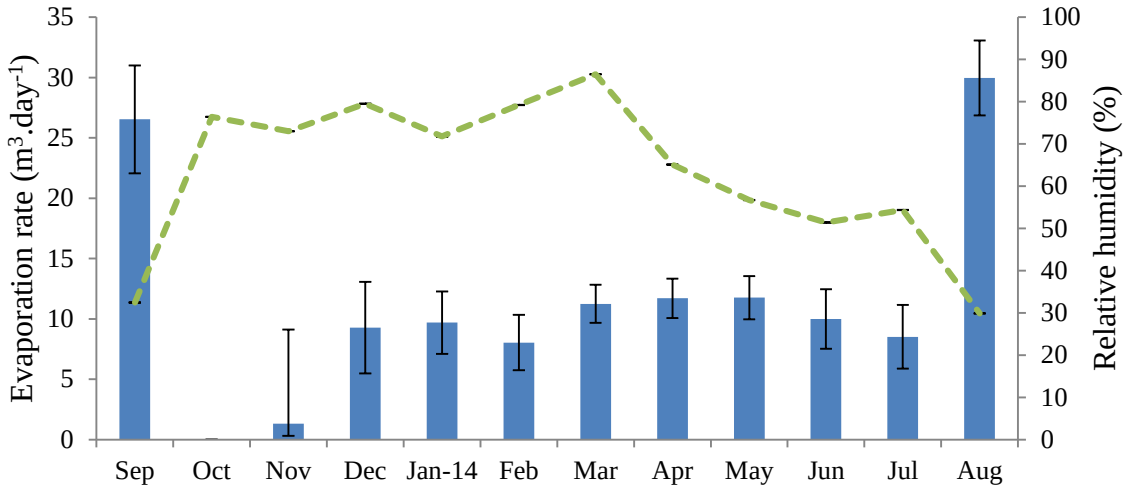

Figure 15: Daily averaged evaporation rates ($m^3.day^{-1}$) and relative humidity (%) in the Charles-Fourie Dam from September 2013 to August 2014. The bars represent the evaporation rate, and the dotted line the relative humidity.

3.1.4 Net groundwater flux

The average outflow discharge from the Charles-Fourie Dam (including surface flow and evaporation) was greater than the inflow (which included surface flow and rain), indicating an average net groundwater gain of 553 $m^3.day^{-1}$ and a total gain of 6 638 m^3 over the twelve observation points. From September to January and April to July there were positive net groundwater fluxes into the Charles-Fourie Dam. In February and March (at the end of the rainfall season) as well as in August (in the dry season) there were net losses of water from the Charles-Fourie Dam to the groundwater. The highest net groundwater gain occurred in June (5 796 $m^3.day^{-1}$), while the highest net groundwater loss occurred in March (8 591 $m^3.day^{-1}$).

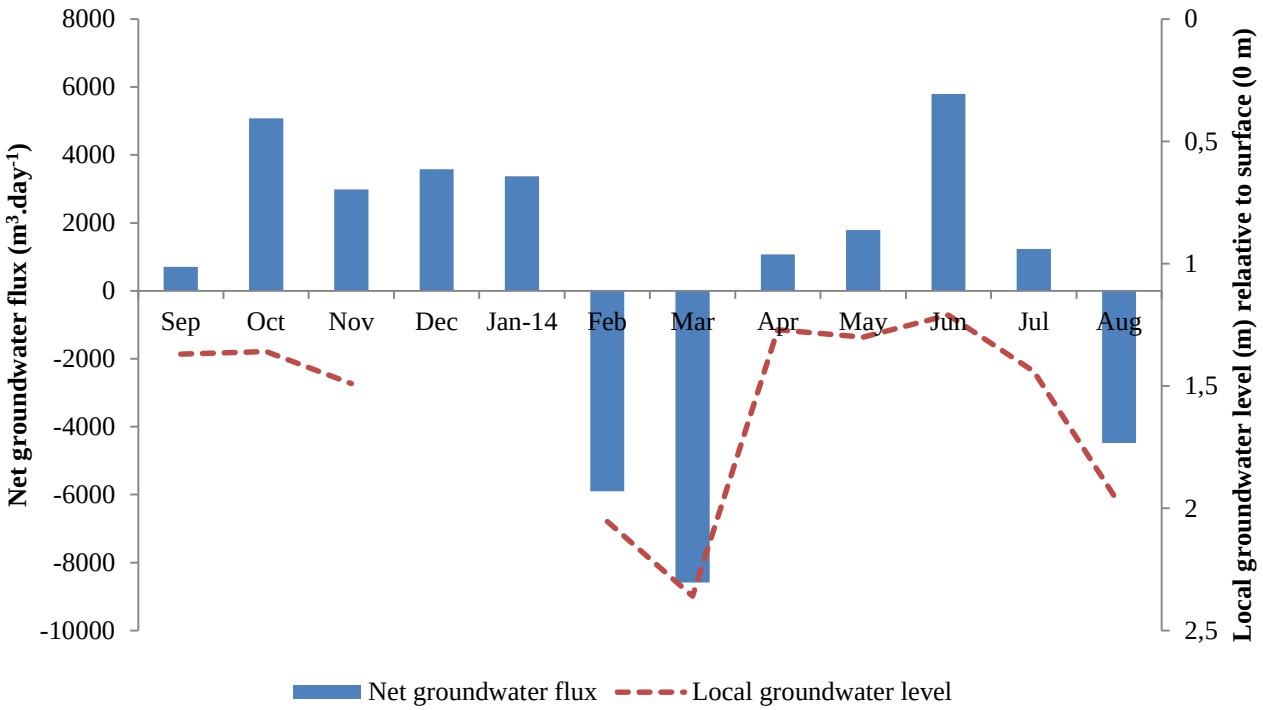

Figure 16: Net groundwater flux ($m^3.day^{-1}$) and borehole water level measurements (m) calculated from a water balance of the Charles-Fourie Dam for 12 observation points measured over a year. The borehole water level values from September 2013 to January 2014 were obtained from the National Groundwater Archive (The National Groundwater Information System, 2012).

Trends in net groundwater flux appear to follow variations in local groundwater level. In February and March a net loss of groundwater was calculated and this corresponds with a lower water level in the borehole (Figure 16). During July and August there was a clear decrease in the water level of the borehole, corresponding to a decrease in the net groundwater flux of the dam.

3.1.5 Daily surface inflow and outflow discharge

Although the rainfall season began in September and ended in March, 71% and 54% increases in the discharge occurred at the inlet and outlet respectively, between the intensive measurement period in February and April. These data were linked to changes in rainfall and groundwater recharge regimen. The rainfall in April was five times less than in February (0.002 $m^3.day^{-1}$ vs. 0.01 $m^3.day^{-1}$) but there was

a net gain from groundwater (5 901 $m^3.day^{-1}$) in February and a net gain from groundwater in April (1 077 $m^3.day^{-1}$) into the Charles-Fourie Dam. Therefore, net groundwater flux is assumed to have had a significant influence on changes in discharge during this period.

A decrease in the discharge measured occurred between the intensive sampling period in April and July at both the inlet (28% decrease) and the outlet (25% decrease) of the Charles-Fourie Dam. Net groundwater flux was similar in April (1 077 $m^3.day^{-1}$) and July (1 236 $m^3.day^{-1}$), however rainfall discharge substantially differed between April (0.002 $m^3.day^{-1}$) and July (0.000 $m^3.day^{-1}$). Thus rainfall had a significant influence on changes in discharge during this period.

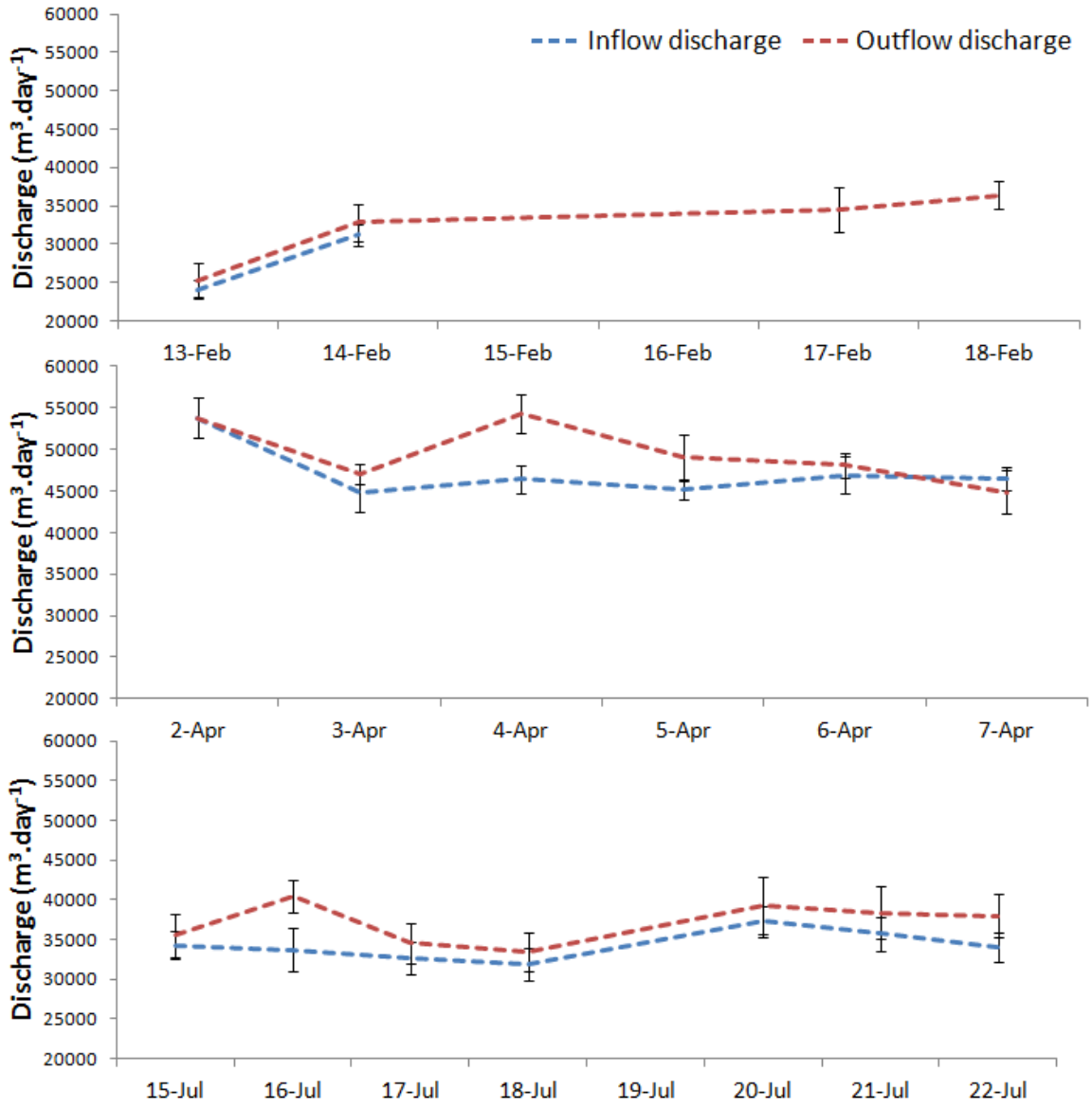

Figure 17: Daily discharge data during intensive sampling periods in February, April and July with discharge error shown.

Between 13 and 14 February surface inflow and outflow discharges increased by an average of 30%, and between 17 and 18 February the discharge at the outlet increased by 6% although no rain fell during this period (Figure 17). Water levels in the borehole increased by 18% during this time indicating that the differences in surface inflow discharges at the surface inflows were likely from changes in net groundwater flux. The presence of hippos at the inlet prevented sampling on the 17th and 18th of February.

From 2 – 7 April discharges at the inlet and outlet decreased by 15% on average (Figure 17). The only rainfall that fell during the sampling period in February

and April was 15.5 mm on the 4th of April. However, the surface discharge data on the 4th of April appear similar to other data in this period (Figure 16); thus direct runoff does not appear to have influenced the surface discharges of this period. Neither rainfall nor local groundwater flux (which increased) accounted for this decrease suggesting that a mechanism upstream influenced daily discharges (such as increased groundwater retention near the mine shaft or abstraction from the river for mining activities).

From 15 to 22 July discharges at the inlet and outlet increased by 3%, and no rainfall occurred during this period. The borehole levels changed by 0.7% during this period, thus the differences in surface flows must be attributable to slight differences in surface discharges upstream of the dam (for example the influence of upstream groundwater fluxes).

Discharge measurements were regressed for the inflow and outflow of each intensive sampling period, with the exception of inflow data for February. The inflow data for February was excluded as only two values were quantified, and thus the data were not sufficient for a regression analysis. The R^2 and p-values (Table 1) generated from the analysis indicated that the discharges on each of the sampling days were significantly different from the other (i.e. $p>0.05$).

Table 1: Regression analysis of discharges recorded at the inflow and outflow of the Charles-Fourie Dam during intensive motioning conducted in February, April and July 2014, respectively denoted "i", "o" "F", "A" and "J".

	Number (n)	R^2-value	p-value
F_o	4	0.638	0.129
A_i	6	0.068	0.307
A_o	6	0.298	0.152
J_i	7	0.015	0.344
J_o	7	-0.092	0.512

These statistical analyses show that the discharge in the river is highly variable between several consecutive days, and no one sample is representative of each sampling period. These data are important as the variation in discharge over consecutive days indicate the accuracy of measurements taken once a month.

3.1.6 Water residence time

The average depth of the dam was 2.7 m (n = 234) with a surface area of 2 631 m^2. The average daily surface outflow was 34 646 $m^3.day^{-1}$, the average daily net groundwater flux was 553 $m^3.day^{-1}$ and the average daily evaporation loss was 11 $m^3.day^{-1}$. The groundwater was excluded when calculating residence time as the total sum was positive – representing an inflow not an outflow. Based on these numbers the volume of the Charles-Fourie Dam was 7 154 m^3 and the water residence time was estimated to be ~0.2 days or 5 hours.

3.2 Constituent mass balance

3.2.1 Water quality of surface and groundwater

Dissolved constituent concentrations, pH and electrical conductivity (EC) varied widely over the study period at the inlet, the outlet and in the borehole (Figure 18). Sulfate concentrations of surface water inflow and outflow appeared to follow similar trends (except from November to December). Iron concentrations, pH and EC for surface inflow and outflow were very similar. Groundwater iron and sulfate concentrations as well as pH and EC differed from surface inflow and outflow in both trends and amounts.

The average water quality of the groundwater showed little variation throughout most of the year, except for pH which increased from 6.2 in May to 9.1 in August (Figure 18). Sulfate concentrations were on average 325 mg L^{-1}, ranging between 170 mg L^{-1} in April and 414 mg L^{-1} in March. Iron concentrations were on average 0.5 mg L^{-1}, with a minimum of 0.1 mg L^{-1} in May and a maximum of 1.6 mg L^{-1} in October. The average EC of the borehole was 696 $\mu S.cm^{-1}$ with a maximum of 824 $\mu S.cm^{-1}$ in February and a minimum of 591 $\mu S.cm^{-1}$ in August.

Trends in pH, EC, sulfate and iron concentrations of the surface waters appeared to change significantly between the months of February and March, and again in August (Figure 18). The average pH of the surface water remained low (pH of 3.2) from March to July relative to a circumneutral pH (pH of 6.7) from September

to February. Therefore, average trends in the surface water quality data will be described from the period of September to February and from March until July.

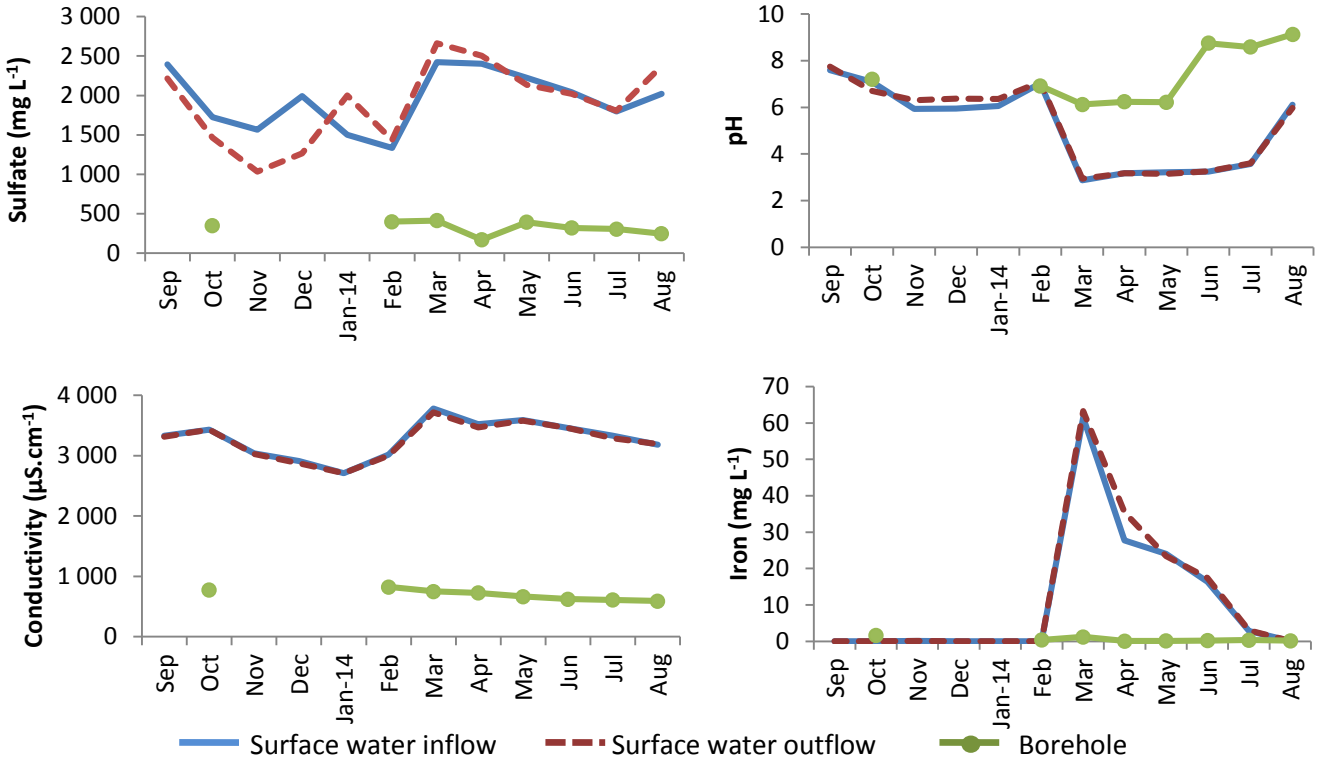

Figure 18: Concentrations of dissolved sulfate and iron, pH and EC of the surface water inflow, outflow and groundwater over the study period.

The concentration of iron in surface waters increased by 688 times from an average of 0.04 mg L^{-1} iron during September to February, to an average of 27.5 mg L^{-1} iron during March to July. These data correspond to a dramatic decrease in pH from 6.9 in February to 2.9 in March at the inlet (Figure 18). Additionally, the average concentration of sulfate and EC increased by 33% (to 2 201 mg L^{-1}) and 15% (3 520 µS.cm^{-1}) respectively between the same periods. Discharge at the inlet increased by 117% on average between the same periods.

The extreme change in water quality for all parameters measured between February and March (Figure 18) was accompanied by a visible change in the water at the inlet and in the dam (Figure 19). In March, when the pH decreased to 2.9, the water was a red-black colour with little clarity compared to the water observed prior to March (when the pH was above 6), which was a yellow-green colour with greater clarity.

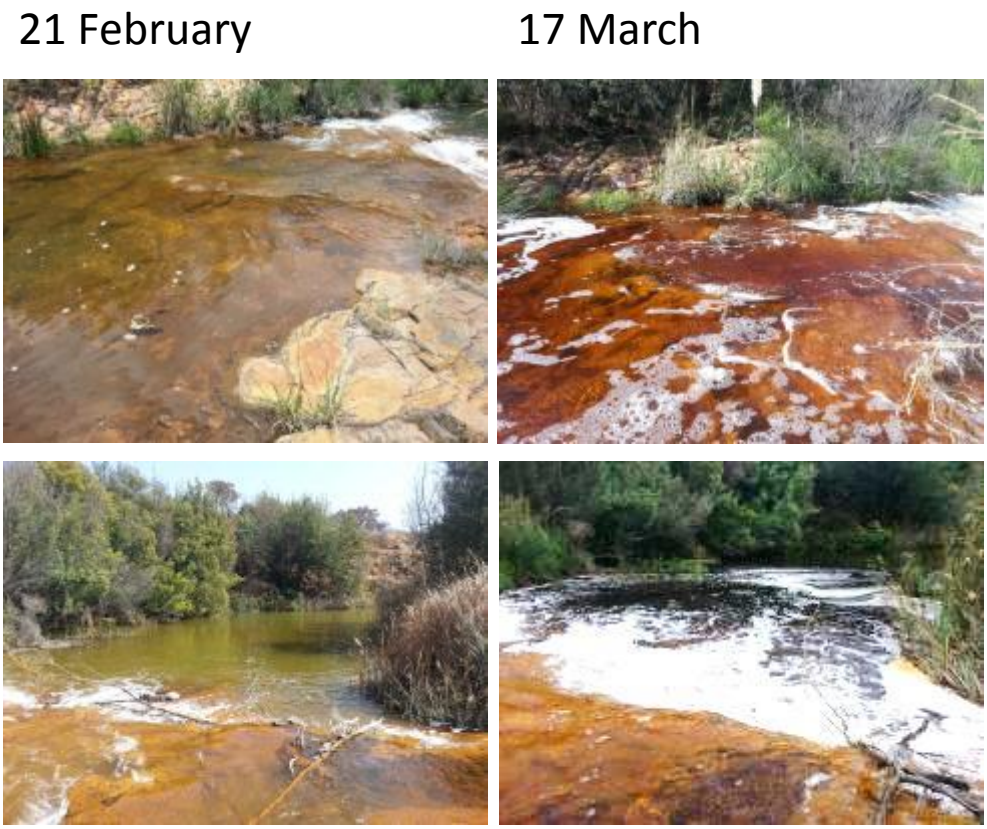

Figure 19: Colour changes in the dam inlet (top) and the Charles-Fourie Dam (bottom) on 21 February and 17 March 2014.

3.2.2 Contaminant concentrations and masses in groundwater, rainfall and dust

Contaminants were present in rainfall in very low concentrations (Figure 20) and thus contributed little to the mass balance. Sulfate concentrations in rainwater were 18 mg L^{-1} on average, with a maximum of 77 mg L^{-1} in August, and a minimum of 8 mg L^{-1} in January. No rain fell in June or July. Iron concentrations in rainwater were 0.02 mg L^{-1} iron on average, with a maximum of 0.06 mg L^{-1} in October and below detection (0.00 mg L^{-1}) in December, February, April and May. Rainwater had an average pH of 6.8 throughout the year, with a minimum of 4.96 in March and a maximum of 7.95 in January. The average EC of rainfall was 54 µS.cm^{-1}, with a maximum of 153 µS.cm^{-1} during May and a minimum of 14 µS.cm^{-1} during December.

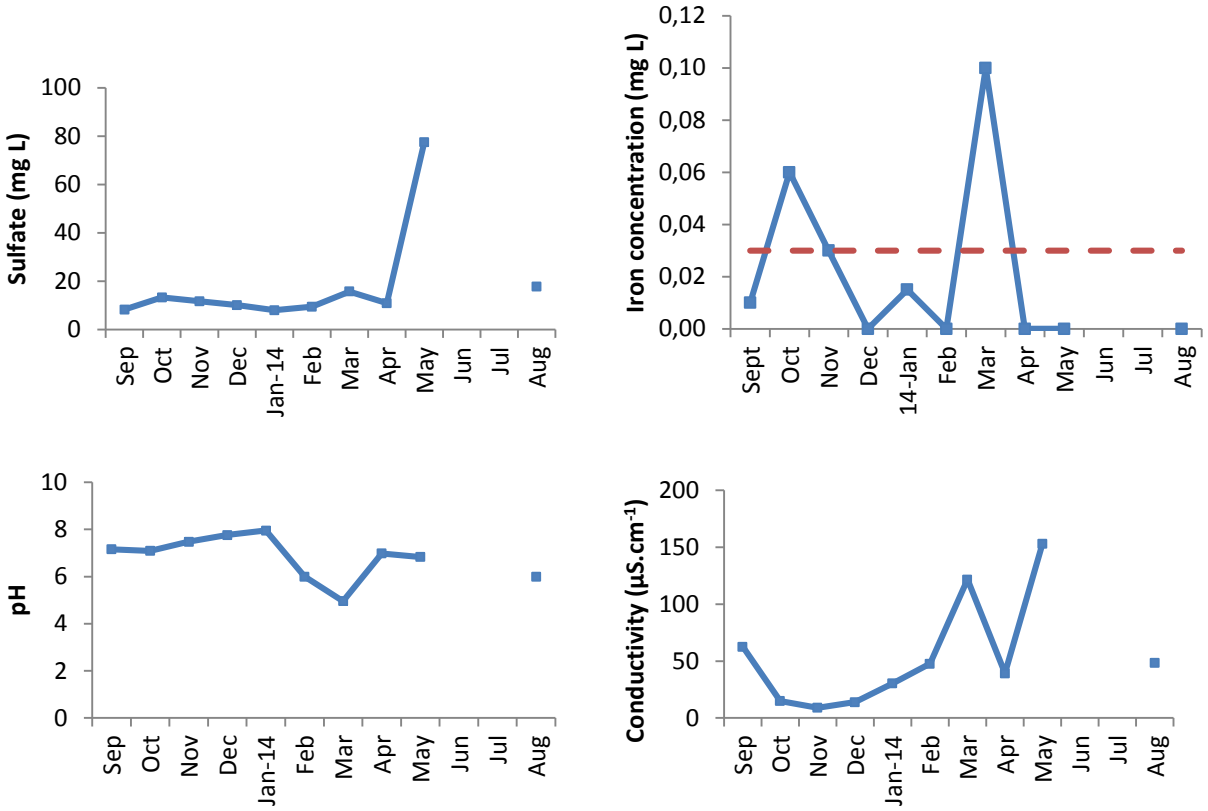

*No rainfall occurred in June and July 2014.

Figure 20: Concentrations of dissolved constituents (sulfate and iron), pH and electrical conductivity of rainfall in the Krugersdorp Game Reserve over the year studied. The dashed line denotes the detection limit for the iron concentration test (0.03 mg.L^{-1}).

Dust was characterised by very low soluble concentrations. Dust contained an average of 47.96 g SO_4^{2-}.day^{-1} and 39 mg Fe.day^{-1} across the study period (Figure 21).

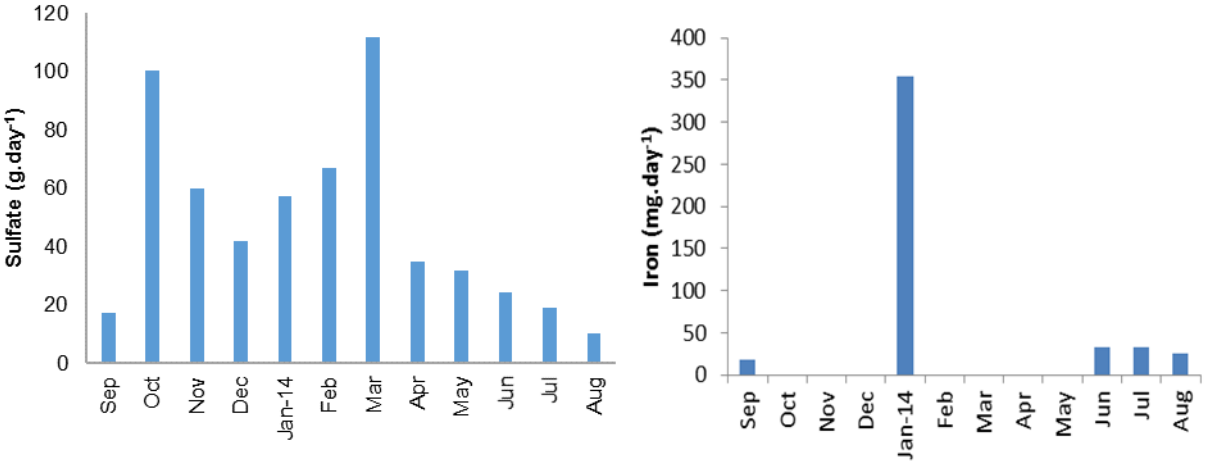

Figure 21: Mass of contaminants in dust per day, as a daily average for each month of 12 points of the year studied in the Krugersdorp Game Reserve, Gauteng Province.

Rain contained and contributed very little sulfate and iron in the mass balance constituent equation, at most a total of 0.9 g sulfate and 3 mg iron (Figures 21 and 22). The total mass of sulfate in the net groundwater exchange was 2% (11 897 kg SO_4^{2-}), compared to the total mass of sulfate in the surface outflow of the Charles-Fourie Dam in the months when groundwater was quantified (680 754 kg SO_4^{2-}).

Throughout the year, all of the observation points reported very low iron concentrations in rainwater relative to those in the surface outflow – a total of 2.688 mg Fe.day^{-1} (Figure 22). Groundwater exhibited the highest sulfate and iron concentration and discharge contribution to the constituent mass balance out of groundwater, rainfall and dust.

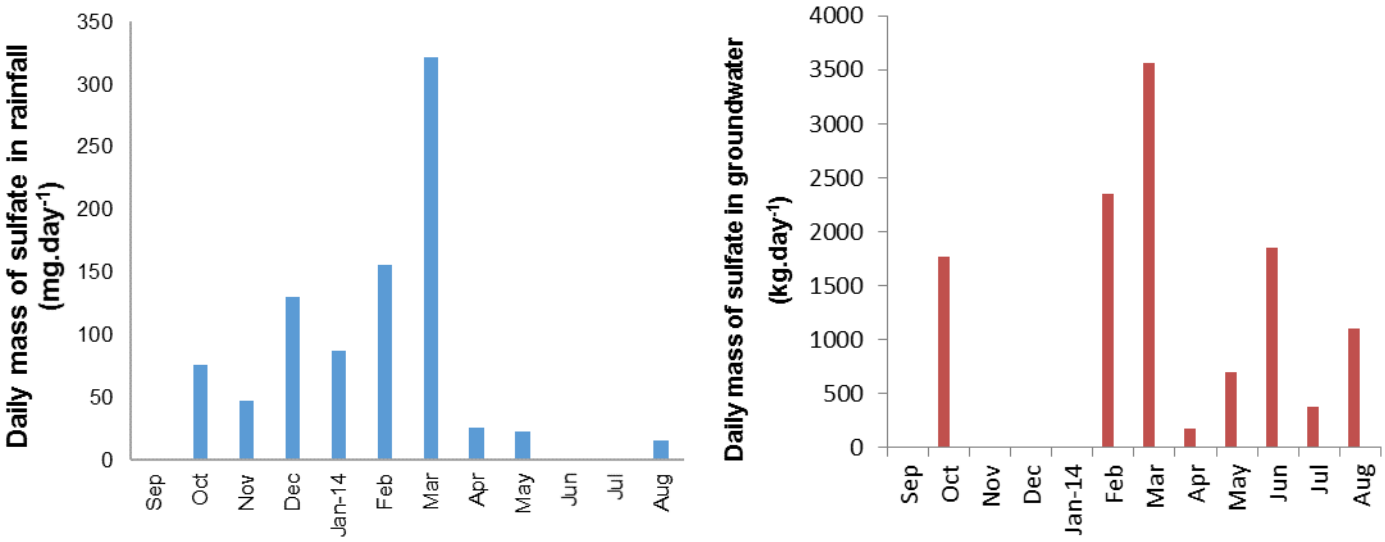

Figure 22: Mass of sulfate in rainwater (left) and groundwater (right) per month, calculated as a daily average.

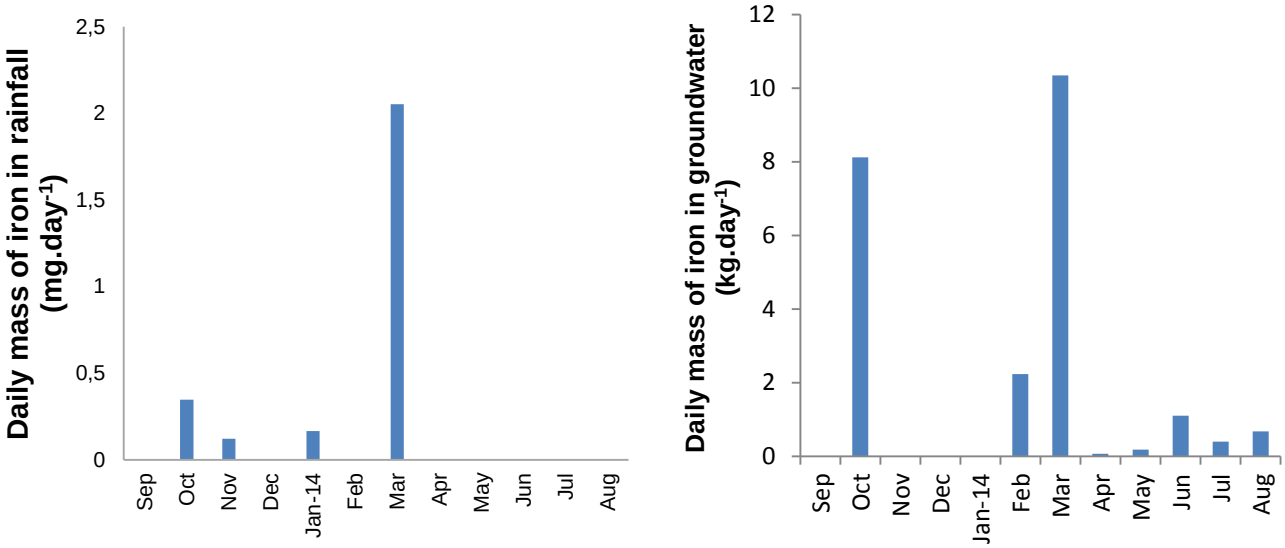

Figure 23: Average daily mass of iron in rainwater (left) and groundwater (right) per month for the 12 points of the year studied in the Krugersdorp Game Reserve, Gauteng Province.

3.2.3 Masses of contaminants retained or released from the dam

3.2.3.1 Sulfate masses

3.2.3.1.1 The Charles-Fourie Dam as a sink for sulfate

The section below details the sulfate mass flows calculated for each observation point (Figures 24 and 25), and presents the total accumulation of sulfate into and from the dam (Figure 26).

The sum of the twelve sulfate mass flows in the inlet and outlet of the Charles-Fourie Dam were 837 112 kg SO_4^{2-} and 858 854 kg SO_4^{2-} respectively over the twelve daily observation points quantified. Similarly, the total mass flows of soluble sulfate in dust, rain and groundwater were 0.6 kg SO_4^{2-}, 0.9 g SO_4^{2-} and 11 898 kg SO_4^{2-} respectively (Figures 24 and 25).

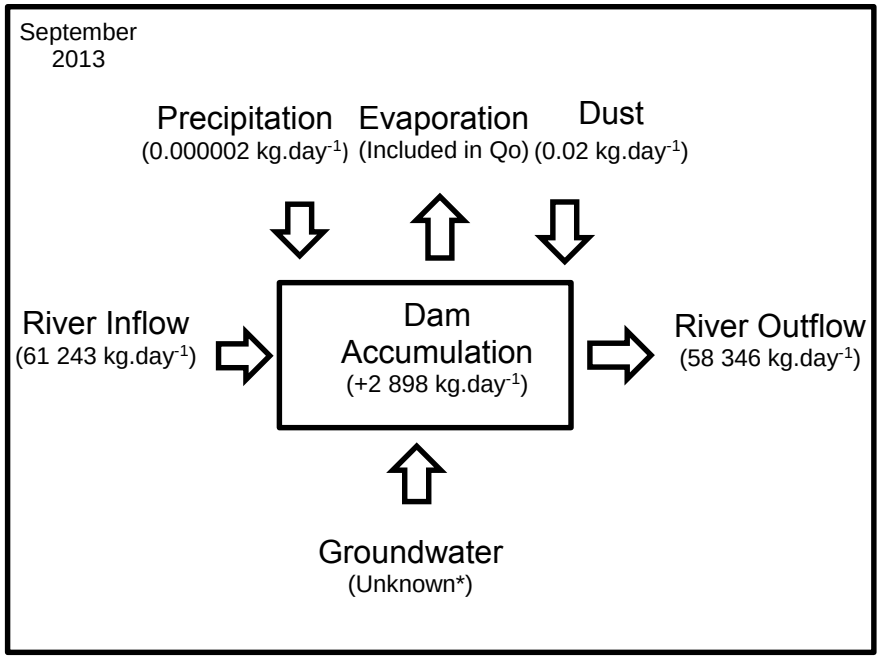
September
2013
Precipitation
(0.000002 kg.day-1)
Evaporation
(Included in Qo)
Dust
(0.02 kg.day-1)
River Inflow
(61 243 kg.day-1)
Dam
Accumulation
(+2 898 kg.day-1)
River Outflow
(58 346 kg.day-1)
Groundwater
(Unknown*)

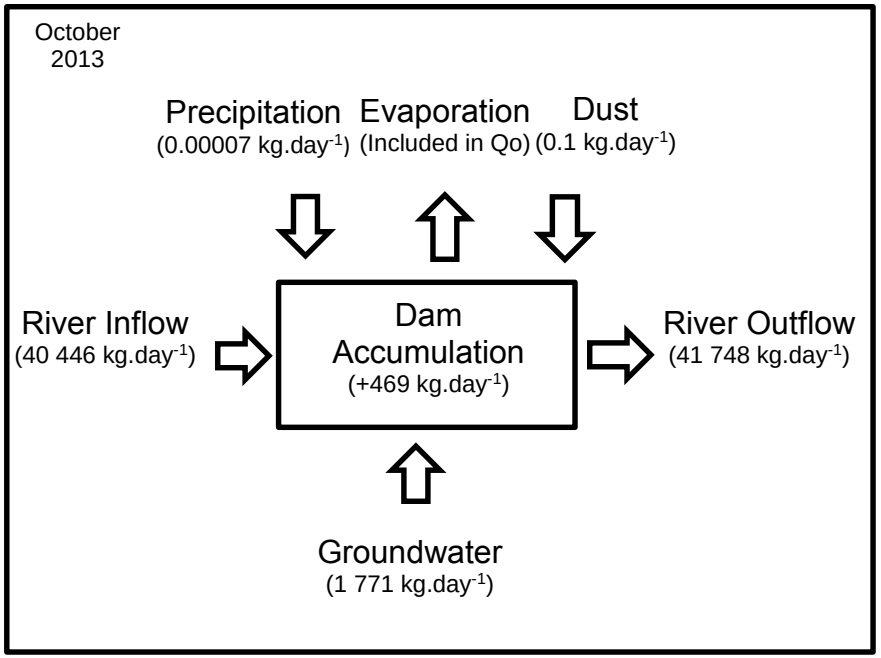
October
2013
Precipitation
(0.00007 kg.day-1)
Evaporation
(Included in Qo)
Dust
(0.1 kg.day-1)
River Inflow
(40 446 kg.day-1)
Dam
Accumulation
(+469 kg.day-1)
River Outflow
(41 748 kg.day-1)
Groundwater
(1 771 kg.day-1)

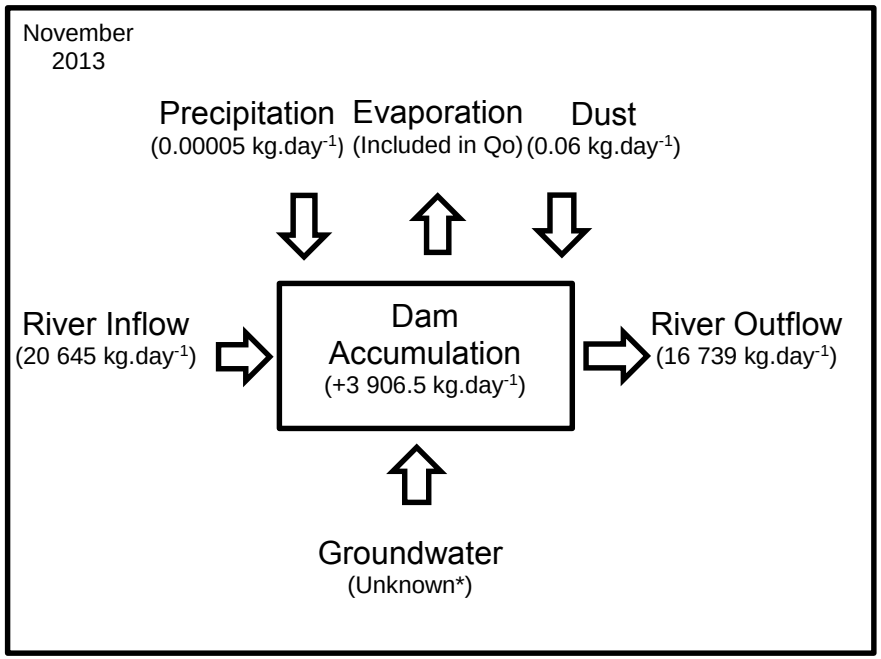
November
2013
Precipitation
(0.00005 kg.day-1)
Evaporation
(Included in Qo)
Dust
(0.06 kg.day-1)
River Inflow
(20 645 kg.day-1)
Dam
Accumulation
(+3 906.5 kg.day-1)
River Outflow
(16 739 kg.day-1)
Groundwater
(Unknown*)

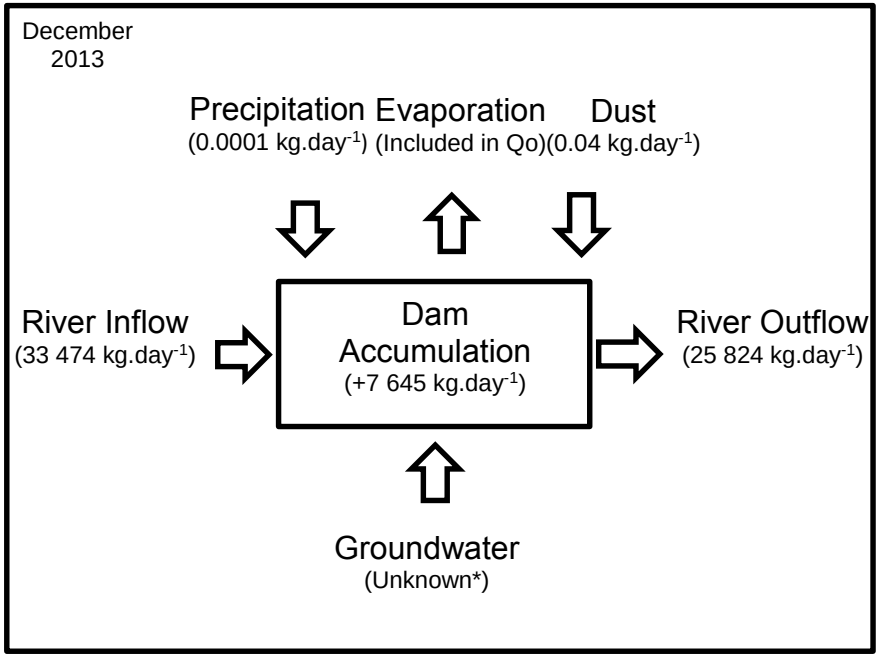
December
2013
Precipitation
(0.0001 kg.day-1)
Evaporation
(Included in Qo)
Dust
(0.04 kg.day-1)
River Inflow
(33 474 kg.day-1)
Dam
Accumulation
(+7 645 kg.day-1)
River Outflow
(25 824 kg.day-1)
Groundwater
(Unknown*)

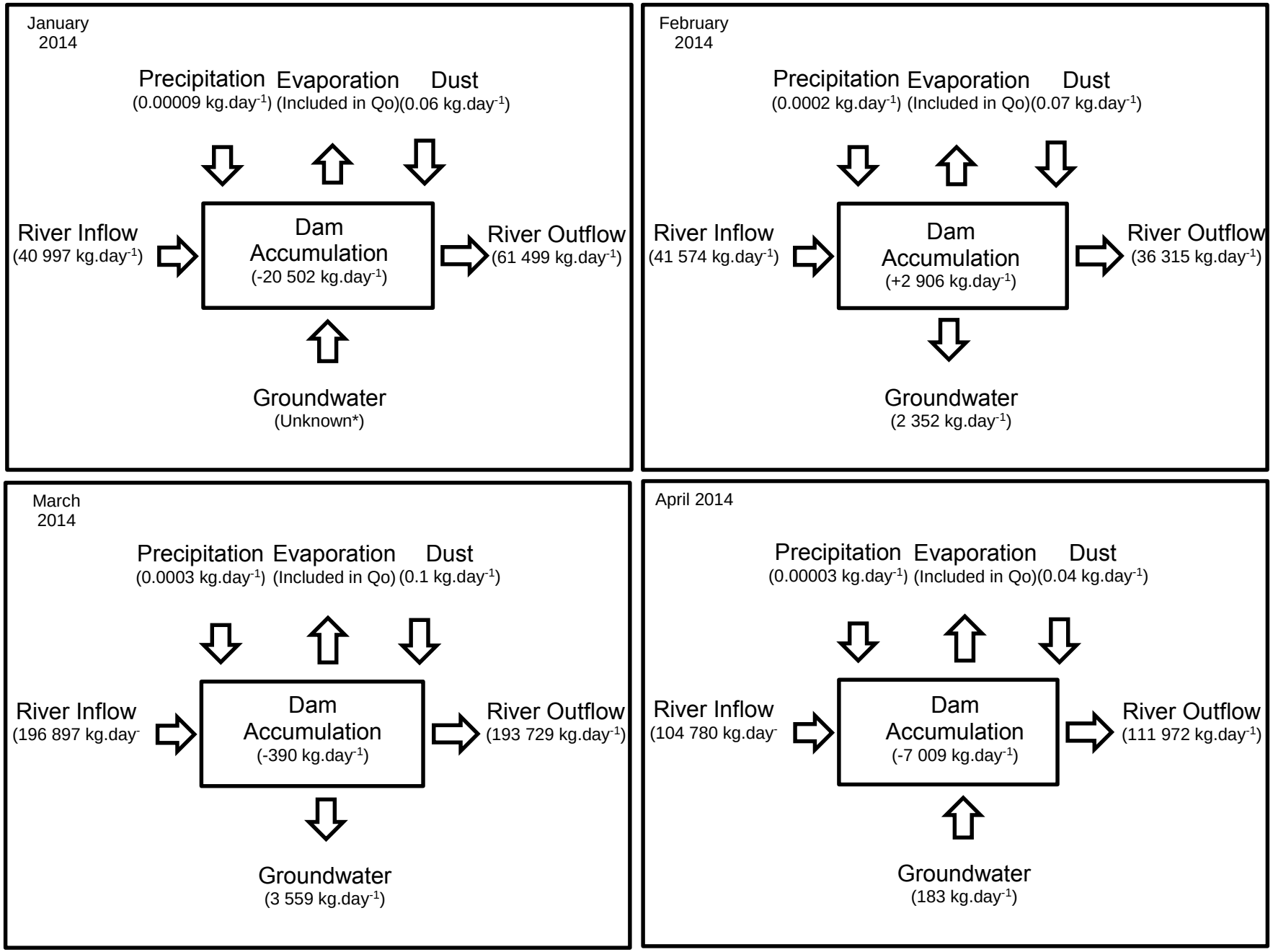
January
2014
Precipitation
(0.00009 kg.day-1)
Evaporation
(Included in Qo)
Dust
(0.06 kg.day-1)
River Inflow
(40 997 kg.day-1)
Dam
Accumulation
(-20 502 kg.day-1)
River Outflow
(61 499 kg.day-1)
Groundwater
(Unknown*)
February
2014
Precipitation
(0.0002 kg.day-1)
Evaporation
(Included in Qo)
Dust
(0.07 kg.day-1)
River Inflow
(41 574 kg.day-1)
Dam
Accumulation
(+2 906 kg.day-1)
River Outflow
(36 315 kg.day-1)
Groundwater
(2 352 kg.day-1)
March
2014
Precipitation
(0.0003 kg.day-1)
Evaporation
(Included in Qo)
Dust
(0.1 kg.day-1)
River Inflow
(196 897 kg.day-
Dam
Accumulation
(-390 kg.day-1)
River Outflow
(193 729 kg.day-1)
Groundwater
(3 559 kg.day-1)
April 2014
Precipitation
(0.00003 kg.day-1)
Evaporation
(Included in Qo)
Dust
(0.04 kg.day-1)
River Inflow
(104 780 kg.day-
Dam
Accumulation
(-7 009 kg.day-1)
River Outflow
(111 972 kg.day-1)
Groundwater
(183 kg.day-1)

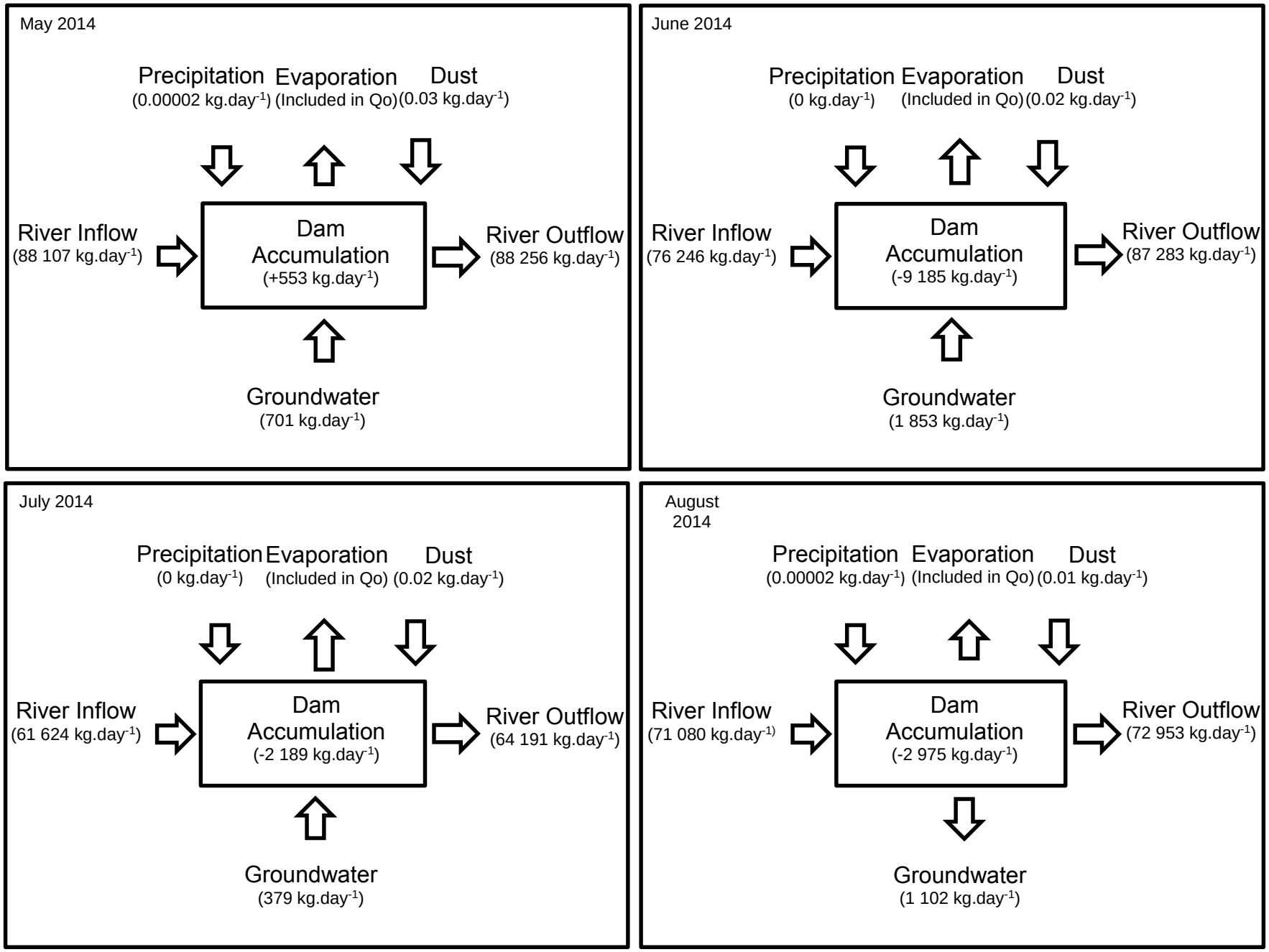

Figure 24: Conceptual diagrams of mass fluxes and accumulation in the Charles-Fourie Dam.

*Groundwater discharge was quantified by means of a water balance, however concentration could not be measured.

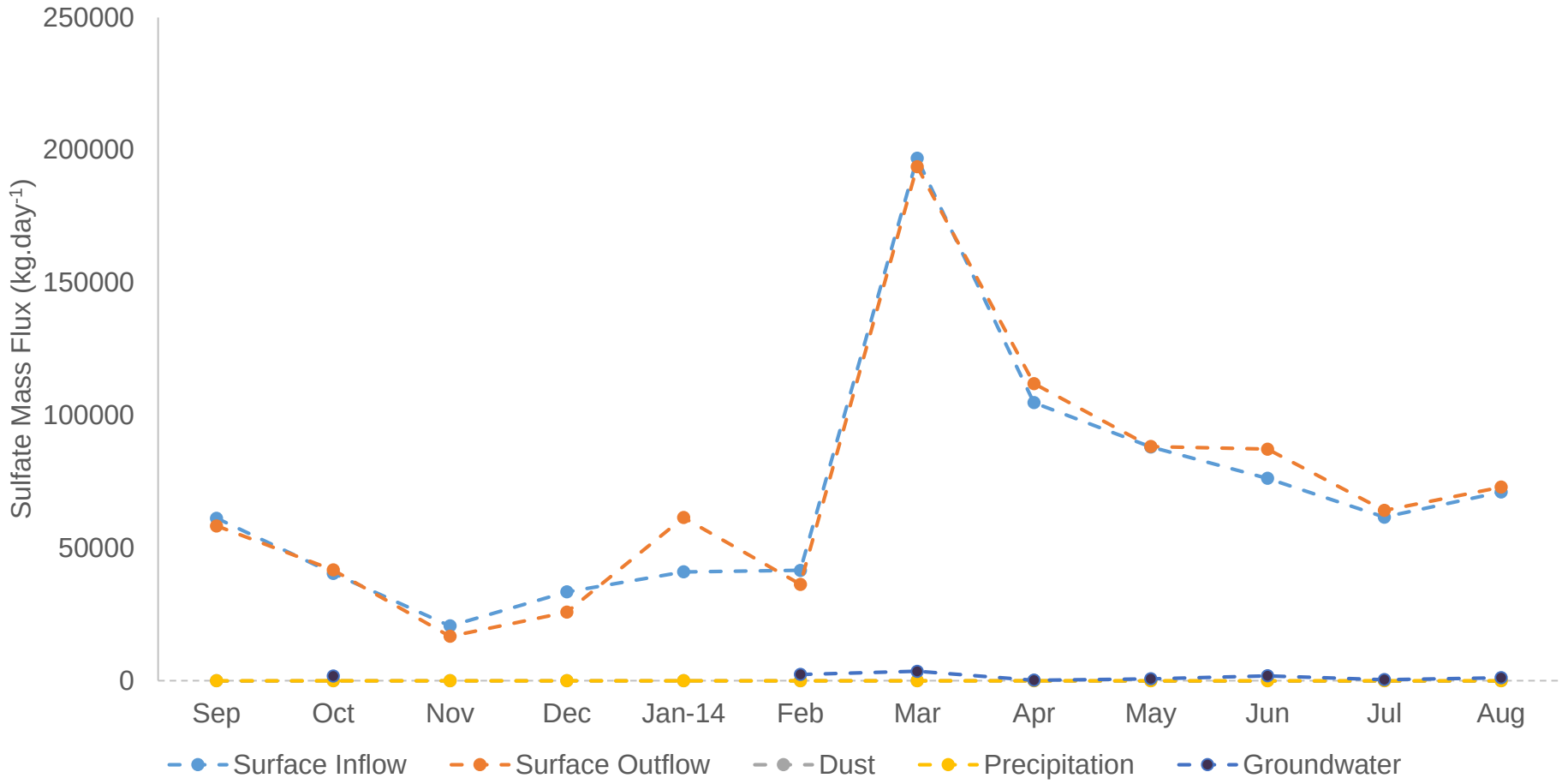

Figure 25: Daily mass fluxes of dissolved sulfate into and from the Charles-Fourie Dam as part of the mass balance calculation.

In total sum, over the twelve observation points studied 23 868 kg SO_4^{2-} of sulfate was remobilised from the species and compounds it was stored in in the dam (please refer to Appendix 2 for calculation) (Figure 26). However, it is important to note that a peak flux event occurred in January alone, whereby 20 502 kg.day^{-1} of sulfate was remobilised from the species and compounds it was stored in in the dam. If the peak flux event is viewed as a standalone event, the dam remobilised a total of 3 366 kg sulfate under normalised flow conditions over eleven observation points.

In respect of the surface area of the dam (2 631 m^2), these data imply that during the peak flux event 7.8 kg SO_4^{2-} per square meter was remobilised, and that over the eleven observation points 1.3 kg SO_4^{2-} per square meter was remobilised from the species and compounds it was stored in in the dam.

Relative to the total flux of sulfate (837 112 kg) passing through the river inflow per day over the twelve observation points, the total net sulfate flux was very small (2.9%) and smaller (0.4%) if the peak flux event in January is excluded. Thus in total, sulfate was remobilised from the dam into the Tweelopies River, increasing the sulfate mass flux by 2.9%. Although the total sum of the mass balance indicated that sulfate was remobilised from the dam, it is evident that the dam acted as a sink for sulfate for half of the observation points (Figure 26).

The observed trend in the sulfate mass balance corresponds with trends measured in the pH of the surface flows. The total flux of sulfate in the river inflow (including the peak flux event) increased by 171% from the high pH period (average 6.7 pH between the September and February observation points) to the low pH period (average 3.2 pH between the March and July observation points). During the high pH period the dam acted as a sink of a sum of 14 853 kg SO_4^{2-} (excluding the peak flux event in January), and during the low pH period a sum of 18 219 kg SO_4^{2-} was remobilised from the species and compounds it was stored in in the dam.

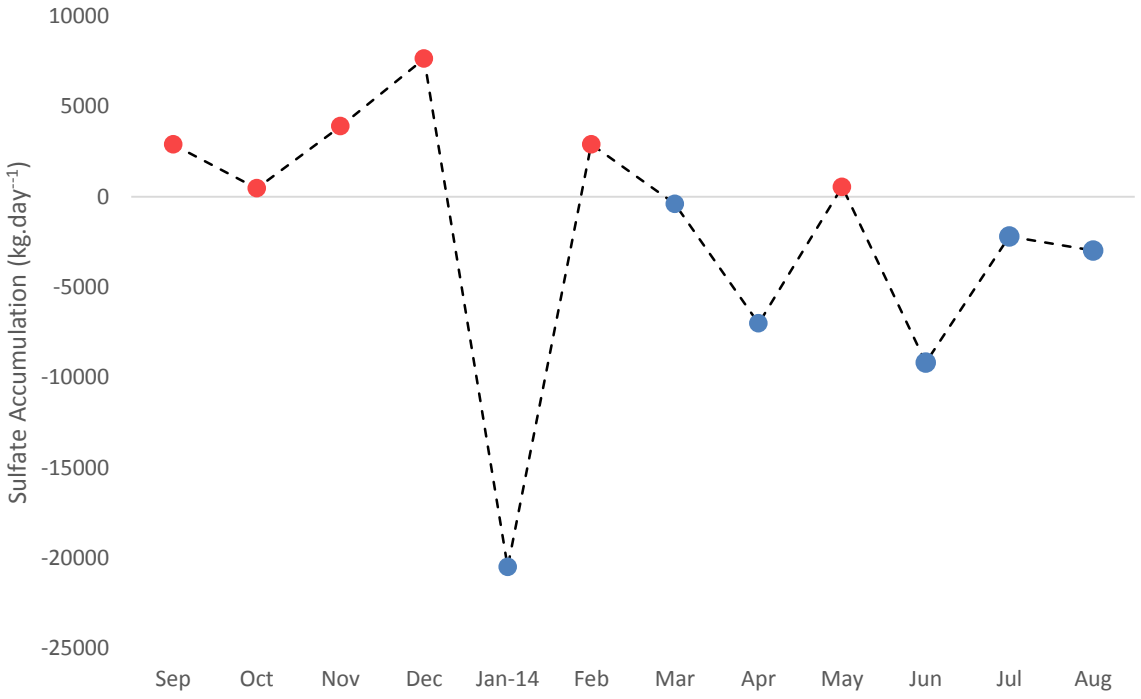

Figure 26: Accumulation of sulfate in the Charles-Fourie Dam. The masses presented on the y-axis are the results of the mass balance described in section 2.3.5 of the methods. The masses show sulfate mass remobilised (blue) from and retained (red) in the Charles-Fourie Dam.

3.2.3.1.3 Contribution of groundwater mass flux to the mass balance

The discharge of groundwater into and from the Charles-Fourie Dam could be calculated for each observation point. However, the borehole could not be accessed until February 2014 so the concentration of sulfate could not be quantified directly for the period September 2013 to January 2014. The concentration of sulfate in the borehole for September 2013 was obtained from the National Groundwater Archive (DWS 2013). The total flux of sulfate that could be measured from the groundwater was 11 898 kg SO_4^{2-}. During the September and February to August observation points, the total accumulation of sulfate in the Charles-Fourie Dam was 17 820 kg SO_4^{2-} and excluding the groundwater flux the total accumulation of sulfate in the Charles-Fourie Dam would be 15 693 kg SO_4^{2-} i.e. the calculation would have shown that 12% less sulfate was remobilised (Figure 27). Therefore, there may be a 12% margin of error in the accumulation calculated in October, and from November to December.

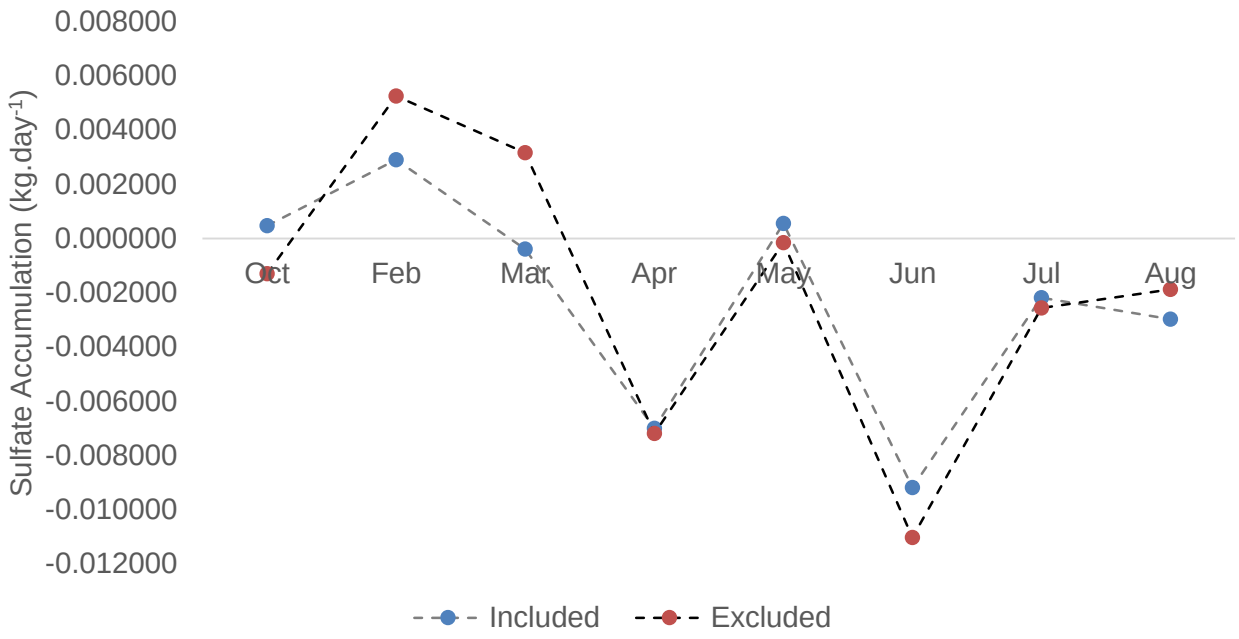

Figure 27: Sulfate accumulation in the Charles-Fourie Dam, calculated with and without the net flux of groundwater.

A comparison of the potential percentage of error with the calculated accumulation rate illustrates that, although the mass flow of groundwater could not be determined for the months of September, and November to January, sulfate was remobilised from the dam (Table 2).

Table 2: Calculated accumulation of dissolved sulfate in the Charles-Fourie Dam and the potential range of error posed by the lack of groundwater data.

	Calculated accumulation (kg SO_4^{2-}.day^{-1})	Range of error (12%)	
		Minimum (kg SO_4^{2-}.day^{-1})	Maximum (kg SO_4^{2-}.day^{-1})
Sep-13	2 898	2 550	3 245
Nov-13	3 907	3 438	4 375
Dec-13	7 649	6 732	8 567
Jan-14	-20 502	-18 042	-22 962

3.2.3.2 Iron masses

3.2.3.2.1 Accumulation of iron in the Charles-Fourie Dam.

The section below details the iron mass flows calculated for each observation point (Figures 28 and 29), and presents the total accumulation of iron into and from the dam (Figure 30).

The total mass flow of iron in the inlet and outlet of the Charles-Fourie Dam was 7 326 kg Fe and 7 139 kg Fe respectively over the twelve daily observation points quantified. The total mass flow of soluble iron in dust, rain and groundwater was 0.5 g Fe, 3 mg Fe and 3.4 kg Fe respectively (Figures 29 and 30).

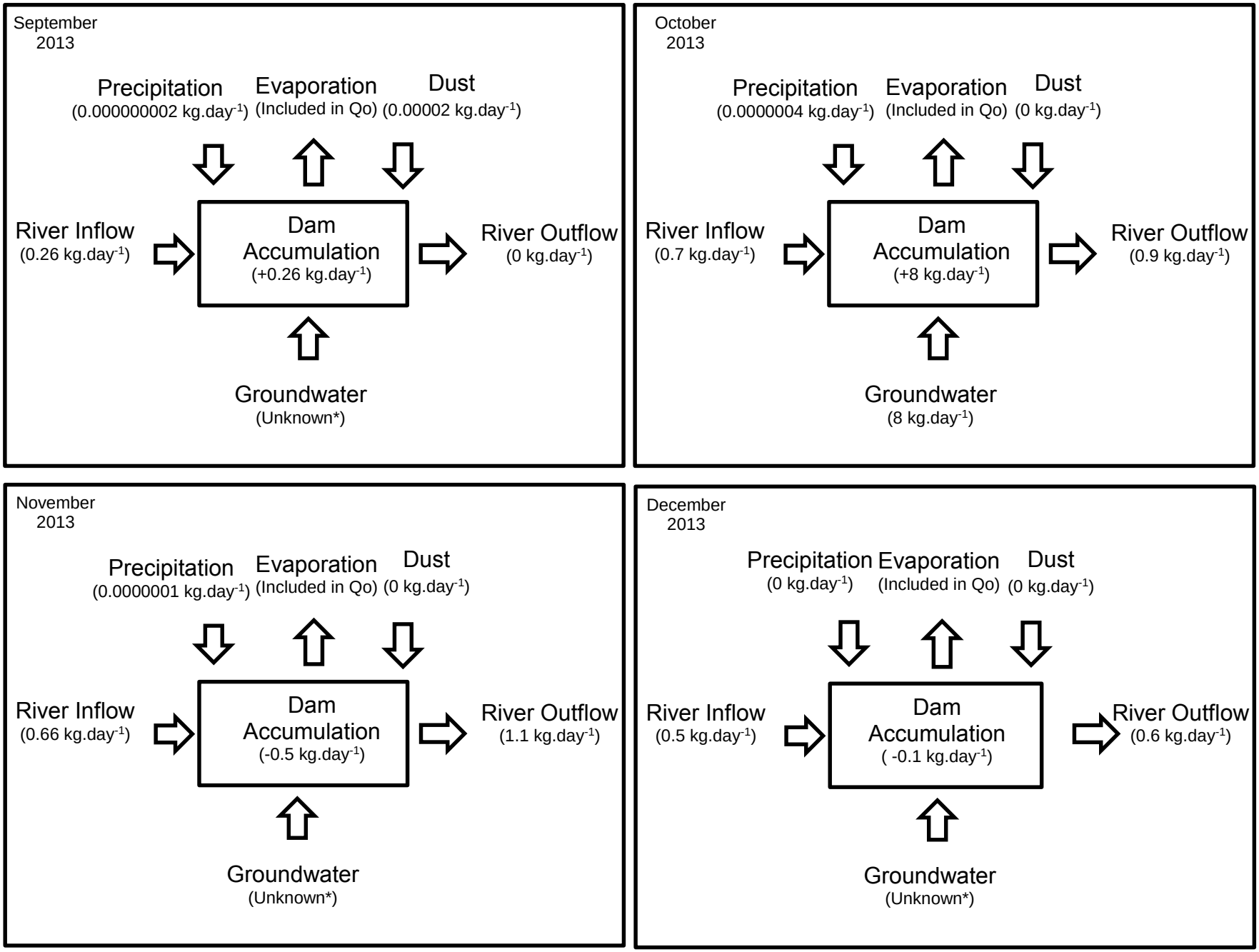
September
2013
Precipitation
(0.000000002 kg.day-1)
Evaporation
(Included in Qo)
Dust
(0.00002 kg.day-1)
River Inflow
(0.26 kg.day-1)
Dam
Accumulation
(+0.26 kg.day-1)
River Outflow
(0 kg.day-1)
Groundwater
(Unknown*)
October
2013
Precipitation
(0.0000004 kg.day-1)
Evaporation
(Included in Qo)
Dust
(0 kg.day-1)
River Inflow
(0.7 kg.day-1)
Dam
Accumulation
(+8 kg.day-1)
River Outflow
(0.9 kg.day-1)
Groundwater
(8 kg.day-1)
November
2013
Precipitation
(0.0000001 kg.day-1)
Evaporation
(Included in Qo)
Dust
(0 kg.day-1)
River Inflow
(0.66 kg.day-1)
Dam
Accumulation
(-0.5 kg.day-1)
River Outflow
(1.1 kg.day-1)
Groundwater
(Unknown*)
December
2013
Precipitation
(0 kg.day-1)
Evaporation
(Included in Qo)
Dust
(0 kg.day-1)
River Inflow
(0.5 kg.day-1)
Dam
Accumulation
(-0.1 kg.day-1)
River Outflow
(0.6 kg.day-1)
Groundwater
(Unknown*)

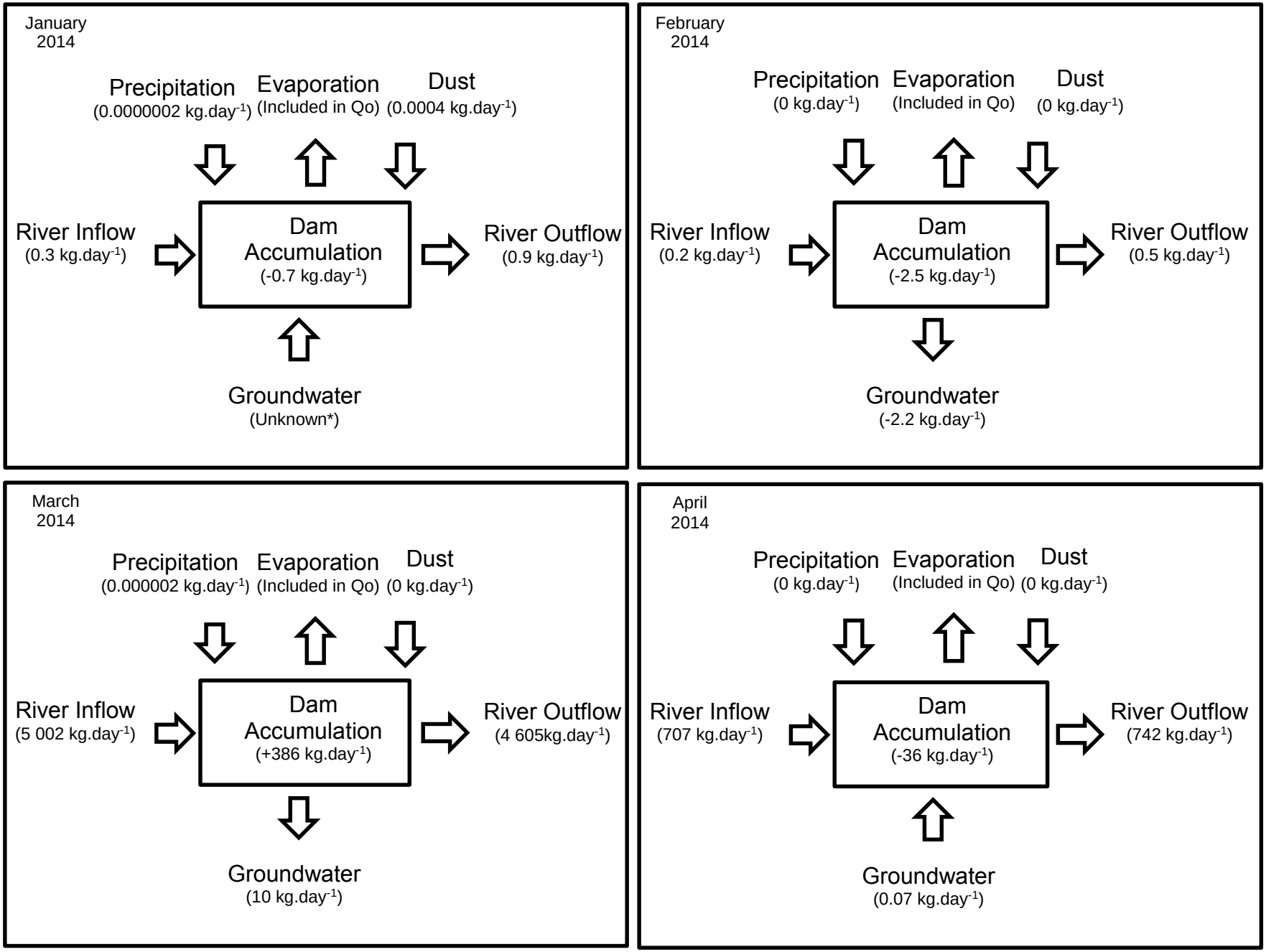
January
2014
Precipitation
(0.0000002 kg.day-1)
Evaporation
(Included in Qo)
Dust
(0.0004 kg.day-1)
River Inflow
(0.3 kg.day-1)
Dam
Accumulation
(-0.7 kg.day-1)
River Outflow
(0.9 kg.day-1)
Groundwater
(Unknown*)
February
2014
Precipitation
(0 kg.day-1)
Evaporation
(Included in Qo)
Dust
(0 kg.day-1)
River Inflow
(0.2 kg.day-1)
Dam
Accumulation
(-2.5 kg.day-1)
River Outflow
(0.5 kg.day-1)
Groundwater
(-2.2 kg.day-1)
March
2014
Precipitation
(0.000002 kg.day-1)
Evaporation
(Included in Qo)
Dust
(0 kg.day-1)
River Inflow
(5 002 kg.day-1)
Dam
Accumulation
(+386 kg.day-1)
River Outflow
(4 605kg.day-1)
Groundwater
(10 kg.day-1)
April
2014
Precipitation
(0 kg.day-1)
Evaporation
(Included in Qo)
Dust
(0 kg.day-1)
River Inflow
(707 kg.day-1)
Dam
Accumulation
(-36 kg.day-1)
River Outflow
(742 kg.day-1)
Groundwater
(0.07 kg.day-1)

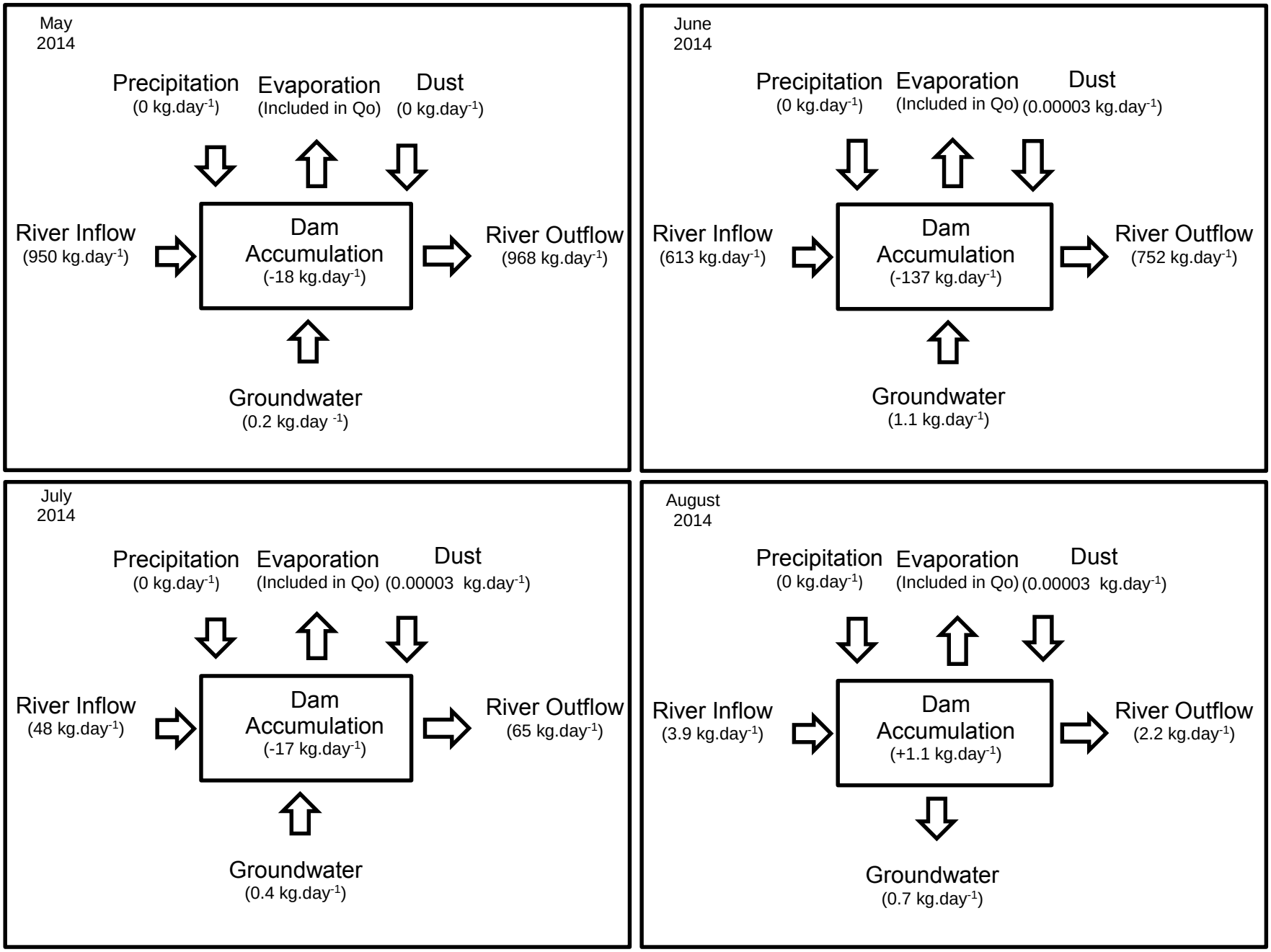

Figure 28: Conceptual diagrams of mass fluxes and accumulation in the Charles-Fourie Dam.

*Groundwater discharge was quantified by means of a water balance, however concentration could not be measured.

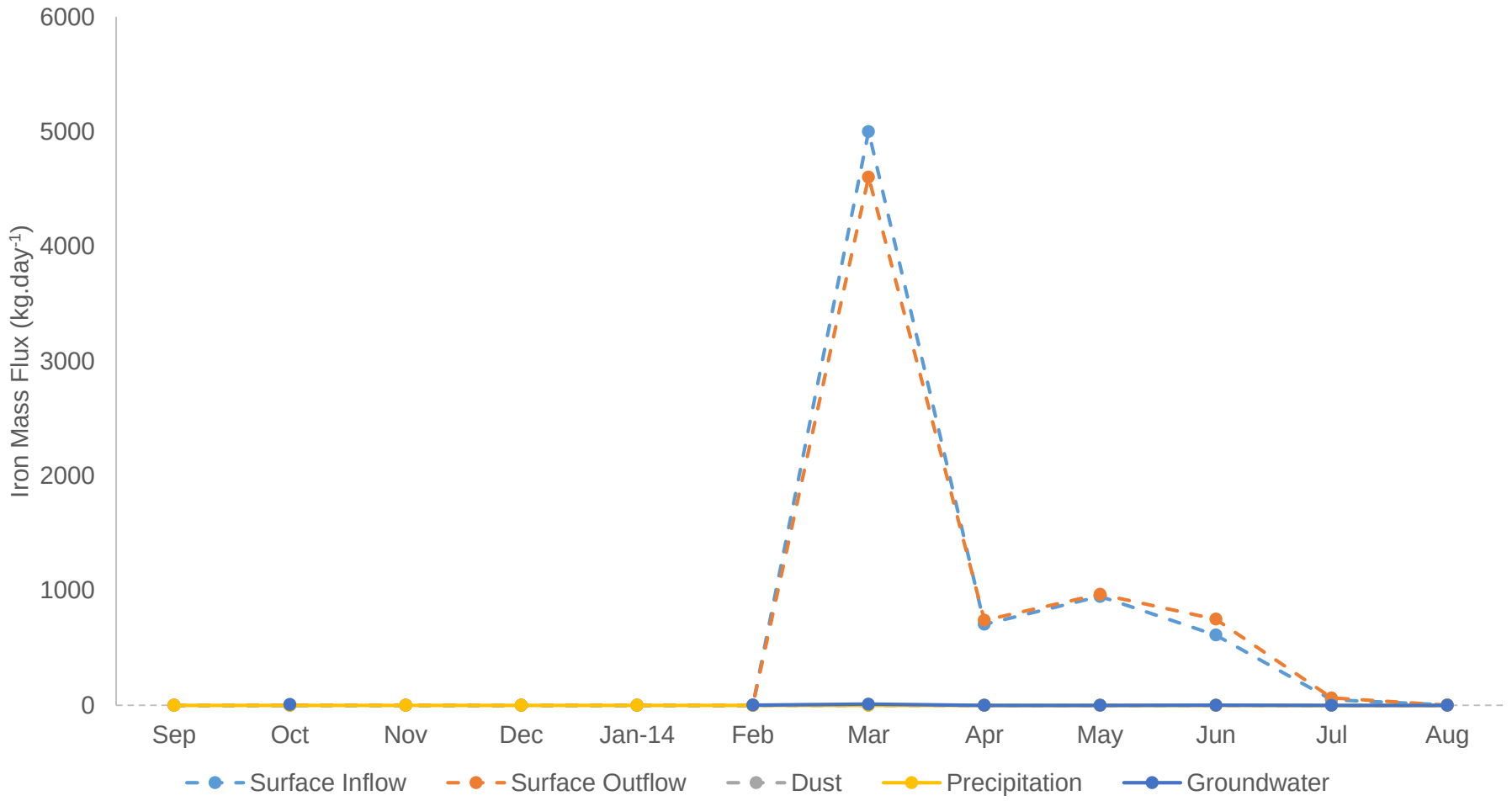

Figure 29:Daily mass fluxes of dissolved iron into and from the Charles-Fourie Dam as part of the mass balance calculation.

Over the twelve daily observation points studied the dam acted as a sink of a sum of 185 kg Fe (Figure 29). However, it is important to note that a peak flux event occurred in March alone, whereby the dam acted as a sink of 386 kg.day^{-1} of iron. If the peak flux event is viewed as a standalone event, the dam remobilised a total of 202 kg iron under normalised flow conditions from the species and compounds it was stored in in the dam. The dam remobilised a maximum of 137 kg Fe.day^{-1} in June and acted as a sink of a maximum of 386 kg Fe.day^{-1} in March.

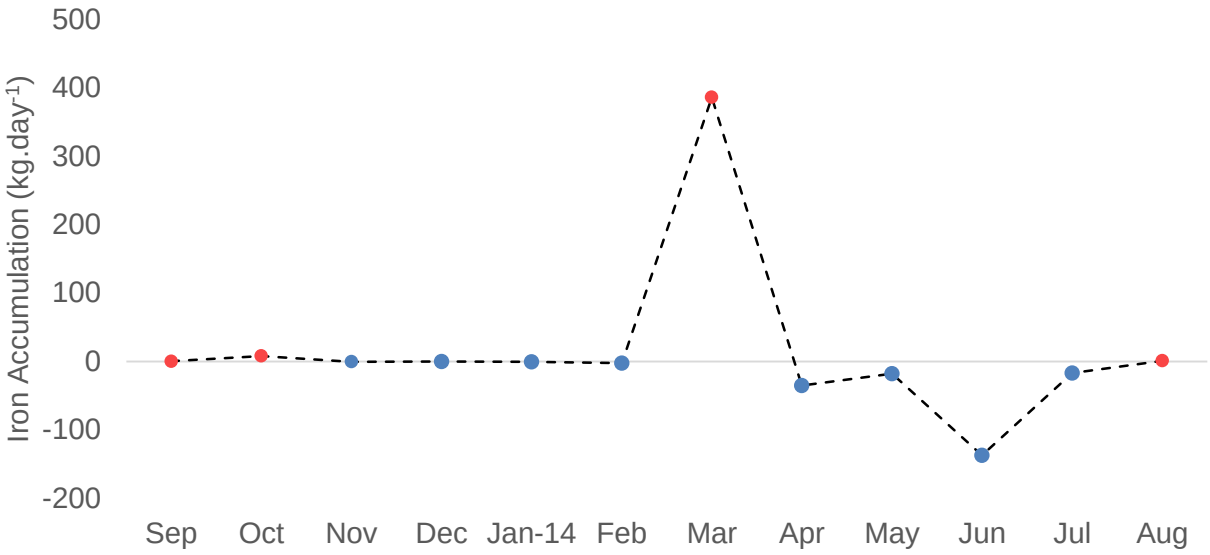

Figure 30: Accumulation of iron in the Charles-Fourie Dam. The masses presented on the y-axis are the results of the mass balance described in section 2.3.5 of the methods. The masses show iron retained into (red) and remobilised from (blue) the Charles-Fourie Dam.

In respect of the surface area of the dam (2 631 m^2), these data imply that during the peak flux event 146 g Fe per square meter was stored in the dam, and that over the eleven observation points 76.77 g Fe per square meter was remobilised from the species and compounds it was stored in in the dam.

The total mass of iron exchange in the Charles-Fourie Dam represents 2.5% of the mass of iron passing the inlet over the twelve observation points (7 326 kg Fe). If the peak flux event in March is excluded, then the Charles-Fourie Dam increased the flux of iron in the Tweelopies River by 8.7%.

There was a clear distinction between chemical fluxes in the high pH period (6.7 pH from September to February at the inlet) compared to the low pH period (3.2 pH between March to July at the inlet). During the high pH period the dam acted as a sink of a total of 5.5 kg Fe, while during the low pH period (excluding the transitional month of March) a total of 179 kg Fe was remobilised.

3.2.3.2.2 *Contribution of groundwater mass flux to the mass water balance*

The discharge of groundwater into and from the Charles-Fourie Dam could be calculated for each observation point. However, the borehole could not be accessed until February 2014 so the concentration of iron could not be quantified directly for the period of September 2013 to January 2014. The concentration of iron in the borehole for September 2013 was obtained from the National Groundwater Archive (DWS 2013). The total flux of iron that could be measured from the groundwater was 3.4 kg Fe. During September, and February to August, the total accumulation of iron in the Charles-Fourie Dam was 185 kg Fe, and excluding the groundwater flux the total accumulation of iron in the Charles-Fourie Dam would be 188.4 kg Fe i.e. the calculation would have shown that 1.8% more iron was stored (Figure 31). Therefore, there may be a 1.8% margin of error in the accumulation calculated in October, and from November to December.

Figure 31: Iron accumulation in the Charles-Fourie Dam, calculated with and without the net flux of groundwater.

A comparison of the potential percentage of error with the calculated accumulation rate illustrates that, although the mass flow of groundwater could not be determined for the months of September, and November to January, iron was remobilised from the species and compounds it was stored in in the dam (Table 3).

Table 3: Calculated accumulation of dissolved iron in the Charles-Fourie Dam and the potential range of error posed by the lack of groundwater data.

	Calculated accumulation (kg Fe·day^{-1})	Range of error (1.8%)	
		Minimum (kg Fe.day^{-1})	Maximum (kg Fe.day^{-1})
Sep-13	0.26	0.25	0.26
Nov-13	-0.47	-0.46	-0.48
Dec-13	-0.11	-0.11	-0.11
Jan-14	-0.65	-0.64	-0.66

3.3 Sediment chemistry

3.3.1 Radiometric dating

Caesium-137 activities were too low to be detected in five of the twelve core sections and thus Caesium-137 could not be used to establish a time series. Lead-210 activities ranged between 11 and 18.7 dpm.gm^{-1}, but did not show decay with depth (Table 4). Thus there is evidence that the core has been re-worked or mixed.

Table 4: Lead-210 and Caesium-137 activities in a core taken from the Charles-Fourie Dam, Gauteng Province.

Core Depth (cm)	Pb-210 (dpm.gm^{-1})	Cs-137 (dpm.gm^{-1})
-1.5	12.2	BD
-3.5	12.8	0.2
-5.5	12.4	BD
-7.5	11	BD
-9.5	12.9	0.3
-11.5	12.8	0.3
-14.5	13	0.2
-16.5	15.8	0.3
-18.5	16.3	BD
-20.5	16.4	0.3
-22.5	17.4	BD
-24.5	18.7	0.4

3.3.2 Contaminant storage in dam sediments

Iron, an AMD constituent, was the most highly concentrated element within the core (120 972 mg/kg) and constituted an estimated 18 ton mass of the sediment in the Charles-Fourie Dam. Aluminium was the next most concentrated element (57.2 g/kg) in the core followed by sulfur (34.7 g/kg), another AMD constituent. The sediment of the dam contained an estimated mass of 5 tons of total sulfur. Calcium constituted 4 tons of the dam sediment, magnesium 600 kg, zinc 300 kg and nickel 100 kg. An estimated 20 kg copper, lead and vanadium were in the sediment of the Charles-Fourie Dam (Table 5).

Table 5: Calculated total accumulation of chemicals within sediments of the Charles-Fourie Dam, Gauteng Province.

Constituent	Concentration (mg/kg)	Sediment quality guideline maxima (mg/kg)	Mass in the core* (g)	Contaminants in dam sediments** (tons)
Al	57 209	N/A	7	8
Fe	120 972	40 000[1]	16	18
Mg	4 101	N/A	0.5	0.6
Ca	28 082	N/A	3	4
S	34 702	500[2]	4	5
Cu	167	197[2]	0.02	0.02
Ni	1 000	49[1]	0.1	0.1
Pb	150	91.3[2]	0.02	0.02
V	120	130[2]	0.02	0.02
Zn	2 265	460[1]	0.3	0.3

* XRF procedures were conducted only on alternating sections of the core so that the other sections could be dated radiometrically, therefore the 'real' depth of the core analysed via XRF was 13 cm.

** Assuming a sediment depth of 19.3 cm

[1] Aartila *et al*., 2003

[2] Canadian Council of Ministers of the Environment, 2001

Total iron mass in the core was the highest of all the elements at 16 g. The range spanned 0.48 g and 2.7 g in sections 14 - 15 cm and 4 - 5 cm respectively (Table 5, Figure 32). Total sulfur masses in the core ranged from 0.12 g in section 24 – 25 and 0.85 g in section 6 - 7 cm. Total sulfur and iron content in the core appeared to have identical increasing or decreasing trends and correlated closely with increasing depth ($R^2 = 0.7501$). The highest masses of total sulfur and iron were measured within the surface 10 cm. These data imply that although the core may be partially re-worked, there is clear evidence of concentrated contamination in the sediment.

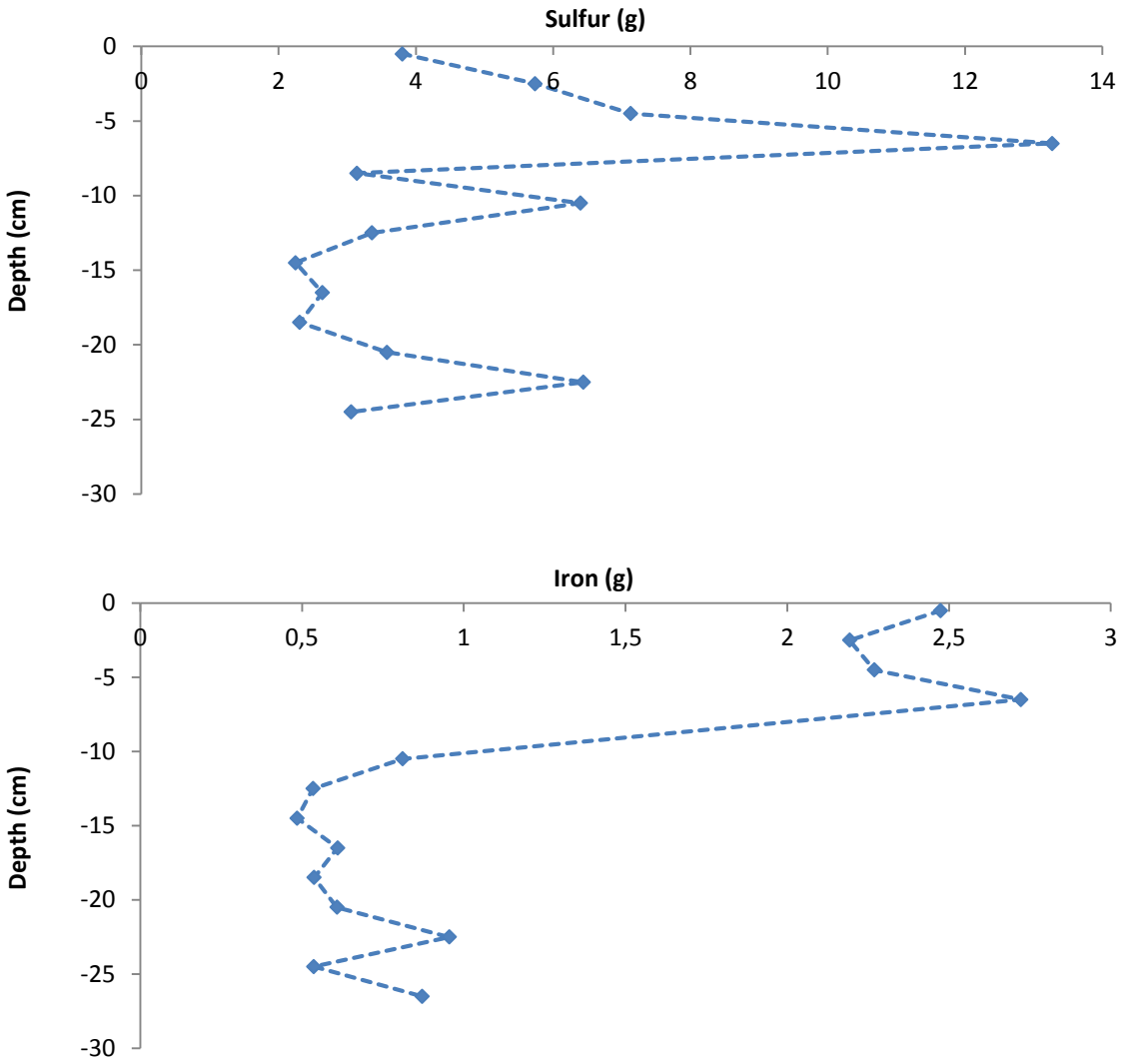

Figure 32: Variation in iron and sulfur (g) accumulation through the 27 cm core taken from the Charles-Fourie Dam, Gauteng Province.

Assuming there was an average sediment depth of 19.3 cm, which was the average depth of the three extracted cores, an estimated 18 tons of iron and 5 tons of total sulfur were present in the sediments of the dam.

3.3) Sediment organic matter

On average organic matter made up 22% of the dry mass of the sediment core. The highest percentages were found mid-core with 44% and 41% in sections 16 - 17 cm and 19 - 20 cm respectively (Figure 33).

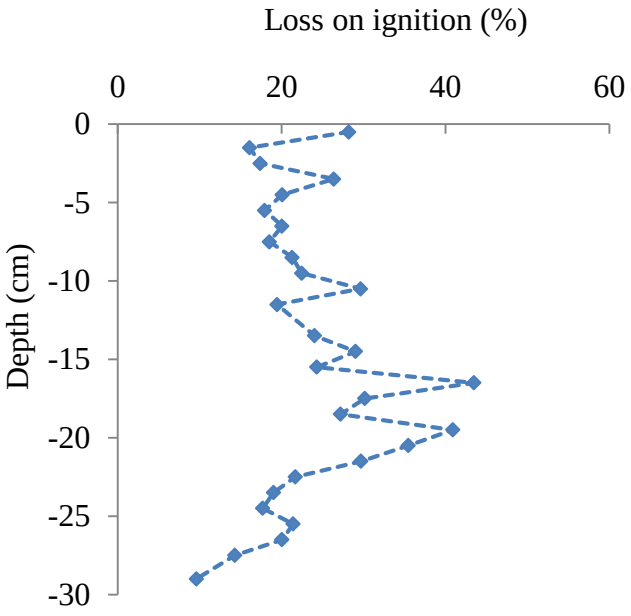

Figure 33: Depth profile plot showing variations in %LOI for the sediment core analysed from the Charles-Fourie Dam, Gauteng Province.

4 DISCUSSION

The aim and key questions of this study centred upon assessing the mitigatory function of the Charles-Fourie Dam on dissolved sulfate and iron (acid mine drainage contaminants) in the Tweelopies River when the dam acted as a sink, and in quantifying the accumulation of total sulfur and iron in the sediment of the dam. The results indicate that in total the dam remobilised dissolved sulfate and iron in the river over the 2013-2014 study period during normalised flows from the species and compounds it was stored in in the dam. However, total iron and sulfur have also accumulated in the sediment since, or prior to, the construction of the dam despite observed re-working in the sediment.

These results provide answers to the key questions posed (which are re-stated and discussed below) and also suggest important pathways in which AMD contaminants are transported and stored, informing recommendations for the management of AMD.

4.1 Key question 1: Does the dam act as a sink for dissolved sulfate and iron (AMD contaminants)?

The ability of the Charles-Fourie Dam to retain either dissolved sulfate or iron was clearly distinguished by two periods, namely what can be considered 'normalised' flows (where flux data for a period were within three standard deviations of the mean) and what can be considered peak flux events (defined as datapoints whose values are three or more times greater or less than the standard deviation of the mean of the population (Osbourne & Overbay, 2004)). Within both of these periods the mitigatory function of the dam to act as a sink for, or remobilise, AMD contaminants varies considerably with, and due to, the significant changes in water quality conditions that occurred in the Tweelopies River. These periods, and their defining characteristics and drivers, are discussed separately below.

4.2.3 Mitigatory function of the Charles-Fourie Dam during 'normalised' flows

During the period of study the Charles-Fourie Dam remobilised dissolved sulfate (3 366 kg or 1.3 $kg.m^{-2}$) and iron (202 kg or 76.77 $g.m^{-2}$) in total (and excluding peak flux events which significantly bias the total sum) from the species and compounds it was stored in in the dam, and contributed to the impairment of downstream water quality in the Tweelopies River. At first glance the remobilisation of sulfate and iron from the Charles-Fourie Dam may appear to be relatively high. However, the concentrations of constituents and the discharge at the inlet and outlet of the dam, which are the primary determinants in the mass balances (Figure 23, 27), are similar to previous studies conducted on the river. The average concentration of sulfate (1 951 $mg.L^{-1}$) at the inlet of the Charles-Fourie Dam was similar to sulfate concentrations previously measured in the Tweelopies River in other studies within 1 km of the inlet. In 2007, 2009 and 2012 sulfate concentrations of 1 772 $mg.L^{-1}$ (Hobbs & Cobbing, 2007), 2 250 $mg.L^{-1}$ (Coetzee *et al.*, 2009), and 2 100 $mg.L^{-1}$ (Olsen *et al.*, 2012) were respectively measured in the Tweelopies River. In 2012, when the pH of the Tweelopies River was 3.3 units, 19 $mg.L^{-1}$ of iron was measured, which is similar to the average iron concentration (27.5 $mg.L^{-1}$) measured by this study when the pH of the river was similarly low (3.2 pH) (Olsen *et al.*, 2012). Furthermore, the average discharge in the Tweelopies River measured in June and July 2014 (0.47 $m^3.s^{-1}$ and 0.40 $m^3.s^{-1}$) were fairly similar to discharges measured in June and July 2012 (0.28 $m^3.s^{-1}$ and 0.26 $m^3.s^{-1}$) (Olsen *et al.*, 2012). Therefore, there is a significant amount of supporting evidence that the data obtained in this study are realistic and typical of the site.

The conduit remobilising dissolved sulfate and iron over the study period was likely the solubilisation and oxidation of sulfide, sulfate and iron minerals in the sediments, including precipitates in the sediment, deposited organic debris and suspended solids. All other influxes and effluxes (river inflow, net groundwater flux, dust and rain influx) were accounted for in mass balance equations aside from the sediment and suspended solids. Sediments (which include detritus) have been shown to contain high masses of sulfur (total) and iron in other water reservoirs contaminated with AMD (Cummings *et al.*, 2000; Box *et al.*, 2005). Additionally, the

desorption and dissolution of constituents (including iron) via physico-chemical and biological processes from sediment have been shown to increase dissolved concentrations in the surface water of rivers (Cummings *et al.*, 2000; Box *et al.*, 2005; Johnson *et al.*, 2005; Luoma & Rainbow, 2011) and lakes (Harrington *et al.*, 1998; Cummings *et al.*, 2000). The remobilisation of iron and sulfate into the water of the Charles-Fourie Dam from the species and compounds it was stored in in the dam was likely, at least partially, facilitated biologically by aerobic decomposition and oxidation of debris or material coated in AMD-derived precipitates or "yellow-boy" (such as organic matter and suspended or top layer/s of bottom sediment). The organic content of the sediments, the depth and very short water residence time in the dam support this supposition. Approximately 22% of the dried sediment core was organic matter, indicating that a large amount of organic matter available for decomposition had accumulated in the dam (the source of the majority of this material is likely to have been the extensive *Phragmites* wetlands located upstream). Additionally, mixed and oxygenated water is an important determinant of bacterial decomposition and thus also of the decomposition of AMD coated organic matter which contains sulfide, sulfate and iron compounds (as discussed in section 1.3.3 of the Literature Review).

The hydraulic residence time of the dam is unusually short (~5 hours) for a reservoir (Bartram & Balance, 1996). However, four reservoirs have been shown to have residence times shorter than five hours (Albrecht *et al.*, 1998). Specifically, Klingnau Reservoir, Aare, Switzerland had a slightly smaller surface area than the Charles-Fourie Dam (0.85 km^2 and 2.6 km^2 respectively) and a slightly deeper average depth (4 m and 2.7 m respectively). The residence time of Klingnau was ~three hours, providing support that the short residence time of the Charles-Fourie Dam is realistic (Albrecht *et al.*, 1998).

Water residence time in a reservoir is a key component determining whether a water body is likely to be well oxygenated (Bushaw-Newton *et al.*, 2001). The short residence time of water in the dam (~5 hours) paired with a shallow average depth of 2.7 m demonstrates that it is highly likely that the dam is fully mixed without any anoxic layers in the water and at the sediment-water interface where the majority of decomposition would occur (Bushaw-Newton *et al.*, 2001). This is important when eliminating sulphidogenisis and anoxic decomposition as a biological process

occurring in the dam. If the water and sediment-water interface were anoxic it is very likely that the dam would act as a sink of sulfate rather than contribute dissolved sulfate as sulfidogenisis would occur.

Sulfidogenesis refers to sulfate-reducing bacteria converting organically derived sulfur to hydrogen sulfide (Machel, 1989; Gibert *et al.*, 2004). Hydrogen sulfide is a gas that once formed will exit the dam and is a mechanism by which the dam would remove sulfide minerals (and remove the conduit from which dissolved sulfate might be remobilised). Artificial addition of organic substrates to facilitate sulphidogenesis and the removal of sulfur from acid mine drainage effluent is a promising new remediation technique (Gibert *et al.*, 2004). However, in the presence of oxygen aerobic decomposition will dominate and organically derived sulfide will oxidise and transform into sulfur, and ultimately dissolved sulfate (as described in detail in section 1.3.3.1.1 of the Literature Review). Although the majority of the sediment of the dam is likely to be anoxic, the sediment-water interface, where the majority of organic decomposition that will interact with the water will occur, will likely still be exposed to sufficient oxygenated water to undergo aerobic decomposition. Thus the low hydraulic residence time of the dam supports aerobic decomposition and oxidation of organic matter resulting in an increase in dissolved sulfate in the water.

Physical and chemical mechanisms that show increased dissolved concentrations of sulfate and iron in other water reservoirs contaminated with AMD include physical re-suspension of sediment from flooding (La Force *et al.*, 1998; Johnson *et al.*, 2005) as well as changes in pH (Chuan *et al.*, 1996). The physical re-suspension of sediment exposes anoxic deep sediments to oxygen and iron- and sulfide-oxidising bacteria. Sulfide-oxidising bacteria decompose organic matter in the sediments and oxidise sulfide minerals releasing dissolved sulfate into the water (Dunn, 1997; Friedrich *et al.*, 2001). Iron-oxidising bacteria decompose organic matter in the sediments and oxidise iron minerals, including ferrous and ferric hydroxides, and iron sulfides (such as pyrite) producing ferrous ions (Akcil & Koldas, 2005). In a circumneutral or alkaline pH environment the resultant ferrous iron would oxidise and form insoluble iron precipitates. However, in a low pH environment (pH<3.5), pH significantly decreases the rate at which insoluble ferric iron precipitates form and more ferrous iron remains dissolved in the water than in a

circumneutral pH environment (Figure 9) (Hem & Cropper 1959; Stumm & Lee, 1961; Brock & Gustafson 1976; Akcil & Koldas 2005). Therefore, the physical resuspension of deep sediment, its exposure to sulfide- and iron-oxidising bacteria in a low pH environment, will increase the concentration of dissolved sulfate and iron in the water. For more information on this process please refer to sections 1.3.2 and 1.3.3 of the Literature Review.

In total, the dam increased the mass of dissolved iron in the river by 8.7% per day (excluding the March peak flux event). However, it was observed that during the observation points from April to July the dam remobilised 210 kg iron, but stored 5.5 kg iron from the observation points between September 2013 and February 2014. This can be linked to changes in water quality that occurred between February and March. In March the concentration of dissolved sulfate in the surface inflow of the dam increased by 33% (to 2 201 mg L^{-1}, Figure 18) most likely due to heavy rain increasing the discharge of contaminated water from the mine shaft and overwhelming neutralisation measures (which are discussed in more detail below). This supposition is supported by data showing that rainfall was highest in March. This occurred concurrently with a dark orange-red colour change of the water, a 237% increase in discharge, a pH drop of four units and a 173 times increase in iron concentrations between the two months. Subsequently the pH of the river remained low (3.2 pH on average) from March until July.

This change in the concentrations and pH in the river are likely partially attributable to increased hydrostatic head facilitating a greater amount of pyrite oxygenation and hydrolysis, and generating greater dissolved sulfate loads in the decanting mine shaft. An increase in hydrostatic head between winter and summer had previously demonstrably increased the decant rate from the mine shaft by 1.8 times (to 36 ML/day) (Hobbs & Cobbing, 2007). Thus it may have had a similar effect on fluxes of sulfate and iron from March onwards. It is also likely that unusual flooding, which closed several roads and schools in Krugersdorp (Viljoen, 2014), caused an overflow in the process water dams, emergency overflow dams and increased runoff from the tailing storage facilities in the West Wits Pit which overlooks the reserve. This highly polluted water might then have drained into the Tweelopies River.

The drastic change in the total daily dissolved iron and sulfate fluxes in the river (38 times and 123% increase respectively (excluding the peak flux events)) between the two periods is linked to changes in pH, which decreased by 3.5 units on average. The solubility of iron drastically increases under low pH conditions. In a low pH environment (pH <3.5), pH increases the availability of dissolved iron (both ferrous and ferric iron) by significantly decreasing the rate at which insoluble ferric iron precipitates form due to a dilution of hydroxyl ions present in the water (Hem, 1975; Luoma & Rainbow, 2011) (Figure 9). Chuan *et al.*, (1995) found this to be true for the solubility of iron in contaminated sediment as well (Chuan *et al.*, 1996), which has bearing on the changes in retention of iron and sulfate in the dam observed during and after March.

The pH of the river decreased from a range of 5.9 to 7.6 during September to February (high pH period), to 2.9 to 3.6 from March to July (low pH period), and then increased to pH 6 in August. During the high pH period the dam acted as a sink of both iron and sulfate (5.5 kg and 14 853 kg respectively). During the low pH period the dam remobilised sulfate (18 219 kg) and iron from April to July (210 kg) from the species and compounds it was stored in in the dam.

Comparing the differences in total accumulation in the dam based on pH changes, excluding the transitional month of March, it is clear that pH plays a pivotal role in determining whether the dam remobilises or acts as a sink for dissolved iron in the water. When the water exhibited a higher, circumneutral pH (5.9 – 7.6) the dam acted as a sink of dissolved contaminants, conversely when the pH was low (2.9 – 3.6) the dam remobilised 38 times more iron when compared to the high pH period.

Changes in pH also affected total sulfate accumulation in the dam. During the high pH period (excluding the peak flux event in January discussed below) the dam acted as a sink of 14 853 kg.SO_4^{2-} and during the low pH period the dam remobilised 18 219 kg sulfate from the species and compounds it was stored in in the dam. These changes are linked to changes in pH due to the co-precipitation of the species of sulfur with iron and other metals. AMD precipitates upon organic matter are predominantly ferrous hydroxide complexes which can contain sulfide and sulfate (Luoma & Rainbow 2011) and the rate at which iron precipitates (including insoluble ferric iron compounds) form is significantly influenced by pH (where for each unit

increase in pH the rate of precipitate formation increases 100 fold (Stumm and Lee, 1961)). Therefore during the high pH period the rate at which sulfide and sulfate containing iron hydroxides precipitated was greatly accelerated. During the low pH period the iron hydroxide precipitates formed at a significantly lower rate. Furthermore, it is also likely that acidification favoured conditions for increased bacterial decomposition and oxidation of AMD coated detritus, which helps to further explain why the dam remobilised a greater mass of sulfate and iron than it retained.

Most bacteria are known to be intolerant to extreme changes in pH over a short period and acid-base flushing is often used to eliminate them (Taylor, 2001). However, acidophilic bacteria, such as *Thiobacillus thiooxidans*, often dominate in AMD contaminated watercourses (Akcil & Koldas, 2006). Acidophilic bacteria are defined as having an optimal growth rate in water with a pH of approximately 3.0 or less (Gerloff-Elias *et al.*, 2005) – thus it is logical that the highest amounts of contaminants are released as a result of decomposition under low pH conditions in an environment mostly containing acidophilic bacteria. That the growth rate of the dominant bacteria in the river will be lower when the pH is above 3 also fits with the lower flux of sulfate and iron measured during the higher, circumneutral pH period.

Historically, water in the Tweelopies River has undergone several periods of low pH caused by the decant of AMD and circumneutral pH caused by liming since the surface decant began in 2002 (Figure 34) (Hobbs & Cobbing, 2007; Coetzee *et al.*, 2009; Olsen *et al.*, 2012). The changes in pH are also likely associated with varying volumes of AMD decanting on the surface over different periods. Liming is used to neutralise the pH making iron and other metals less soluble, thus removing them from solution. Liming took place at the mine shaft at the start of the study period (Turton *et al.*, 2014) which is why the pH of the river was circumneutral during the start of the study period and why the site has historically undergone multiple changes in pH (Department of Agriculture and Rural Development, 2014; Turton *et al.*, 2014). These changes in pH are evident in several separate studies (Figure 34).

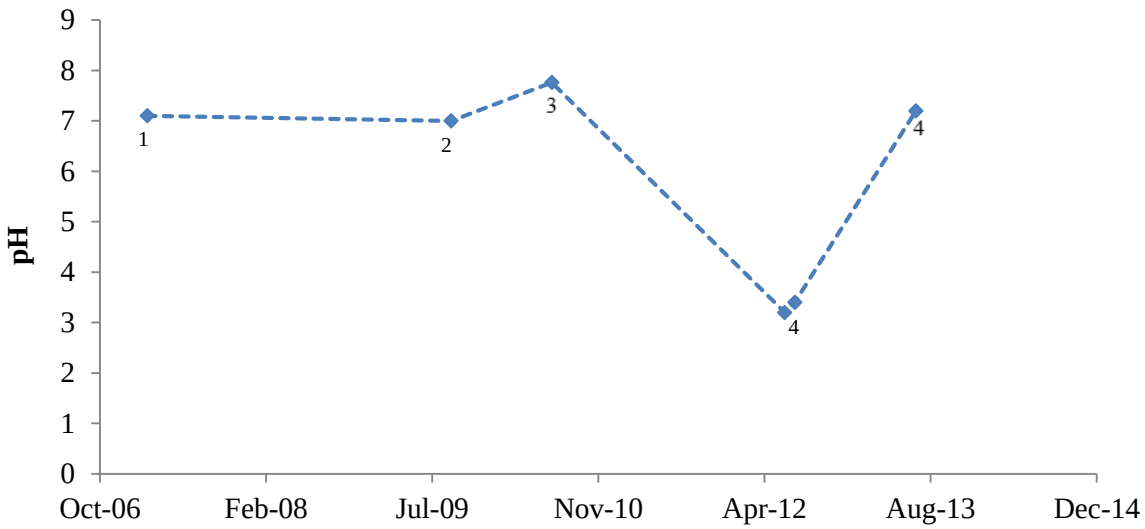

Figure 34: Historical trends in pH of the surface water of the Tweelopies River, within 1 km of the Charles-Fourie Dam inlet.

[1] Hobbs and Cobbing, 2007
[2] Coetzee *et al.*, 2009
[3] Lusilao-Makiese, 2012
[4] Olsen *et al.*, 2012

Through liming, from June 2013 to February 2014, the pH of the river and the iron concentrations had not been detrimental to aquatic life. From March 2014 to July 2014 they were detrimental based on the South African water quality guidelines for the protection of aquatic life (Department of Water Affairs and Forestry, 1996).

The DWAF (1996) guideline states that should pH values vary by 0.5 pH or 15% of background levels (whichever is the most conservative) then there will likely be a detrimental impact on the biodiversity of the ecosystem. The severity of this impact will increase with the non-compliance of pH, leading to an acute or chronically toxic system. Additionally, significant changes in pH over a short time compound the severity of the impact. When considering the background pH level of the dam to be 6.6 (the average pH of the inlet during the September to February period) and the minimum pH (2.9) measured in March, then the maximum variation in pH of the system was 57%, with a change of four pH units occurring within a month.

Additionally, the low pH of the water during the months of March to July 2014 increased the availability of dissolved iron, generating a maximum concentration of 61.5 $mg.L^{-1}$ at the inlet in March and 27.5 $mg.L^{-1}$ on average (including the iron concentration quantified in March). The DWAF (1996) guideline determined detrimental ecosystem impacts above a variation of 10% from background iron

concentrations. Considering the background iron concentrations as 0.04 mg.L^{-1} (the average concentration at the inlet between September and February), the concentration of iron at the inlet during March was 1 398 times greater than the maximum value recommended for the protection of aquatic life (0.044 mg.L^{-1}) and 625 times greater on average during the low pH period. Although iron is an essential element to life, high concentrations in living tissue become toxic through the dilution of trace metals present in the body which results in the 'forced' substitution of iron to binding sites during protein synthesis. Proteins that were formed due to incorrect iron substitution are geometrically/spatially distorted leading to changes in function and the risk of cancer amongst other health concerns (Luoma & Rainbow, 2011). Additionally, iron precipitation onto the exoskeletons and gills of invertebrates can lead to oxygen deprivation and limited mobility (Figure 1).

It is important to note that ecosystems in the Tweelopies River might have started reverting to an improved ecological state during the extended circumneutral pH period. However, the decrease in pH would have caused impairment of the ecosystem once more – therefore the financial resources spent on treatment of the water did not result in any meaningful improvement in the ecological state of the river. As the amount of rainfall has been very typical of the area since 2000 (World Weather Online, 2013) and there have previously been low to high pH periods (Figure 34) it is clear that the current treatment strategy (such as amount of lime used during the wet season) needs to be re-evaluated to take rainfall considerations into account and prevent these significant changes in pH.

4.2.4 Mitigatory function of the Charles-Fourie Dam during peak flux events

Two peak flux events in the dam occurred during this study (one for each sulfate and iron flux in the dam). In terms of iron flux, one peak flux event occurred when in March the dam acted as a substantial sink of iron (386 kg.day^{-1} or 146 g.day^{-1}.m^{-2}), decreasing iron flux in the Tweelopies River by 8%. The iron flux in March can be explained by considering the buffering capacity of water in the dam and changes in pH. The pH in the dam in February (6.9) was significantly higher than in March (2.9), thus dilution from the dam would have significantly increased the pH of the contaminated water and reduced the solubility of iron, reducing the

concentration of dissolved iron as it flowed through the dam. Additionally, the concentration of iron in the inlet was highest in March (61.5 $mg.L^{-1}$) which would have contributed to the amount of iron sequestered. Once the dilution capacity of the dam was exhausted (which would have occurred within a few days after the decant due to the short residence time), the dam remobilised a significant mass of iron from the species and compounds it was stored in in the sediment. The physical re-suspension of deep sediment allowed iron-oxidising bacteria to dissolve ferric and insoluble ferrous hydroxide complexes, and non-biological oxidation to dissolve soluble ferric and ferrous hydroxide complexes (La Force *et al.*, 1998; Johnson *et al.*, 2005). The low pH of the water significantly slowed the rate at which the precipitates reformed and resulted in a significant increase in the dissolved iron concentration both within the dam as well as up and downstream. This is reflected in the data between April and July.

A peak also occurred in the sulfate flux of the dam, where the dam remobilised 20 502 $kg.day^{-1}$ sulfate or 7.8 $kg.day^{-1}.m^{-2}$ at the observation point in January, with no corresponding change in iron flux (likely because there was no change in pH and it remained circumneutral at 6.2 on average). When compared to the mass of sulfate flowing through the river inlet per day in the month of January (40 997 $kg.day^{-1}$) the 20 502 $kg.day^{-1}$ remobilised mass implies that the mass of sulfate in the water doubled; an extremely large increase from inlet to outlet. This value is the result of the difference in flux where the concentration of sulfate and discharge in the outflow were respectively 34% and 12% higher than the inflow. Dissolved particulates in the dust and masses of contaminants in the rain contributed negligibly (0.06 $kg.day^{-1}$ and 0.00009 $kg.day^{-1}$ respectively) to the mass balance equation while groundwater concentration was not measured.

This significantly high remobilisation (20 502 $kg.day^{-1}$) of sulfate might have originated from the dissolution of salts near the dam wall by rain, the net groundwater inflow (the concentration was not measured in January and thus not taken into account in the constituent mass balance) and/or fluxes from the sediment.

Quantification of the sulfate concentration in groundwater in January was not possible due to access delays, however the net groundwater discharge within the water balance was calculated at 3 369 $m^3.day^{-1}$. Back calculation of the mass balance equation allowed for determination of the groundwater sulfate concentration

needed to account for the sulfate flux of 20 502 kg.day^{-1} (where the sulfate flux of groundwater in January was the flux of sulfate in the outflows minus the inflows and then the groundwater sulfate flux was divided by the water flux to yield concentration). Assuming that groundwater was the only conduit of sulfate, then the concentration of sulfate in the groundwater during January would have been 6 084 mg. L^{-1}, 15 times greater than the maximum concentration measured in the groundwater (414 mg.L^{-1} in March) and 5.8 times greater than the maximum sulfate groundwater flux (3 559 kg.day^{-1} in March). Thus, if sampling error is not considered to be the cause of the peak flux in sulfate, then the flux can only be explained by a major groundwater contamination event. A groundwater contamination event would have been caused by overflow, spillage or seepage from a mining process water system such as a slimes dam upstream. Differences in the groundwater recharge regimen would account for the lack of a corresponding peak in sulfate concentrations in the Tweelopies River.

Groundwater demonstrably can have a large influence on the flux of contaminants in the dam. However, it is important to also note that the large influence of groundwater on the accumulation of sulfate in the Charles-Fourie Dam may only have occurred in January. During the months where the groundwater flux was quantified in the mass balance, it was determined that inclusion and exclusion of the groundwater flux only changed the accumulation of sulfate in the dam by 12% (Table 2, Figure 27).

Groundwater contained the greatest quantity of contaminants compared to dust and rain and appears to increase the iron and hydrogen ion concentrations in the outlet more than rain and dust. This was especially true before the pH of the river dropped in March.

Rain had a maximum concentration of 0.06 mg.L^{-1} iron, 77 mg.L^{-1} sulfate and a conductivity of 153 µS.cm^{-1}. All concentrations were well within the recommended guidelines for the protection of aquatic life (Department of Water Affairs and Forestry, 1996).

Dust contained a total of 0.6 kg SO_4^{2-} and 0.4 g Fe.day^{-1} across the study period. Despite the occurrence of a large, high intensity fire (flames in excess of ~2.5 m in height) (Figure 35), an hour after the July sampling was completed, the

conductivity and concentrations of iron and sulfate in the dust in August did not spike above the general trends observed previously. However, it is likely that ash did contribute some of the soluble concentrations of iron and sulfate measured in August.

Figure 35: Landscape of the Krugersdorp Game Reserve approximately an hour after a large fire event had been extinguished. The dam lies approximately 120 m downhill and to the left.

Although only soluble concentrations of iron and sulfate were measured in the dust, the low masses shed doubt on theories that dust blown off mine tailings facilities are a significant source of acid mine drainage (Diamond, 1995; Turton, 2013) specifically in the West Rand (Turton, 2013) where several large mine tailings facilities overlook the game reserve (~3.5 km south-west of the Charles-Fourie Dam).

4.2.5 Summary of key findings

General trends (excluding peak flux events) indicate that the Charles-Fourie Dam remobilised dissolved sulfate and iron in the river from the species and compounds it was stored in in the dam (increasing the total flux by 0.4% or 3 366 kg, and 8.7% or 202 kg respectively over eleven observation points). Thus there is evidence that damming of the river has impaired the water quality through the provision of a remobilisation conduit for dissolved sulfate and iron during the 2013-2014 study period. However, the dam also stored constituents concurrent with changes in pH. During a low pH period (pH 3.2 on average) the dam remobilised both dissolved iron and sulfate from the species and compounds it was stored in in the dam (18 219 kg SO_4^{2-} and 210 kg Fe respectively). However, during a period where the pH was more circumnetural (pH 6.7 on average) the dam stored both sulfate and iron (14 853 kg SO_4^{2-} and 5.5 kg Fe respectively) (where sulfate was stored in the form of a metal sulfate or sulfide). This evidence suggests that continual neutralisation of the water will decrease the degree to which the dam is remobilising contaminants.

4.2 Key Question 2: What is the estimated reservoir and accumulation of total sulfur and iron (AMD contaminants) in sediment of the Charles-Fourie Dam?

There are clear covariant trends in the mass of total sulfur and iron in the extracted core and a correlation coefficient of 0.75 (75.01%) which indicates a fairly strong correlation (Rubin, 2012). This implies that sulfur and iron contamination in the sediments are closely related. These data, although a concentration of total sulfur, compliment the results obtained in the water flux study indicating that the dam remobilised and acted as a sink of both sulfate and iron during periods of differing pHs in normalised flows. Therefore, both lines of evidence indicate that the flux of sulfate and iron are linked (likely through co-precipitation processes as explained above).

Data indicate that the sediments clearly contained variable concentrations of iron and sulfur (Table 5, Figure 32). The average concentrations of vanadium and copper (167 mg $Cu.kg^{-1}$, 120 mg $V.kg^{-1}$) complied with international standards of the

protection of aquatic life (Canadian Council of Ministers of the Environment, 2001; Aartila *et al.*, 2003). However, average concentrations of total iron, sulfur, nickel, lead, and zinc (120 972 mg $Fe.kg^{-1}$, 34 702 mg $S.kg^{-1}$, 1 000 mg $Ni.kg^{-1}$, 150 mg $Pb.kg^{-1}$, and 2 265 mg $Zn.kg^{-1}$) exceeded the maxima of the sediment quality guidelines for the protection of aquatic life (Table 2). The maxima guidelines represent the probable effect level, where adverse biological effects are always observed. Iron concentration exceeded the maxima guideline by 3 times, sulfur by 69 times, nickel by 20 times, lead by 1.6 times and zinc by 4.9 times (Canadian Council of Ministers of the Environment, 2001; Aartila *et al.*, 2003). Thus it is apparent that the concentrations of metals and total sulfur in the sediment are likely reducing the biodiversity of aquatic invertebrates, fish communities, macrophytes and microbial communities to a significant degree (Luoma & Rainbow, 2011).

Radiometric dating of the sediment core indicated that the core was re-worked or mixed. However, if it is assumed that only a limited degree of mixing or re-working occurred, it is possible to discuss potential trends in the concentration of total iron and sulfur with depth as there appear to be clear corresponding trends (Figure 32). Between a depth of 0 cm and 6.5 cm the concentrations of total sulfur and iron increased by 9.4 $g.cm^{-1}$ and 0.3 $g.cm^{-1}$ to respectively peak at 13.2 $g.cm^{-1}$ and 2.7 $g.cm^{-1}$. The sediment core was extracted in April 2014, therefore the lower 0 cm concentration of total iron and sulfur might be attributable to biological or non-biological oxidation of iron, sulfide and sulfate minerals in the sediments and/or physical resuspension as a result of flooding in March.

The 0 cm to 6.5 cm increases and peaks in the concentrations of total sulfur and iron might be representative of long term storage of AMD in the sediments during a period when the pH of the water was more circumneutral and sulfur and iron were stored in the dam. Historical studies conducted within 1 km of the inlet of the Charles-Fourie Dam (Figure 34) indicated that from at least 2006 (four years after the surface decant began) until 2010 the pH of the river may have remained circumneutral.

The concentration of total iron and sulfur significantly decreased by 70% and 77% respectively from the 6.5 cm to 10 cm depth interval, and thereafter remained relatively stable to 20.5 cm depth. On average the sediment core contained 22% organic matter, but the highest percentages of organic matter (44% and 41%) were

located between 16 cm and 20 cm. Given the interval of 3.5 cm and the high accumulation of organic matter, the 10 cm to 20.5 cm interval might represent the period from the dam's establishment in 1968 until 2006. Houel *et al.* (2006) demonstrated that following impoundment the organic content of the sediment in a dam increased three-fold which supports this hypothesis. Additionally, the older sediments of the dam will likely contain an increased amount of organic matter as the sediment might represent a time when upstream diversions, abstraction, municipal stormwater management and anthropogenic development within the catchment (specifically large scale mining activities which have cleared a significant amount of vegetation) were significantly lower (van Metre & Callender, 1996; Findlay *et al.* 2001). In the past the river channel and associated riparian zone would likely have been significantly greater in extent generating a greater amount of organic debris than the present (Allan, 2004), and might have received a greater amount of stormwater containing organic debris. The organic matter content of the sediment core significantly decreases from 20.5 cm and the lowest percentage of organic matter (10%) is recorded at 27 cm. The 20.5 cm to 27 cm section might then represent river sediment (which is usually low in organic matter due to the fluvial nature of rivers (Boehrer & Schultze, 2008) in the area before the dam was developed i.e. pre-1968.

It should be noted that the above discussion of trends in the sediment core should be considered with great caution given that radiometric dating indicated that the sediment core had been mixed or reworked. In this instance it is considered prudent to apply the precautionary principle and assume that the sediment core was completely mixed. If it is assumed that the sediment core was completely mixed, no local baseline of sediment considered "tailings free" can be used for comparison. However, it is still considered useful to compare the concentration of major and minor ions in the sediment of the Charles-Fourie Dam with the sediment of another watercourse unaffected by AMD contamination. The concentration of iron, lead and zinc in the sediments of the Charles-Fourie Dam are four, two and three times higher respectively than uncontaminated lake sediments in the Coeur d'Alene lake delta region (Harrington *et al.*, 1998). This region is also being influenced by AMD contamination and therefore is a useful site of comparison, considering no local baseline is available. The concentrations of constituents (iron and zinc) are within a

similar range to the Coeur d'Alene lakes that have been exposed to a century of sulfidic ore mining (Table 6). Thus the comparable concentrations of contaminants in the Charles-Fourie Dam (information on other elements was not available) reflect major relatively short-term pollution from acid mine drainage.

Table 6: Mean concentrations of total iron and zinc in the Charles-Fourie Dam and Lake Coeur d'Alene (Harrington *et al.,* 1998).

	Mean concentrations in the Charles-Fourie Dam ($mg.kg^{-1}$)	Mean concentrations in Coeur d'Alene Lake ($mg.kg^{-1}$)
Iron	120 972	82 486
Zinc	2 265	2 995

Primarily, iron and sulfur in the sediment of the Charles-Fourie Dam are likely to be in the form of precipitates sorbed to organic matter particulates (Harrington *et al.*, 1998; Cummings *et al.*, 2000). The amount of organic matter in the sediment core (22%) provides some evidence for this supposition. Studies have previously directly demonstrated that bacteria decompose organic debris and increase iron and sulfate concentrations in the water (Box *et al.*, 2005; Johnson *et al.*, 2005; Luoma & Rainbow, 2011). Organic matter content in sediments of dams older than 30 years are typically lower than 22% and range between 3 and 10% (Ghrefat & Yusuf, 2006; Dean, 2006; Çevik *et al.*, 2009). Thus these data indicate that the Charles-Fourie Dam is likely a highly depositional system containing an atypically high amount of detritus, likely coated in AMD precipitates prior to deposition and that could support a large decomposer community and provide a significant conduit by which dissolved sulfate and iron are remobilised.

Assuming that the average sediment depth in the dam was 19.3 cm, 18 tons of total iron and 5 tons of total sulfur were contained within the sediment of the Charles-Fourie Dam. Eighteen tons of iron is a relatively small amount of iron compared to 37 000 000 tons extracted per year by a large South African iron mine (Anglo American, 2013). The same is true for sulfur – mining operations in the United States that are considered small produce around 100 000 tons of sulfur per year (United States Geological Survey Mineral Resources Programme *et al.*, 2001), thus 5 tons of sulfur is a small amount. With the price of iron set at ~$81 US per metric ton (Index Mundi, 2014) and sulfur at around $160 per ton (U.S. Geological Survey,

2012), this sediment does not contain enough contaminants to be economically feasible for mining.

In a geochemical cycle it is important to evaluate whether the quantitative data for fluxes and pools complement each other in order to provide parallel lines of evidence supporting any conclusions made. However, it is evident that in the short term (the 2013-2014 study period) the dam remobilised dissolved iron and sulfate (dependent upon pH) from the species and compounds it was stored in in the dam, but the accumulation of elevated levels of metals and total sulfur in the sediment indicate that in the long term the dam acted as a sink. The conclusions drawn from the water flux assessment indicate that the dam acted as a sink of iron and sulfate for a portion of the study period that was characterised by water with a circumneutral pH. This finding, paired with the pH timeline that has been constructed (Figure 34), indicates that historically the Tweelopies River has experienced extended periods of circumneutral pH interrupted by short periods of low pH. This explains why and how the Charles-Fourie Dam acted as a long-term sink, but overall remobilised dissolved AMD contaminants in the short term (sulfur and iron) from the species and compounds it was stored in in the dam.

4.3 Key question 3: Do the sediments of the dam show reliable temporal trends?

The longest core taken from the Charles-Fourie Dam did not display consistent radiometric activity and was considered mixed (Table 1). The core was probably reworked due to substantial fluxes between the sediment and water, a short residence time, as well as bioturbation from the two hippopotami living in the reserve. Changes in hydrostatic pressure and turbidity currents generated by varying river discharges into the dam would also have mixed sediment, particularly in conjunction with the less saline groundwater influx likely causing density driven mixing (Cesare *et al.*, 2001; Boehrer & Schultze, 2008). However, sediment cores had never before been taken from this dam, nor any other dam in South Africa experiencing AMD contamination as far as could be determined by a review of the available literature. Therefore, these results still provide valuable data including an estimate of sediment stored in the dam, determination that the chemical content of

the sediment is detrimental to aquatic life, that the organic content of the sediment core supports theories generated from the water quality flux data and that the total iron and sulfur content in the sediment do not constitute a viable economic opportunity.

4.4 Acknowledgement of short-comings and limitations

This study estimated that the average net groundwater exchange (533 $m^3.day^{-1}$) constituted approximately 1.6% of the average inflow of the river (34 081 $m^3.day^{-1}$). However, net groundwater exchange into a watercourse is inherently challenging to measure directly and indirect measurement, as conducted in this study, can only be considered as a rough estimate (Kalbus *et al.*, 2006). Unfortunately, equipment to directly measure net groundwater flux (such as bag-type seepage meters and heat pulse meters) were not available and were also considered dangerous and impractical to use regularly due to the frequent presence of hippopotami in the dam. Although this study did indirectly quantify net groundwater exchange it utilised two USGS approved methods for such a determination (Rosenberry & LaBaugh, 2008); 1) a water balance quantifying in-stream flow, rain and evaporative loss, and 2) direct measurement of local groundwater levels in a nearby borehole. The results of each method employed complement each other, thus the error in estimation of groundwater is likely to be limited and not significantly bias the results of the mass constituent balance.

The lack of data available on groundwater quality from September 2013 to January 2014 may be a source of error for retention and release of contaminants during these months. Unfortunately, administrative procedures and scheduling of the National Groundwater Archive of the Department of Environmental Affairs (who own the boreholes sampled) only allowed for supervised and approved sampling of the groundwater to begin in February (pH and conductivity measurements reported in October were recorded by the department alone before the requests from this project were approved). Although the error is likely to be small in the month of September (as little groundwater entered the dam) from October to January relatively high discharges did enter the dam. In November, December and January groundwater discharges were of similar values and – based on the groundwater data that is

available – are likely to have had similar salinities, which lend some reliability when comparing results between these months.

A bailer was used to collect groundwater samples from a borehole in close proximity to the Charles-Fourie Dam. A limitation of the study is that the borehole was not purged. The water sampled from the lower depths of the borehole likely contains a higher content of dissolved oxygen than groundwater in a sealed environment (which is inherently oxygen deficient). Therefore, there may be some degree of error in the content of iron in the groundwater sample collected. This is based on the reduction-oxidation reactions of iron, which can change the species of iron present in the water.

Additionally, the best practice sampling protocol for the extraction of groundwater is for the borehole to be purged prior to the extraction of a sample, in order to ensure that the water column is mixed. The DWS NGA field technician indicated that he had previously compared borehole water extracted with a purging vehicle against borehole water extracted with a bailer at the borehole sampled in the Krugersdorp Game Reserve and others in the area. Moolman indicated that in his opinion the quantified data did not differ when the two different methods were used (*pers. comm,* T. Moolman). Therefore, based on his more than twenty years of experience, any degree of error between the two methods used is likely to be limited.

The dam's inlet and outlet were only sampled once a month (except during a week in February, April and July, two consecutive days in October and three consecutive days in March). This casts some doubt on the reliability of trends reported during certain months. Statistical analysis of data in April and July – which each spanned a week of consecutive sampling days – showed a large amount of variation from the start to the end of each week (Figure 17). Thus one observation point in each month cannot be considered as a good representative for the month and the observations can only be viewed as 12 points taken in a time series spanning a year.

The total deposition of sulfur, sulfide, sulfate and iron precipitates into the dam encompassed organic detritus as well as suspended solid and particulate matter. However, only the inflow and outflows of the dissolved forms of iron and sulfate were directly measured, which is why the mass constituent balance only shows these

fluxes. As organic detritus, suspended solids and particulate matter entering and exiting the dam were not measured, the conduit for the flux of dissolved sulfate and iron cannot be conclusively determined. However, the significantly high (22%) organic content of the sediment, together with the literature (Harrington *et al.*, 1998; Cummings *et al.*, 2000; Box *et al.*, 2005; Johnson *et al.*, 2005; Luoma & Rainbow, 2011), do provide support that the dominant conduit of the dissolved fluxes was likely organic matter coated in sulfide, sulfate and iron precipitates. Although not all of the mass flows of dissolved iron and sulfate were quantified the aim of the study, to determine dissolved fluxes, was still met.

5 CONCLUSIONS AND RECOMMENDATIONS

The accumulation of elevated levels of metals and non-metals in the sediment indicated that in the long term the dam stored both total sulfur and iron. However, the accumulation of this pool has also enabled the dam to become a conduit for the re-mobilisation of dissolved sulfate and iron from the species and compounds it was stored in in the dam during periods when the pH in the Tweelopies River was low. This was indicated by the mass balance, whereby normalised flows indicate that the Charles-Fourie Dam remobilised dissolved sulfate from the species and compounds it was stored in in the dam over the 2013-2014 study period, increasing the dissolved sulfate flux in the river by 0.4% or 3 366 kg in total over eleven observation points. Additionally, the Charles-Fourie Dam remobilised dissolved iron from the species and compounds it was stored in in the dam during normalised flows over the 2013-2014 study period, increasing the flux of dissolved iron in the river by 8.7% or 202 kg. Thus there is evidence that damming of the river has impaired the water quality through the creation of a store of sulfate-, sulfide- and iron-rich precipitates, which can be remobilised into dissolved sulfate and iron from the species and compounds it was stored in in the dam.

Fluxes of dissolved iron and sulfate were highly dependent upon pH and the dam remobilised both dissolved iron and sulfate (18 219 kg SO_4^{2-} and 210 kg Fe respectively) under low pH (2.9 – 3.6) conditions. However, during a period where the pH was more circumnetural (pH 6.1 – 7.6) the dam acted as a sink of both sulfate and iron (14 853 kg SO_4^{2-} and 5.5 kg Fe). This finding, paired with the pH timeline that has been constructed, provides some evidence that historically the Tweelopies River may have experienced extended periods of circumneutral pH interrupted by short periods of low pH, similar to the pH changes recorded in this study. Available evidence suggests that pH is the main driver causing the Charles-Fourie Dam to act as a long-term sink, but also as a periodic short-term conduit for the remobilisation of AMD constituents, as quantified during the 2013-2014 study period. Evidence indicates that neutralisation of the water through liming limits the degree to which dissolved contaminants are remobilised from the species and compounds they are stored in in the dam. Additionally, if liming is discontinued, and the pH remains low for an extended period of time, the dam might confound rehabilitation efforts (including decreasing biodiversity).

Total iron, sulfur, nickel, lead and zinc were present in the sediment at concentrations detrimental to the protection of aquatic life. Therefore, even with improvements in water quality, benthic micro-flora and micro-faunal biodiversity would likely remain low for an extended period of time. Additionally, bioturbation of the sediments could cause short-term pollution plumes through the exposure and oxidation of iron sulfide complexes that were stored in the sediment – this could possibly confound fish stocking of the dam. Future management plans should avoid high investment loss to short-term remediation efforts and rather take a long-term approach that incorporates these findings.

Surface runoff during the wet season likely caused a major decant of AMD into the river in March, increasing discharge of the river by 237%, decreasing the pH by four units, and increasing the concentration of iron and sulfate in the water by 173 times and 1.3 times respectively between February and March. Iron and sulfate concentrations in the river then remained higher (688 times and 1.3 times on average) between March and July compared to September to February. As the amount of rainfall has been very typical of the area since 2000 (World Weather Online, 2013) it is clear that the current treatment strategy needs to be re-evaluated to take rainfall considerations into account. In the short term, the water capacity of the new neutralisation plant at the surface decant point, which is currently between 25 and 35 million litres per day, should be at least doubled. In the long term, the flooded mine shaft and associated workings should be de-watered via continuous pumping. Water should be continually extracted from this aquifer in order to lower water levels to beneath the underground mining operations and thereby limit generation of AMD by limiting the exposure of pyrite to water. The water that is pumped from the aquifer should be treated if required - as it may be polluted from other mining activities in the area. Alternatively, the low pH of the AMD currently contaminating the aquifer might have dissolved some of the underlying dolomite and exposed an additional pyrite ore body. The treatment of water should encompass high loads during the wet season and treated effluent should be released back into the Tweelopies River so as to dilute any contaminated groundwater seepages downstream (however these will likely also have been reduced as a consequence of de-watering the aquifer). Concurrent liming (with calcium oxide) downstream will also address seepages of contaminated groundwater by increasing the pH and removing

iron from the water. Liming should be intensified during the wet season, for the entire length of the river, and possibly beyond (depending upon the extent of groundwater contamination). This will induce the precipitation of iron and, as the mass constituent balance has shown, decrease the flux of dissolved sulfate and iron remobilised from the species and compounds they are stored in in the dam. Additionally, as less AMD is generated upstream less debris and sediments coated in sulfide, sulfate and iron precipitates will enter and be stored in the dam.

Annual water monitoring of the West Wits Pit should be reported to the Department of Water and Sanitation (as required for permissible mining operations (Department of Water Affairs and Forestry,1998)). Should this annual report note overflows of process water from the containment facilities and spikes in groundwater contamination, then the mine/s must be subject to an audit and potentially held liable for damages to the Krugersdorp Game Reserve and downstream users. It is recommended that the Krugersdorp Game Reserve and other downstream receiving bodies (such as the Cradle of Humankind) investigate this matter with the (current) Department of Water and Sanitation, with particular mention of groundwater quality in January and surface and process water quality in March 2014 (including that of slimes dams and waste water).

The mass sulfate and iron balance data suggest that removal of the organic matter (via dam dredging or upstream netting) would remove a conduit by which dissolved sulfate and iron is remobilised. However, the dam only increased the dissolved sulfate and iron flux of surface outflow by 0.4% and 8.7% respectively. Thus the effort and cost of dredging might be better spent on alternative remediation measures. It is recommended that the feasibility of this and the other mitigation measures mentioned above, be investigated when next an environmental management plan is compiled for the Krugersdorp Game Reserve.

6 LITERATURE CITED

Aartila, T., Amrhein, J., Brunette, M., Fitzpatrick, B., Galarneau, S., Grefe, B. & Hosch, J., 2003. Consensus-Based Sediment Quality Guidelines report WT-732 2003. Available at: http://dnr.wi.gov/topic/brownfields/documents/cbsqg_interim_final.pdf.

Abbot, R., 2005. Loss on Ignition (LOI) procedures. Available at: http://www.pitt.edu/~mabbott1/climate/mark/Teaching/GEOL_3931_PaleoAnalysis/0909LOIProtocol.pdf.

Adler, R.A., Claassen, M., Godfrey, L. & Turton, A., 2007. Water, mining and waste: an historical and economic perspective on conflict management in South Africa. *The economics of peace and security journal*, 2(2), pp.32–41.

Akcil, A. & Koldas, S., 2006. Acid Mine Drainage (AMD): causes, treatment and case studies. *Journal of Cleaner Production*, 14(12), pp.1139–1145.

Allan, J. D. 2004. Landscapes and Riverscapes: the influence of land use on stream ecosystems. *School of Natural Resources and Environment, University of Michigan, Michigan*.

Alavian, V., Gerhard, H.J., Denton, R.A., Johnson, M.C., & Heinz, G.S. 1992. Density currents entering lakes and reservoirs. *Journal of Hydraulic Engineering*, 118(11), pp. 1464–1489.

Albrecht, A., Reiser, R., Luck, A., Stoll, J.A, & Giger, W., 1998. Radiocaesium dating of sediments from lakes and reservoirs of different hydrological regimes. *Environmental science & technology*, 32(13), pp.1882–1887.

Anglo American, 2013. Kumba Iron Ore Limited. Integrated report 2012.

Baker, B.J. & Banfield, J.F., 2003. Microbial communities in acid mine drainage. *FEMS Microbiology Ecology*, 44(2), pp.139–152.

Bartram, J. & Ballance, R., 1996. *Water quality monitoring: a practical guide to the design and implementation of freshwater quality studies and monitoring programmes*, CRC Press.

Bege, S., 2014. New treatment plant opened as acid water pours. *The federation for a sustainable environment*. Available at

http://www.fse.org.za/index.php/water/item/365-new-treatment-plant-opened-as-acid-water-pours.

Bencala, K. E., & Ortiz, R. F., 1999. Theory and(or) reality: analysis of sulfate mass-balance at Summitville, Colorado poses process questions about the estimation of metal loadings. *U.S. Geological Survey Toxic Substances Hydrology Program - Proceedings of the Technical Meeting, Charleston, South Carolina.*

Boehrer, B. & Schultze, M., 2008. Stratification of lakes. *Reviews of Geophysics*, 46(2). Available at: http://doi.wiley.com/10.1029/2006RG000210 [Accessed November 3, 2014].

Bowman, J., 2009. Acid Mine Drainage abatement and treatment plan for Upper Rush Creek Watershed. *Ohio University, Ohio*.

Box, S.E., Bookstrom, A.A. & Ikramuddin, M., 2005. *Stream-sediment geochemistry in mining-impacted streams: sediment mobilized by floods in the Coeur d'Alene-Spokane River system, Idaho and Washington*, US Department of the Interior, US Geological Survey. Available at: http://pubs.usgs.gov/sir/2005/5011/ [Accessed June 16, 2015].

Brock, T. D., & J., Gustafson. 1976. Ferric Iron Reduction by Sulfur- and Iron-oxidising Bacteria. *Applied and Environmental Microbiology* (32)4, pp 567-571.

Brown, T.L., 2009. Chemistry: *The Central Science*. Pearson Education.

Bruker AXS GmbH, 2013. Document-B80-EXS006, Bruker S2 Ranger. *Bruker AXS GmbH.*

Bruyns, L., 2013. Phytoremediation of acid mine drainage using commonly occuring aquatic macrophytes. University of the Witwatersrand, Johannesburg.

Bushaw-Newton, K.L., Ashley, J.T., Boettner, A.R., De Alteris, J., Kiry, P., Kreeger, D.A., Raksany, D. & Velinsky, D.J., 2001. The Manatawny Creek dam removal: biogeochemical processes and sediment contaminants. Drexel University. Available at: http://www.ansp.org/research/environmental-research/projects/manatawny/references/ [Accessed January 14, 2015].

Canadian Council of Ministers of the Environment, 2001. Canadian Environmental Quality Guidelines. Available at http://st-ts.ccme.ca/en/index.html.

Cesare, G.D., Schleiss, A. & Hermann, F., 2001. Impact of turbidity currents on reservoir sedimentation. *Journal of Hydraulic Engineering*, 127(1), pp.6–16.

Çevik, F., Goksu, M.Z.L., Derici, O.B., & Findik, O., 2009. An assessment of metal pollution in surface sediments of Seyhan dam by using an enrichment factor, geo-accumulation index and statistical analyses. *Environmental Monitoring and Assessment*, 152(1-4), pp.309–317.

Chamber of Mines South Africa, 2012. *Facts and Figures 2012*, Johannesburg, South Africa: Chamber of Mines South Africa. Available at: www.chamberofmines.org.za.

Charles, D.F., Whitehead, D.R., Goldstein, R.A., 1990. Paleo-ecological investigation of recent lake acidification in the Adirondack Mountains, N. Y. *Journal of Paleolimnology*, 3, pp.195–241.

Chen, C.J. & Jiang, W.T., 2012. Influence of waterfall aeration and seasonal temperature variation on the iron and arsenic attenuation rates in an acid mine drainage system. *Applied Geochemistry*, 27(10), pp.1966–1978.

Chen, D. & Chen, H.W., 2013. Using the Köppen classification to quantify climate variation and change: an example for 1901–2010. *Environmental Development*, 6, pp.69–79.

Chuan, M.C., Shu, G.Y. & Liu, J.C., 1996. Solubility of heavy metals in a contaminated soil: effects of redox potential and pH. *Water, Air, and Soil Pollution*, 90(3-4), pp.543–556.

Coetzee, H., Chirenje, E., Hobbs, P. & Cole, J., 2009. Ground and airbourne geophysical surveys identify potential subsurface acid mine drainage pathways in the Krugersdorp Game Reserve, Gauteng Province, South Africa. In 11th SAGA Biennial Technical Meeting and Exhibition. Swaziland.

Costello, C., 2003. Acid mine drainage: Innovative treatment technologies. *National Network of Environmental Management Studies Fellow for US Environmental Protection Agency, Washington, DC*. Available at: http://helsenet.info/pdf/drainage/6.pdf [Accessed April 13, 2013].

Cummings, D.E., March, A., Bostick, B., Spring, S., Caccavo, F., Fendorf, S. & Rosenzweig, R.F., 2000. Evidence for Microbial Fe(III) Reduction in Anoxic, Mining-Impacted Lake Sediments (Lake Coeur d'Alene, Idaho). *Applied and Environmental Microbiology*, 66(1), pp.154–162.

Dabrowski, J., Oberholster, P.J., Dabrowski, J.M., Le Brasseur, J. & Gieskes, J., 2013. Chemical characteristics and limnology of Loskop Dam on the Olifants River (South Africa), in light of recent fish and crocodile mortalities. *Water SA*, 39(5), pp.675–686.

Daneshmand, S., Mortaji, A. & Mortaji, Z., 2012. Investigation and design of seawater desalination with solar energy. *Life Science Journal*, 9(3), pp.770–773.

Dasch, J.M, 1985. Direct Measurement of Dry Deposition to a Polyethylene Bucket and Various Surrogate Surfaces. *Environmental Science & Technology* 19(8), pp. 721–25.

Dean, W.E., 2006. *Characterization of organic matter in lake sediments from Minnesota and Yellowstone National Park*, U.S. Geological Survey.

Department of Agriculture and Rural Development, 2014. SA: Statement by the Department of Agriculture and Rural Development, on the Gauteng's plan to avoid Acid Mine Drainage. Available at: http://www.polity.org.za/article/sa-statement-by-the-department-of-agriculture-and-rural-development-on-the-gautengs-plan-to-avoid-acid-mine-drainage-30042014-2014-04-30

Department of Water Affairs, 2010. List of registered Dams - September 2009. Available at: https://www.dwaf.gov.za/DSO/Documents/List%20of%20Registered%20Dams%20Oct%202011.xls

Department of Water Affairs, the Council for Geoscience, Department of Mineral Resources, Council for Scientific and Industrial Research, Mintek and the Water Research Commission, 2010. Mine Water Management in the Witwatersrand Gold Fields with special emphasis on acid mine drainage. Report to the inter-ministerial committee on acid mine drainage, Pretoria.

Department of Water Affairs, 2012. Classification of significant water resources in the Mokolo Catchment: Limpopo Water Management Area (WMA) and Crocodile (West) and Marico WMA: WP 10506. Available at: https://www.dwa.gov.za/rdm/WRCS/doc/Gap%20Analysis%20Report_Croc%20West%20and%20Marico_final_29%20Mar%20l12.pdf

Department of Water Affairs and Forestry, 1998. Republic of South Africa National Water Act. Act No 36 of 1998. Available at: https://www.dwaf.gov.za/Documents/Legislature/nw_act/NWA.htm.

Department of Water Affairs and Forestry, 1996. South African Water Quality Guidelines Volume 7: Aquatic ecosystems. First Edition. Available at: https://www.capetown.gov.za/en/CSRM/Documents/Aquatic_Ecosystems_Guidelines.pdf.

Diamond, M.L., 1995. Application of a mass balance model to assess in-place arsenic pollution. *Environmental science & technology*, 29(1), pp.29–42.

Dunn, J.G., 1997. The oxidation of sulfide minerals. *Thermochimica Acta* 300(1-2), pp.127-139.

Els, B.G., Van den Berg, W.A. & Mayer, J.J., 1995. The Black Reef Quartzite Formation in the western Transvaal: sedimentological and economic aspects, and significance for basin evolution. *Mineralium Deposita*, 30(2), pp.112–123.

Findlay, S., Quinn, J. M., Hickey, C. W., Burrell, G., & Downes, M. 2001. Effects of land use and riparian flowparth on delivery of dissolved organic carbon to streams. *American Society of Limnology and Oceanography, Inc*. 46(2), pp. 345 - 355.

Friedrich, C. G., Rother, D., Bardischewsky, F., Quentmeier, A., and Fischer, J., 2001. Oxidation of reduced inorganic sulfur compounds by bacteria: emergence of a common mechanism. *Applied and Environmental Microbiology*, 67(7), pp.2873-2882.

Gerloff-Elias, A., Spijkerman, E. & Pröschold, T., 2005. Effect of external pH on the growth, photosynthesis and photosynthetic electron transport of Chlamydomonas acidophila Negoro, isolated from an extremely acidic lake (pH 2.6). *Plant, Cell & Environment*, 28(10), pp.1218–1229.

Ghrefat, H. & Yusuf, N., 2006. Assessing Mn, Fe, Cu, Zn, and Cd pollution in bottom sediments of Wadi Al-Arab Dam, Jordan. *Chemosphere*, 65(11), pp.2114–2121.

Gibert, O., de Pable, J., Luis Cortina, J. & Ayora, C., 2004. Chemical characterisation of natural organic substrates for biological mitigation of acid mine drainage. *Water Research*, 38(19), pp.4186–4196.

Gold One International Limited, 2012. *Completion of the Rand Uranium Acquisition Senior Corporate Appointments*, Johannesburg: Gold One International Limited.

Google Earth 6.0, 2014. *Krugersdorp Game Reserve, 26° 5'18.53"S 27°42'55.27"E, elevation 1 594m.*

Grande, J.A., Beltran, R., Sainz, A., Santos, J.C., de la Torre, M.L. & Borrego J., 2004. Acid mine drainage and acid rock drainage processes in the environment of Herrerias Mine (Iberian Pyrite Belt, Huelva-Spain) and impact on the Andevalo Dam. *Environmental Geology*, 47(2), pp.185–196.

Gray, N.F., 1998. Acid mine drainage composition and the implications for its impact on lotic systems. *Water Research*, 32(7), pp.2122–2134.

Gray, N.F., 1997. Environmental impact and remediation of acid mine drainage: a management problem. *Environmental Geology*, 30(1-2), pp.62–71.

Hach Company, 2013. *Hach DR/890 Colorimeter Procedures Manual*, Hach Company.

Harries, J., 1997. *Acid Mine Drainage in Australia: Its extent and potential future liability*, Canberra: Environment Australia.

Harrington, J.M., La Force, M.J., Rember, W.C., Fendorf, S.E. & Rosenzweig, R.F., 1998. Phase associations and mobilization of iron and trace elements in Coeur d'Alene Lake, Idaho. *Environmental science & technology*, 32(5), pp.650–656.

Hauer, F.R. & Lamberti, G.A., 2011. *Methods in stream ecology*, Academic Press. Available at:http://books.google.co.za/books?hl=en&lr=&id=rlclsSCF_dQC&oi=fnd&pg=PP2&dq=Methods+in+stream+ecology.+Amsterdam%3B+Boston:+Academic

+Press/Elsevier%3B+2006.&ots=4wzD4YmQEi&sig=Z_9R9Hwp8MJRVFqB74oSbgu78Lw [Accessed November 10, 2014].

Hedin, R.S., 2003. Recovery of marketable iron oxide from mine drainage in the USA. *Land Contamination and Reclamation*, 11(2), pp.93–98.

Hem, J.D., & W.H., Cropper. 1959. Chemistry of iron in natural water: Survey of ferrous-ferric chemical equilibria and redox potentials. *Geological Survey Water-Supply* (1459), pp: 1 - 33.

Hem, J.D., 1975. *Study and Interpretation of the Chemical Characteristics of Natural Water: Second Edition*, United States Government Printing Office.

Herlihy, A.T. & Mills, A.L., 1985. Sulfate reduction in freshwater sediments receiving acid mine drainage. *Applied and environmental microbiology*, 49(1), pp.179–186.

Hobbs, P.J. & Cobbing, J.E., 2007. The hydrogeology of the Krugersdorp Game Reserve area and implications for the management of mine water decant. In *Groundwater Division of the Geological Society of South Africa Conference, Bloemfontein, October*.

Hontelez, J., 2000. *The environmental performance of the mining industry and the action necessary to strengthen European legislation in the wake of the Tisza-Danube pollution*, Brussels: European Environmental Bureau.

Houel, S., Louchouarn, P., Lucotte, M., Canuel, R., & Ghaleb, B. 2006. Translocation of soil organic matter following reservoir impoundment in boreal systems: Implications for *in situ* productivity. *The American Society of Limnology and Oceanography, Inc.* 51(3), pp. 1497 - 1513.

Hudson-Edwards, K.A., Schell, C. & Macklin, M.G., 1999. Mineralogy and geochemistry of alluvium contaminated by metal mining in the Rio Tinto area, southwest Spain. *Applied Geochemistry*, 14(8), pp.1015–1030.

Index Mundi, 2014. Iron Ore Monthly Price. Available at: http://www.indexmundi.com/commodities/ [Accessed 28 July, 2015].

International Atomic Energy Agency, 2003. Guidelines for radioelement mapping using gamma ray specrometry data. Nuclear Fuel Cycle and Materials Section of the International Atomic Energy Agency, Vienna, Austria.

Johnson, D.B. & Hallberg, K.B., 2005. Acid mine drainage remediation options: a review. *Science of the total environment*, 338(1), pp.3–14.

Johnson, V.G., Peterson, R.E. & Olsen, K.B., 2005. Heavy Metal Transport and Behavior in the Lower Columbia river, USA. *Environmental Monitoring and Assessment*, 110(1-3), pp.271–289.

Kalbus, E., Reinstorf, F. & Schirmer, M., 2006. Measuring methods for groundwater, surface water interactions: a review. *Hydrology and Earth System Sciences Discussions*, 10(6), pp.873–887.

Keyser, N. & The Council for Geoscience, 1986. Metallogeny of the West Rand area: 2626 Wes-Rand. The Council for Geoscience.

Kirby, C.S., Dennis, A. & Kahler, A., 2009. Aeration to de-gas CO_2, increase pH, and increase iron oxidation rates for efficient treatment of net alkaline mine drainage. *Applied Geochemistry*, 24(7), pp.1175–1184.

Küsel, K., Roth, U., Trinkwalter, T. & Peiffer, S., 2001. Effect of pH on the anaerobic microbial cycling of sulfur in mining-impacted freshwater lake sediments. *Environmental and Experimental Botany*, 46(3), pp.213–223.

La Force, M.J., Fendorf, S.E., Li, G.C., Schneider, G.M. & Rosenzweig, R.F., 1998. A Laboratory Evaluation of Trace Element Mobility from Flooding and Nutrient Loading of Coeur d'Alene River Sediments. *Journal of Environment Quality*, 27(2), p.318.

Luoma, S.N. & Rainbow, P.S., 2011. *Metal Contamination in Aquatic Environments: Science and Lateral Management* Reissue., Cambridge University Press.

Luther, G.W., Findlay, A.J., MacDonald, D.J., Owings, S.M., Hanson, T.E., Beinart, R.A. & Girguis, P.R., 2011. Thermodynamics and Kinetics of Sulfide Oxidation by Oxygen: A Look at Inorganically Controlled Reactions and Biologically Mediated Processes in the Environment. *Frontiers in Microbiology*, 2. Available at: http://www.ncbi.nlm.nih.gov/pmc/articles/PMC3153037/ [Accessed October 30, 2014].

Machel, H.G., 1989. Relationships between sulfate reduction and oxidation of organic compounds to carbonate diagenesis, hydrocarbon accumulations, salt

domes, and metal sulfide deposits. *Carbonates and Evaporites*, 4(2), pp.137–151.

Maree, J., Theron, D., Nengovhela, R. & Hlabela, P., 2005. Sulfur from smelter gases and sulfate-rich effluents. In The Third Southern African Conference on Base Metals. South African Institute of Mining and Metallurgy, p. 641. Available at: http://www.platinum.org.za/Kitwe2005/515-522_Maree.pdf [Accessed December 9, 2014].

McCarthy, T.S., 2011. The impact of acid mine drainage in South Africa. *South African Journal of Science*, 107(5/6). Available at: http://www.sajs.co.za/index.php/SAJS/article/view/712 [Accessed October 20, 2012].

McCullough, C.D. & Lund, M.A., 2006. Opportunities for sustainable mining pit lakes in Australia. *Mine water and the environment*, 25(4), pp.220–226.

McCully, P., 1996. *Silenced rivers: the ecology and politics of large dams.*, Zed Books. Available at: http://www.cabdirect.org/abstracts/19971801995.html [Accessed November 4, 2014].

Meade, R.H., 1982. Sources, sinks, and storage of river sediment in the Atlantic drainage of the United States. *The Journal of Geology*, pp.235–252.

Michalková, E., Schwarz, M., Pulisova, P., Masa, B. & Sudovsky, P., 2013. Metals recovery from acid mine drainage and possibilities for their utilization. *Polish Journal of Environmental Studies*, 22(4). Available at: http://www.pjoes.com/pdf/22.4/Pol.J.Environ.Stud.Vol.22.No.4.1111-1118.pdf [Accessed December 9, 2014].

Moreno-Amich, R., & Garcia-Berthou, E., 1989. A new bathymetric map based on echo-sounding and morphometrical characterization of the Lake of Banyoles (NE-Spain). *Hydrobiologica* 185(1), pp. 83-90.

Moses, C.O., Nordstrom, D.K., Herman, J.S. & Mills, A.L., 1987. Aqueous pyrite oxidation by dissolved oxygen and by ferric iron. *Geochimica et Cosmochimica Acta*, 51(6), pp.1561–1571.

National Research Council - Division on Earth and Life Studies, Committee on Superfund Site Assessment and Remediation in the Coeur d' Alene River

Basin & Board on Environmental Studies and Toxicology, 2005. *Superfund and mining megasites: lessons from the Coeur D'Alene River Basin.*, Washington D.C.: The National Academies Press. Available at: http://earth1.epa.gov/superfund/accomp/coeur/pdfs/coeur.pdf. [Accessed 7 June, 2015).

Nicholas, D.J.D., 1967. Biological sulfate reduction. *Mineralium Deposita*, 2(3), pp.169–180.

Nordstrom, D.K., 2011. Mine Waters: Acidic to Circumneutral. *Elements*, 7(6), pp.393–398.

Nordstrom, D.K., Alpers, C.N., Ptacek, C.J. & Blowes, D.W., 2000. Negative pH and Extremely Acidic Mine Waters from Iron Mountain, California. *Environmental Science & Technology*, 34(2), pp.254–258.

Nordstrom, D.K. & Alpers, C.N., 1999. Negative pH, efflorescent mineralogy, and consequences for environmental restoration at the Iron Mountain Superfund site, California. *Proceedings of the National Academy of Sciences*, 96(7), pp.3455–3462.

Oelofse, S.H.H., Hobbs, P.J., Rascher, J. & Cobbing, J.E., 2007. The Pollution and Destruction Threat of Gold Mining Waste on the Witwatersrand: A West Rand Case Study. In *10th International Symposium on Environmental Issues and Waste management in Energy and Mineral Production (SWEMP, 2007), Bangkok*. pp. 11–13. Available at: http://www.infomine.com/publications/docs/oelofse2007b.pdf [Accessed March 23, 2013].

Olsen, K.A.A., Drake, D.C. & Harrison, J., 2012. *Natural Remediation of Acid Mine Drainage in the Tweelopiespruit, Krugersdorp, South Africa.* Honours research report. University of the Witwatersrand.

Osbourne, J.W. & Overbay, A., 2004. The power of outliers (and why researchers should always check for them). *Practical Assessment, Research & Evaluation.*, 9(6).

Oxford Business Group. 2012. The Report: South Africa 2012. *Oxford Business Group*.

Rosenberry, D.O. & La Baugh, J.W., 2008. Field techniques for estimating water fluxes between surface water and ground water: U.S. Geological Survey Techniques and Methods 4-D2. Available at: http://pubs.usgs.gov/tm/04d02/.

Rubin, A., 2012. *Statistics for Evidence-Based Practice and Evaluation*, Cengage Learning.

Runkel, R.L. & Kimball, B.A., 2002. Evaluating remedial alternatives for an acid mine drainage stream: application of a reactive transport model. *Environmental science & technology*, 36(5), pp.1093–1101.

Smit, C. 2013. The Role of Mining in the South African Economy. *KPMG South Africa Business Blog.*

Stumm, W., & G. F. Lee. 1961. Oxygenation of ferrous iron. *Industrial and Engineering Chemistry* (53), pp: 143.

Taylor, J., 2001. *Microorganisms and Biotechnology*, *University of Bath, Science 16 - 19*. Second Edition, Nelson Thornes.

The National Groundwater Information System, 2012. *The National Groundwater Archive*, Pretoria: The Department of Water and Sanitation. Available at: https://www3.dwa.gov.za/NGANet/ [Accessed 25 April, 2015].

The World Commission on Dams Report, 2000. Dams and development: a new framework for decision-making. *The World Commission on Dams*. Available at: http://www.internationalrivers.org/files/attached-files/world_commission_on_dams_final_report.pdf [Accessed 7 May, 2015].

Turton, A., Molewa, E. & Mining Weekly, 2014. Government lauded for AMD paradigm shift, but complexity not fully grasped. *Mining Weekly*. Available at: http://www.miningweekly.com/article/govt-lauded-for-amd-paradigm-shift-but-detractors-insist-it-hasnt-fully-grasped-complexity-of-the-issue-2014-04-18-1 [Accessed 5 September, 2015].

Turton, A. 2013. On acid mine drainage in the West Rand. DHI SA Symposium, Professional Development Hub, University of the Witwatersrand.

United States Environmental Protection Agency, 1980. USEPA FerroVer Method 8008.

United States Geological Survey Mineral Resources Programme, & Ober, J.A., 2001. Sulfur. Available at: http://minerals.usgs.gov/minerals/pubs/commodity/sulfur/sulfmyb01.pdf [Accessed 23 March, 2015].

U.S. Geological Survey, 2012. Mineral Commodity Summaries. Available at: http://minerals.usgs.gov/minerals/pubs/mcs/2012/mcs2012.pdf [Accessed 15 October 2014].

Van Metre, P. C., & Callender, E. Water-quality trends in White Rock Creek Basin from 1912-1994 identified using sediment cores from White Rock Lake reservoir, Dallas, Texas. *Journal of Paleolimnology* 17, pp. 239-249..

Viljoen, J., 2014. Krugersdorp flooded during heavy rain fall. Available at: http://krugersdorpnews.co.za/226496/krugersdorp-flood/ [Accessed 18 August, 2015].

Weaver, T.J., 2014. Refinement of iron oxide recovery methods for AMD treatment systems. In *Abandoned Mine Drainage: Impacts, Treatment and Developing Novel Uses for AMD*. Northeastern Section - 49th Annual Meeting. The Geological Society of America. Available at: https://gsa.confex.com/gsa/2014NE/finalprogram/abstract_236427.htm [Accessed December 9, 2014].

Webb, J.S., McGinness, S. & Lappin-Scott, H.M., 1998. Metal removal by sulfate-reducing bacteria from natural and constructed wetlands. *Journal of Applied Microbiology*, 84(2), pp.240–248.

Whitehead, P., & Jeffrey, H., 1995. Heavy metals from acid mine drainage - impacts and modelling strategies. *International Association of Hydrological Sciences - Proceedings of a Boulder Symposium*.

World Weather Online, 2013. *Average Rainfall for Krugersdorp, South Africa 2000 - 2012.*, World Weather Online. Available at: http://www.worldweatheronline.com/Krugersdorp-weather-averages/Gauteng/ZA.aspx [Accessed 16 June, 2015].

Yu, J. Y., 1998. A mass balance approach to estimate the dilution and removal of the pollutants in stream water polluted by acid mine drainage. *Environmental Geology*, 36(3-4), pp.271-276.

7 APPENDICES

Appendix 1: Meteorological conditions

Weather patterns over the year varied considerably. Based on monthly averages wind-speed was highest in spring (~4.0 $m.s^{-1}$) followed by summer (~2.8 $m.s^{-1}$), winter (~2.5 $m.s^{-1}$) and autumn (~2.1 $m.s^{-1}$) (Figure A1).

Monthly average temperatures of the dam's water surface remained similar (~16.6^{0}C) during autumn and spring, peaking in summer (~20.7^{0}C) and were at their lowest in winter (~11.1^{0}C). The highest daily temperature in the dam occurred in summer (~22.0^{0}C), and the lowest in winter (~8.0^{0}C) (Figure A1).

Based on monthly averages, relative humidity was highest at the study site during summer (~77%), autumn (~71%), spring (~66%) followed by winter (~54%) (Figure 14).

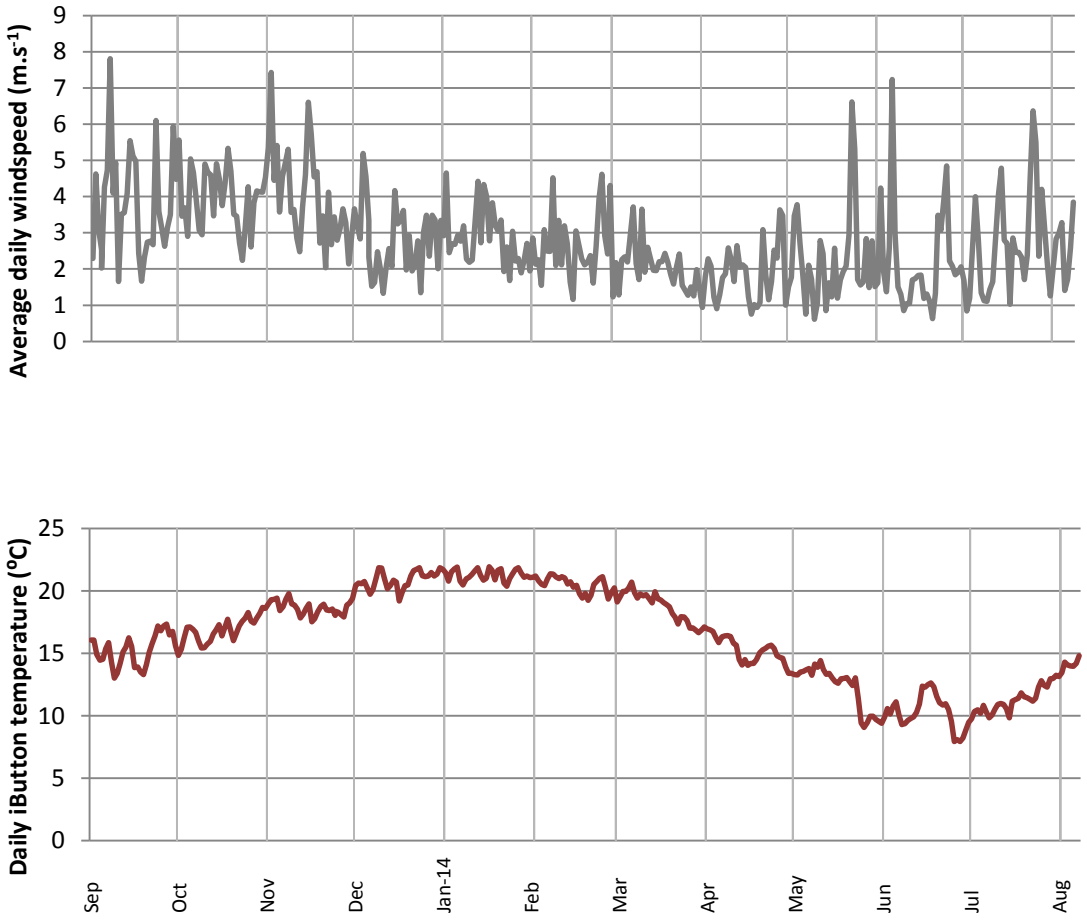

Figure A1: Meteorological data (daily mean) of wind-speed ($m.s^{-1}$), surface water temperature (^0C) and relative humidity of the air around the Charles-Fourie Dam. Hourly data for relative humidity and wind-speed were sourced from an iWeathar station at the Krugersdorp airfield and surface water temperatures were sourced from iButtons left in the dam.

Appendix 2: Calculation of the average mass of dissolved sulfate in the surface waters of the Charles-Fourie Dam

The daily mass of dissolved sulfate (and iron) in the inlet and outlet of the Charles-Fourie Dam was calculated via the following process (Tables 4 and 5):

1. Discharge ($m^3.s^{-1}$) was multiplied by 86400 to convert the value into $m^3.day^{-1}$;
2. The concentration (mg. L^{-1}) was multiplied by 0.001 to convert the value to $kg.m^{-3}$;
3. The product of 1) and 2) yielded the flux of sulfate ($kg.day^{-1}$) in the Charles-Fourie Dam for each observation point.

Table A1: Calculation of the daily mass of dissolved sulfate in the inlet of the Charles-Fourie Dam over the 2013-2014 study period.

Observation point	Discharge ($m^3.s^{-1}$)	Discharge ($m^3.day^{-1}$)	Concentration (mg. L^{-1})	Concentration ($kg.m^{-3}$)	Flux of sulfate ($kg.day^{-1}$)
September	0.30	25 592	2393	2.39	61 243
October	0.27	23 473	1723	1.72	40 446
November	0.15	13 193	1565	1.56	20 645
December	0.19	16 796	1993	1.99	33 473
January-14	0.32	27 337	1500	1.50	40 997
February	0.28	24 106	1332	1.33	32 112
March	0.94	81 328	2421	2.42	196 897
April	0.50	43 615	2402	2.40	104 780
May	0.46	39 588	2226	2.23	88 107
June	0.43	37 385	2039	2.04	76 245
July	0.40	34 284	1797	1.80	61 624
August	0.41	35 173	2021	2.02	71 080
Total					837 112

Table A2: Calculation of the accumulation of dissolved sulfate in the Charles-Fourie Dam over the 2013-2014 study period.

Observation point	Surface Inflow (Qi.Ci)	Surface Outflow (Qo.Co)	Dust (QdCd)	Rain (Qr.Cr)	Groundwater (Qr.Cr)	Accumulation (dM/dt)
September-13	61 243	58 346	0.02	0.000002		2 898
October-13	40 446	41 748	0.10	0.000076	1 771	469
November-13	20 645	16 739	0.06	0.000047		3 907
December-13	33 473	25 824	0.04	0.000130		7 649
January-14	40 997	61 499	0.06	0.000088		-20 502
February-13	41 574	36 315	0.07	0.000156	2 352*	2 906
March-13	196 897	193 729	0.11	0.000322	3 558*	-390
April-13	104 780	111 972	0.03	0.000026	183	-7 009
May-13	88 107	88 256	0.03	0.000023	701	553
June-13	76 245	87 283	0.02	0.000000	1 852	-9 185
July-13	61 624	64 191	0.02	0.000000	378	-2 188
August-13	71080	72 953	0.01	0.000016	1 102*	-2 975
Total Accumulation						**-23 868**
Total Accumulation during normalised flows						**-3 366**

*Denotes observation points where groundwater exited the dam

Appendix 3: Bathymetric map

A bathymetric map was developed using OriginPro 9 software.

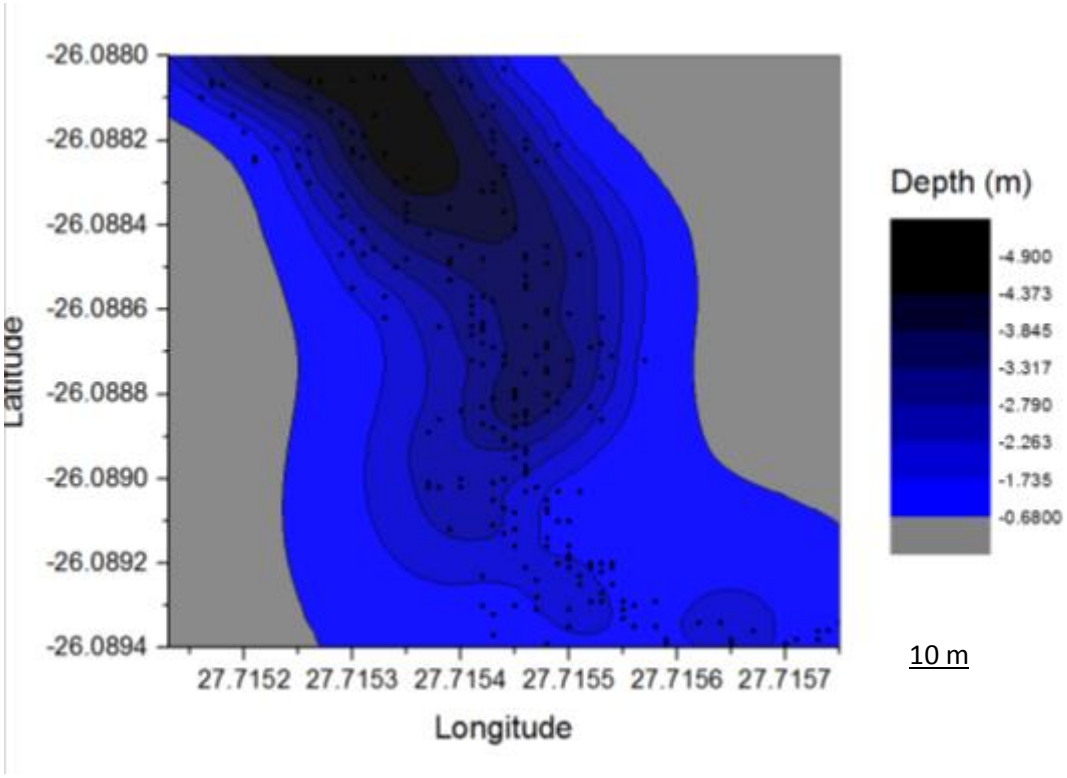

Figure A2: Bathymetric map of the Charles-Fourie Dam, Gauteng Province.